FACULTY OF SCIENCES

INVESTIGATING LONG NON-CODING RNAS IMPLEMENTED IN MYELOID NEUROINFLAMMATION DURING MULTIPLE SCLEROSIS PATHOGENESIS

Jo De Vos
Student number: 01806466

Supervisors: Prof. Dr. Geert van Loo and Prof. Dr. Pieter Mestdagh
Scientific tutor: Prof. Dr. Geert van Loo

Master's dissertation submitted to Ghent University to obtain the degree of Master of Science in Biochemistry and Biotechnology: Major Biomedical biotechnology

Academic year: 2022 – 2023

UNIVERSITEIT GENT

Ghent University – Department of Biomedical Molecular Biology
VIB – Center for Inflammation Research
Research Group: van Loo unit

VIB-UGENT CENTER FOR INFLAMMATION RESEARCH

Acknowledgements

As the semester draws to a close, I can almost taste the bittersweet blend of relief and nostalgia that accompanies the end of my master's education. Once, the entrance exam of medicine denied me the opportunity to pursue my dream in neurology. As a consequence, I changed path and entered the fascinating world of biochemistry and biotechnology. It was a challenging path, no doubt. However, I seized every chance that came my way, eventually still pursuing my dream of solving the mysteries of the nervous system as a scientist.

These past five years have brought more than just an infinite wealth of knowledge in biochemistry and biotechnology. They have gifted me with encounters with the most fascinating individuals, and a lot of opportunities that shaped my journey. I have had the honour of serving as the president of the student association, forging bonds and creating memories that will last a lifetime. I have ventured afar to South-Korea, immersing myself in a vibrant culture while pursuing my studies. And at last, I had the privilege of diving into captivating research within the realm of my passion of neuroscience in the van Loo unit. Truly, they say that your student years are the best time of your life, and I can attest that it is no mere myth. Now the time has come to appreciate every person who contributed to this unbelievable journey.

First and foremost, I would like to express my deep gratitude to Professor Geert van Loo, one of the supervisors my thesis research. Over a year ago, I approached him with my proposal to investigate epigenetics in neurobiology, specifically in neuroinflammation, at his lab. He was incredibly supportive and open-minded, allowing me to explore this area and propose an experimental setup while offering his expertise to refine it. He also approached Prof. Pieter Mestdagh (Faculty of Medicine, UGent) for his expertise in research on long non-coding (lnc)RNAs. Through the making of the research proposal and the subsequent execution of the thesis this academic year, Prof. van Loo provided me with all the tools and knowledge necessary to conduct the research of my interest. Working under his guidance, I gained independence, technical insights, and a deeper understanding of the subject matter. Furthermore, his interest in my ideas and results gave me the motivation and encouragement needed to persevere through the semester, and I am truly grateful for the opportunities he gave me to develop as a young scientist. I would also like to extend my thanks to Professor Pieter Mestdagh, copromotor of this thesis, for his contribution to our research project. He provided me with a lot of information to become more familiar with lncRNA research and performed the RNA sequencing of our samples in his lab, which made it possible to conduct high quality research. I also wanted to thank the bioinformation of the Mestdagh lab, Jasper Ankaert, who gave me plenty help in the analysis of the RNA sequencing dataset.

I am deeply grateful to the individuals who provided invaluable assistance throughout my research and putted a smile on my face every day. Their contributions were inevitable in the success of my project, and I would like to extend my appreciation to each of them. First, I want to express my gratitude to Pieter Hertens, my cell culture hero, for training me in working with primary cell cultures and his assistance in setting up my experiments. Beyond his technical expertise, Pieter was a supportive friend in the lab, always available to provide guidance and advice. I am also thankful to Maarten Ciers, our talented bioinformatician, for his extensive help with all aspects of bioinformatic analysis. Without his expertise and tips and tricks, I

would not have been able to obtain the results I have achieved. Mozes Sze, our dedicated lab technician, deserves special recognition for bringing joy to my work and for his continuous support in various technical aspects. His guidance ensured that I conducted my experiments accurately, making him a key contributor to the overall success of my lab work. I also highly appreciated the help of Xenia Ghysels, who was always open to answering my questions and providing assistance in different technical aspects, including her valuable help with various protocols. I am also grateful to Murali for his kindness and cooperation in allowing me to utilize his findings for my study. I would like to thank Edith De Bruycker and Manon Bouckaert from the Coppieters lab for generously sharing their time and expertise, assisting me with the design of antisense oligonucleotides and experimental setup. Lastly, I would like to express my sincere thanks to all other members of the lab who were readily available to offer assistance in every aspect possible. The collaborative and supportive environment within the van Loo unit contributed significantly to my overall experience and the fun I had.

My gratitude extends to all my professors who have enriched my education with their teachings. Crossing paths with such remarkable individuals has been an honour. A special thank you goes to the professors who collaborated with me in organizing events for all students, creating lasting impactful moments.

I deeply appreciate the unwavering support and love of my parents and family throughout my academic journey. Their belief in me has been the driving force behind my accomplishments as a scientist. To my partner Sandra, whom I met during my exchange in South Korea, I am also grateful. Your unwavering support in both my studies and personal life has been instrumental in overcoming challenges and achieving my goals.

Heartfelt appreciation goes to all my friends who have been part of my academic journey. Your friendship has enriched my experiences, both within and beyond academia. I will cherish the late-night study sessions with all of you as well as the adventures we had, the many parties, the cosy diners and definitely the coffee breaks at the VIB. I am looking forward to extend our adventures in the future and hope that everyone will achieve the dreams they want.

Table of Contents

List of Abbreviations

Word	Abbreviation
1-Methyl-4-phenyl-1,2,3,6-tetrahydropyridine	MPTP
5-methylcytosine	m5C
A20$^{Cx3Cr1\text{-}KO}$	A20 KO
A20$^{Myel\text{-}Ko}$	A20 KO
Adeno-associated virus	AAV
Alzheimer's disease	AD
Amyloid-beta	Aβ
Amyotrophic lateral sclerosis	ALS
Antisense oligonucleotides	ASOs
Apoptosis-associated speck-like protein	ASC
Base pairs	bp
Blood-brain barrier	BBB
Bone-marrow derived macrophages	BMDMs
Central nervous system	CNS
Chemokine (C-C motif) ligand	CCL
Chromatin immunoprecipitation	CHIP
CNS-associated macrophages	CAMs
Complete Freud's adjuvant	CFA
Crosslinking immunoprecipitation	CLIP
Damage-associated molecular patterns	DAMPS
Disease-associated microglia	DAM
Dentritic cells	DCs
Extracellular signal-regulated kinases	ERK
Epstein barr virus	EBV
Experimental autoimmune encephalomyelitis	EAE
Extracellular matrix	ECM
Gasdermin-D	GSDMD
Gene ontology enrichment	GOE
Granulocyte-macrophage colony-stimulating factor	GM-CSF
Growth arrest-specific 5	*Gas5*
Insulin growth factor	IGF
Integrated DNA technologies	IDT
Integrative genome viewer	IGV
Interferon	IFN
Interleukin	IL
Janus kinases	JAK
Lipopolysaccharide	LPS
Locked nucleic acid	LNA

Long non-coding RNAs	LncRNAs
Macrophage-colony stimulating factor	MCSF
Magnetic resonance imaging	MRI
Major histocompatibility complex	MHC
Metastasis Associated Lung Adenocarcinoma Transcript	Malat1
MicroRNAs	miRNAs
Mitogen-activated kinases	MAPKs
Multiple Sclerosis	MS
Myelin oligodendrocyte glycoprotein	MOG_{35-55}
N6 -methyladenosine	m6A
Nitric oxide synthase	iNOS
Nuclear paraspeckle assembly transcript 1	*Neat1*
Nod-like receptor protein	Nlrp
Non-coding RNAs	ncRNAs
Nuclear factor erythroid-derived)-like-2	NRF2
Nuclear factor kappa-light-chain-enhancer of activated B cells	NF-κB
Nucleotides	nt
OTULIN$^{Cx3cr1\text{-}KO}$	OTU KO
Piwi-interacting RNAs	piRNAs
Parkinson's disease	PD
Pathogen-associated molecular patterns	PAMPS
Peripheral blood mononuclear cells	PBMCs
Pggt1b$^{CD4\text{-}KO}$	Pggt KO
Peroxisome proliferator-activated receptor γ	PPARγ
Platelet derived growth factor	PDGF
Polycomb repressive complexes	PRC
Primary progressive MS	PPMS
Protein Geranyl gerany ltransferase Type I Subunit Beta	PGGT1B
Pseudouridine	Ψ
PTEN-induced putative kinase 1	PINK1
Reactive nitrogen species	RNS
Reactive oxygen species	ROS
Relapsing-remitting MS	RRMS
Regulatory B-cells	Bregs
Ribosomal RNAs	rRNAs
RNA *in situ* conformation sequencing	RIC-seq
RNA polymerases	Pol
Secondary progressive MS	SPMS
Signal transducer and activator of transcription	STAT
Single nucleotide polymorphism	SNPs
Small interfering RNAs	siRNAs
Split ends homologue	SPEN
Staufen 1	STAU1

Transmembrane protein 119	TMEM119
T-helper cell	Th
T-regulatory cell	Treg
Toll like receptor	TLR
Tumor necrosis factor	TNF
TNF receptor	TNFR
Untranslated region	UTR
Ultraviolet	UV
Vascular endothelial growth factor	VEGF
Weightened correlation network analysis	WGNA
Wild-type	WT

English Summary

In the recent decade, there has been a significant increase in the number of articles dedicated to research on long non-coding RNAs (lncRNAs), which were once regarded as transcriptional 'noise'. These transcripts have garnered attention due to their complex and multifaceted roles in regulating diverse biological processes and numerous pathologies on DNA, RNA, and protein level. Furthermore, lncRNAs exhibit intriguing therapeutic potential attributed to their cell and context-specific characteristics. Consequently, they are now recognized as pivotal players in neurodegenerative and neuroinflammatory disorders, including Alzheimer's and Parkinson's disease. However, our understanding of the involvement of lncRNAs in the pathophysiology of Multiple Sclerosis (MS), the most prevalent neuroinflammatory condition afflicting young adults, remains significantly limited. Our study aimed to identify and characterize a group of lncRNAs involved in neuroinflammation during experimental autoimmune encephalomyelitis (EAE), an MS mouse model, in order to decrease the gap of knowledge. As a start, we investigated the behaviour of lncRNAs during LPS-induced neuroinflammation, identifying and correlating 10 lncRNAs with elevated levels of neuroinflammation. Furthermore, using unbiased RNA-seq profiling, we identified the presence of 51 inflammation-related lncRNAs that are significantly altered in the spinal cord of EAE mice. From these analyses, *Malat1, Neat1, Miat*, and *Zfas1* exhibit interesting characteristics, which led us to undertake comprehensive characterization studies in both *in vivo* and *in vitro* settings to better comprehend and validate their roles in EAE and neuroinflammation. First, we revealed similar expression patterns of these lncRNAs in Pggt1b$^{CD4\text{-}KO}$ EAE mice, which are resistant to EAE and neuroinflammation, compared to unchallenged wild-type mice, further indicating a correlation between the lncRNAs and neuroinflammation. Furthermore we analysed their expression in A20$^{Cx3cr1\text{-}KO}$ and OTULIN$^{Cx3cr1\text{-}KO}$ mice, which are both 'hypersensitive' to EAE and display hyperactivated microglia. Interestingly, while we revealed the downregulation of *Malat1, Miat,* and *Neat1* in unchallenged A20$^{Cx3cr1\text{-}KO}$ mice as well as in EAE mice compared to non-immunized wild-type mice, they show upregulation in unchallenged OTULIN$^{Cx3cr1\text{-}KO}$ mice. These observations support the notion that these lncRNAs, namely *Malat1, Miat,* and *Neat1*, function as "brakes" to balance and counteract the inflammatory response. However, the ability of these lncRNAs to restrain inflammation appears to be compromised under conditions of prominent neuroinflammation, as observed in EAE. Finally, we conducted expression characterization of the identified lncRNAs *in vitro* using bone marrow-derived macrophages (BMDMs) under conditions of NF-κB, NLRP3, and STAT6 activation to elucidate the *in vivo* results. Additionally, we employed antisense oligonucleotides targeting *Miat* to gain insights into the role of this particular lncRNA. Although our results demonstrated trends of differential expression during all stages of stimulation, we encountered technical difficulties, and no conclusive findings are obtained. In summary, this M.Sc. thesis study provides valuable insights into the involvement of specific lncRNAs in neuroinflammation during EAE, shedding light on potential regulatory mechanisms and emphasizing their significance in modulating the immune response. However, further 'multi-omics' approaches, including single-cell cross-linking immune precipitation (CLIP) and total RNA-sequencing within our experimental framework, are required to validate our hypothesis and gain deeper knowledge of their precise regulatory mechanisms during EAE pathology, particularly in the context of neuroinflammation.

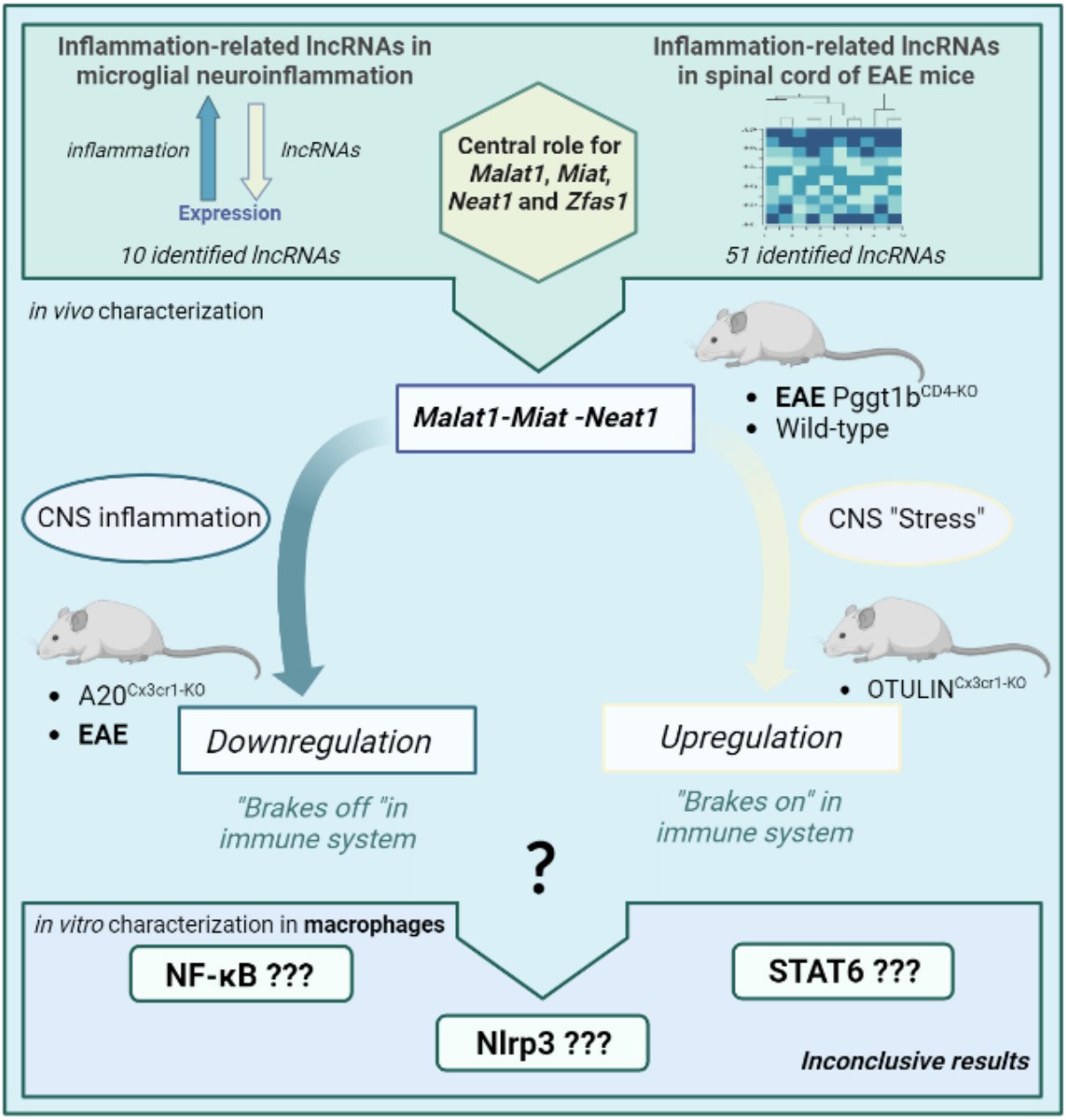

Long non-coding RNAs *Malat1, Miat* and *Neat1* exhibit a regulatory role in neuroinflammation during experimental autoimmune encephalomyelitis (EAE). Figure created with BioRender.

Part 1: Introduction

Long non-coding RNAs (lncRNAs) play a critical role in biology and are key regulators in many cellular processes as well as in various pathologies, including neuroinflammatory ones. While numerous studies have demonstrated their complex involvement in Alzheimer's (AD) and Parkinson's diseases (PD), there is still a lack of knowledge on their role in other conditions, such as in Multiple Sclerosis (MS). MS is a highly complex neuroinflammatory disease, with myeloid cells driving both the chronical phase of inflammation as well as its resolution. Exploring the significance of lncRNAs in the regulation of these cellular responses could lead to the development of more effective and broad-ranging therapies.

1.1 LncRNAs

For many years, research in molecular biology focused solely on the involvement of protein-coding genes. However, more recently, a class of molecules known as non-coding RNAs (ncRNAs) has emerged as critical regulators of all aspects of cellular activity (Mattick et al., 2023; Statello et al., 2021). It became clear that around 95 % of the genome is not translated into proteins. Initially, these transcripts were considered to be non-functional and seen as "junk-transcripts". Nevertheless, more and more evidence, points to an important and highly complex role for different types of ncRNAs, including microRNAs (miRNAs), Piwi-interacting RNAs (piRNAs), ribosomal RNAs (rRNAs), and lncRNAs, in cellular regulation (Carninci et al., 2005; Cheetham et al., 2020). In particular, lncRNAs have garnered significant attention in the fields of cancer and neurodegenerative diseases. Despite the increasing number of publications on these RNAs, there is still much to uncover about their function and potential therapeutic applications.

1.1.1 LncRNAs: Definition and Appearance

Although the name ‘long non-coding RNA’ defines what they are, a precise definition of lncRNAs is currently lacking. Originally, lncRNAs have been defined as non-coding transcripts longer than 200 base pairs (bp), a convenient cut-off that distinguishes them from smaller non-coding RNAs, such as miRNAs and small interfering RNAs (siRNAs). However, given the functional similarity of many RNAs in the 200-500 bp range, it is proposed that lncRNAs should be categorized as transcripts longer than 500 bp (Deng et al., 2006; Mercer et al., 2009).

LncRNAs are transcribed by all three RNA polymerases (Pol I, II, and III), and can be polyadenylated, spliced and 5’-capped such as mRNAs (Figure 1) (Cheng et al., 2005; H. Wu et al., 2016; Yin et al., 2012). They can be classified as intergenic, antisense, or intronic, based on their genomic localization relative to protein-coding genes (Cheetham et al., 2020). While the human genome contains approximately 20.000 protein-coding genes, it is estimated that there are around 100.000 lncRNAs (Uszczynska-Ratajczak et al., 2018). The remarkable abundance of lncRNAs can be attributed to the fact that the non-coding genome constitutes approximately 95 % of the genetic material, as previously mentioned. Furthermore, with the rapid evolution of sequencing technologies, there is a strong likelihood of identifying an even greater number of lncRNAs (Cabili et al., 2015; Seifuddin et al., 2020). Despite their great abundance in many species, lncRNAs are less conserved compared to mRNAs (Pang et al., 2006), probably due to their non-strict structure-function relationship (Pheasant & Mattick,

2007). Still, there are lncRNAs that are highly conserved throughout evolution and have been shown to play indispensable roles in cellular processes (Tavares et al., 2019).

LncRNAs not only play a critical role in the general organization and regulation of organisms but also exhibit limited and cell-specific expression, contributing to the evolutionary complexity of organisms (Gloss & Dinger, 2016). They are involved in crucial processes such as stemness, differentiation, and cell state, with particular significance during organismal development (Flynn & Chang, 2014). The observed low expression of lncRNAs may be essential for their functional role, as low amounts of transcripts increase the likelihood of on-target binding and reduce off-target effects. Fascinating, lncRNAs can even harbour different epitranscriptomic marks, namely pseudouridine (Ψ), N6 -methyladenosine (m6A) and 5-methylcytosine (m5C). These modifications have been shown to affect their fate, functions and efficacy, thereby expanding the diversity of the transcriptome(Jacob et al., 2017). However, our comprehension of their biological function, particularly in relation to lncRNAs, is still at an early stage. Moreover, environmental factors, including stress responses in animals and drug resistance in cancer, can influence their expression, the modifications and signalling functions. Consequently, the regulatory mechanisms governing lncRNAs are intricate and multifaceted, mirroring the diverse functions they fulfil within the cellular context (Kopp & Mendell, 2018).

1.1.2 LncRNAs: Regulatory Mechanisms

The diverse regulatory functions of lncRNAs are mediated by their capacity to engage in a wide range of interactions, encompassing RNA-protein, RNA-RNA, and RNA-DNA interactions (Ramilowski et al., 2020). The repeated sequence elements present in lncRNAs, such as small interspersed nuclear elements, provide multiple binding sites that allow lncRNAs to regulate various cellular processes, including chromatin architecture, transcription, splicing as well as translation, and localization of proteins (Cao et al., 2021; Hacisuleyman et al., 2016; Morrissy et al., 2011; Pisignano & Ladomery, 2021; Zhao et al., 2008; Zucchelli et al., 2015).

The importance of chromatin structure in the regulation of differentiation and development is well documented, with modifications such as methylation, acetylation and ubiquitination on histones altering the chromatin structure and thereby regulating gene expression (Schuettengruber et al., 2007). Fascinatingly, the intricate regulation of polycomb repression complexes 1 and 2 (PRC1/2), which employ histone-modifying enzymes, involves diverse and complex interactions with lncRNAs. (Trotman et al., 2021). PRC1/2 catalyses the monoubiquitylation of aminoacids on histones as well as dimethylation and trimethylation, but do not contain sequence-specific DNA binding domains in mammals (Laprell et al., 2017). Therefore, the recruitment of PRC1/2 to specific genes is achieved through the interaction of the complexes with controlling RNAs, such as lncRNAs (Figure 1). Moreover, recent studies have shown that a significant proportion of lncRNAs (~20%) interacts with PRC2, and silencing of several of these lncRNAs has been found to restrict the expression of genes that are normally silenced by PRC2 (Davidovich & Cech, 2015).

The second class of lncRNA regulatory mechanisms involves interactions between these transcripts and other RNA molecules. LncRNAs can act as decoys for specific RNAs, thereby preventing their translation or binding to their targets, as is the case for miRNAs (Figure 1)(Täuber et al., 2019). Furthermore, some lncRNAs directly target mRNAs for degradation, a process mediated by the protein Staufen 1 (STAU1). This protein recognizes a particular motif

in the 3' untranslated region (UTR) of mRNAs and facilitates their degradation through nonsense-mediated mRNA decay. Specifically, STAU1 binds to double-stranded RNA motifs in the 3'UTR of mRNAs. The lncRNAs appear to contain a single-stranded complementary sequence that binds to mRNAs, creating that double-stranded motif which is subsequently recognized by STAU1 (Gong & Maquat, 2011). Another example of RNA-RNA interaction involves the function of lncRNAs in the splicing of mRNAs and even other lncRNAs. They regulate this process through interaction with splicing protein factors, generating RNA-RNA duplexes, or with chromatin modifiers, which consequently have an effect on how transcripts are spliced (Romero-Barrios et al., 2018).

Next, lncRNAs have emerged as key regulators of transcription by binding to DNA. For most genes, transcription involves the interaction between a proximal promoter and distant enhancer elements, which are often located far from the transcription start site. Active enhancers are bound by RNA Pol II, suggesting that they interact with the promoter (Ray-Jones & Spivakov, 2021). Intriguingly, lncRNAs appear to direct RNA Pol II and transcription factors to specific enhancer elements and promoters of target genes (Figure 1). This spatiotemporal regulation allows lncRNAs to modulate cellular specific processes which are highly important during development (W. Li et al., 2016).

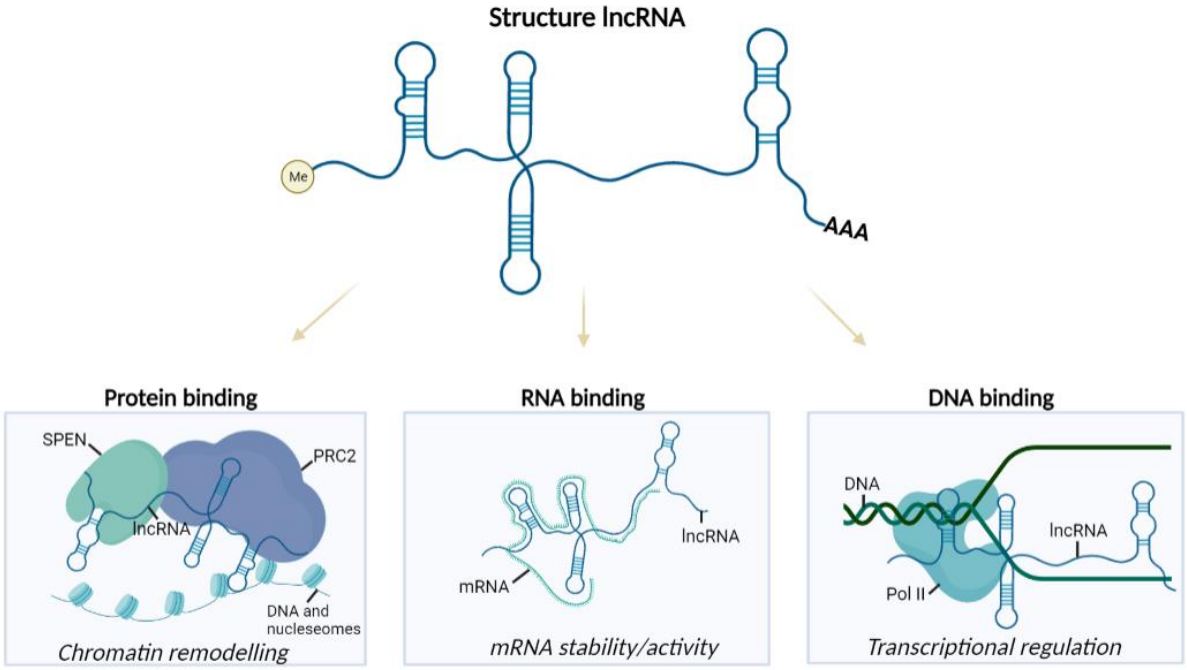

Figure 1. Structure and function of long non-coding (lnc)RNAs. LncRNAs can be transcribed by all three RNA polymerases (Pol I,II & III). In case of Pol II, lncRNAs can be 5'- capped and polyadenylated at the 3' of the transcript. LncRNAs are characterized by complex secundairy and tertiary structures, hence they can interact with proteins, RNA and DNA. As scaffolds, lncRNAs will bind and gather different protein complexes to optimize their functions or guide them to other protein complexes such as DNA nucleosomes. Split ends homologue (SPEN) and Polycomb repressive complex 2 (PRC2) are guided to nucleosomes of DNA to remodel chromatin and consequently influence hetero -and euchromatin (left). Next, lncRNAs can bind other RNAs such as messenger -and microRNAs to alter their activity and stability. More specifically, lncRNAs can act as decoys for these RNAs and inhibit translation or the binding of microRNAs to their targets (middle). Last, Pol II and transcription factors can be guided by lncRNAs to specific DNA sequences to regulate transcription (right). Figure created with BioRender.

The array of mechanisms by which lncRNAs operate is indeed remarkable. Given their significant impact on cellular functionality, their role in various pathologies is becoming increasingly notable. While much of the research on lncRNAs has focused on their role in cancer, there is significant evidence supporting their pivotal involvement in other pathological conditions, including diabetes, cardiovascular diseases, autoimmune diseases, and neurodegenerative and neuroinflammatory pathologies such as AD and PD (Huarte, 2015; Sparber et al., 2019; Wan et al., 2017). Neuroinflammation involves strict regulation through complex signalling pathways, in which lncRNAs notably play an unmissable role.

1.2 Neuroinflammation and The Regulation by LncRNAs

The central nervous system (CNS) is a highly complex system with many different cell types, including immune cells, that work together to ensure the proper functioning and integrity of the CNS. In a healthy brain, these immune cells tightly regulate neuroinflammation, ensuring a balanced immune response within the CNS. However, pathological disruptions, including viral or bacterial infections, exposure to neurotoxins, accumulation of aggregated proteins, ischemia, degenerative conditions, autoimmune reactions, or traumatic events, have been identified as factors that can disturb the immune response within the CNS. Consequently, these disturbances can lead to neurotoxicity and potentially result in neuronal degeneration (Lyman et al., 2014). Although this field has been extensively studied, the precise mechanisms regulating neuroinflammation are not fully understood (Shabab et al., 2017a). However, recent studies suggest that lncRNAs exert important roles in modulating neuroinflammation and can possibly serve as interesting targets for therapy (Y. Liu et al., 2022a; Wan et al., 2017).

1.2.1 Myeloid Cells in the CNS

Myeloid cells are a diverse group of immune cells and, if not the most prominent, important drivers of neuroinflammation and immune responses in the CNS. They include monocytes, macrophages, dendritic cells (DCs), neutrophils, eosinophils, basophils, and microglia (Herz et al., 2017). While the majority of myeloid cells originate from hematopoietic stem cells in the bone marrow, microglia arise from the yolk-sac and are known as supportive glial cells in the CNS (Epelman et al., 2014; Kierdorf et al., 2013). Microglia constitute approximately 5 to 12 % of the total brain cells and fulfil various functions. These cells are strategically positioned within the parenchyma of the CNS, allowing them to be in close proximity to neurons (Nimmerjahn et al., 2005). In contrast, CNS-associated macrophages (CAMs), also known as border-associated macrophages, are a small population of specialised macrophages localised at the border areas of the CNS in the choroid plexus, meningeal and perivascular spaces (Prinz et al., 2017; Prinz & Priller, 2014). Both microglia and CAMs have relative longevity and high motility, and can suppress or drive immune responses during CNS development, health, and disease (Ousman & Kubes, 2012; Prinz et al., 2017). During disease, microglia and CAMs are accompanied by infiltrating monocytes. One subtype of the murine monocytes, the $CX3CR1^{low}/CCR2^{+}/Ly6C^{high}/PD\text{-}L1^{-}$ monocytes, have the ability to cross through a compromised blood-brain barrier (BBB) and become activated in both inflamed and non-inflamed areas (Lund et al., 2018; Mildner et al., 2007). Because these cells originate from monocytes out of the bone marrow, we refer to this myeloid population as bone-marrow derived macrophages (BMDMs). They express cellular markers, such as CD11b, Iba-1, and CX3CR1, which are also seen on microglia (Lund et al., 2018). However, specific cell surface markers such as transmembrane protein 119 (TMEM119) and purinergic receptor P2Y12 can distinguish microglia from BMDMs or other myeloid cell types under pathological conditions (M. L.

Bennett et al., 2016). One study has shown that over time, graft-derived macrophages acquire characteristics similar to microglia, including ramified morphology, longevity, radio-resistance, and clonal expansion. However, even after prolonged residence in the CNS, the transcriptomes and chromatin accessibility landscapes of engrafted bone marrow-derived macrophages remain distinct from those of host microglia. Moreover, engrafted bone marrow-derived cells exhibit distinct responses to peripheral endotoxin challenge compared to the host microglia (Shemer et al., 2018). Indeed, although both cell populations exhibit similar characteristics, BMDMs and microglia serve notably different functions in disease and homeostasis (J. Lyu et al., 2021).

1.2.2 Immune Functions of Myeloid Cells in the CNS

Microglia play a prominent role in the development and maintenance of the CNS. One of their key functions is mediating synapse pruning, which is essential for organizing neuronal circuits during both development and adulthood. Disruptions in microglial number or activation have been associated with functional and structural deficits in cortical circuits (Ueno et al., 2013). Intriguingly, microglia secrete mediators of the complement cascade, including C1q, C4, C3, and CR3, which are critical for synaptic connectivity and neuroinflammation (Györffy et al., 2018). Deficiencies in these mediators have been shown to result in synaptic connectivity defects in mice (Shi et al., 2015). Additionally, microglia, along with other myeloid cell types, participate in the removal of apoptotic and healthy cells in the developing and adult brain, a process crucial for preventing inflammation and autoimmunity (Damisah et al., 2020). Yet, despite their vital roles in CNS development and homeostasis, microglia and the other myeloid cells, primarily function to drive neuroinflammation in response to pathogens, toxins, or damage within the CNS (Hanisch, 2002).

In an inflammatory environment, activated microglia undergo a morphological change, adopting an amoeboid shape with larger, rounder cell bodies and shorter, thicker branches (Jinno et al., 2007). This morphological transformation is accompanied by increased secretion of cytokines, chemokines as well as by the production of matrix metalloproteases (Merson et al., 2010a). These metalloproteases are crucial in inducing BBB leakage and the infiltration of monocytes and other immune cells into the CNS (Brkic et al., 2015; Z. Jiang et al., 2014). Furthermore, the activated microglia and residential macrophages secrete chemokines such as chemokine (C-C motif) ligand (CCL)-2, CCL5, CCL12, and CCL22, which not only recruit monocytes and macrophages but also stimulate the proliferation and migration of additional microglia in the CNS, thereby creating positive feedback loops that amplify inflammation (Z. Jiang et al., 2014). Tumor necrosis factor (TNF), interleukin (IL)-6, IL1-β, and IL-12 are well-known inflammatory mediators that induce expression of inflammatory genes via different signalling pathways, including nuclear factor kappa-light-chain-enhancer of activated B cells (NF-κB), Janus kinase/signal transducer and activator of transcription (JAK/STAT), c-jun N-terminal kinase (JNK), mitogen- activated protein kinases/ extracellular signal-regulated kinases (MAPK/ERK1/2), as well as nitric oxide synthase (iNOS) (Kaltschmidt & Kaltschmidt, 2009). The latter pathway leads to the production of reactive nitrogen species (RNS) such as NO, which, together with reactive oxygen species (ROS), triggers cytosolic stress pathways, DNA damage, and upregulation of pathways involved in inflammation. These effects can result in the degeneration of neurons and glial cells (Figure 2) (Metodiewa & Kośka, 2000; Ransohoff, 2016b). Interesting, the myeloid secreted cytokines have both neuroprotective and neurotoxic actions based on complex signals within their microenvironment. However, TNF, IL6, and IL1β

are primarily associated with neurotoxicity due to their ability to inhibit neurogenesis, and induce cellular stress and apoptosis (Merson et al., 2010b).

The pro-inflammatory response is further characterized by antigen presentation. Although originally thought to be an exclusive characteristic of DCs, microglia and macrophages can also present antigens, activate and guide the adaptive immune response in the CNS (Jordão et al. 2019; Roche and Cresswell 2016). Microglia play an essential role in antigen presentation by expressing low levels of major histocompatibility complex (MHC) molecules at steady-state, but rapidly induce MHC expression when activated in disease conditions, which is crucial in promoting and reactivating T-cell responses. For example, antigen presentation by myeloid cells in the CNS promotes T-cell responses and phagocytosis of myelin in MS, increasing disease severity (Riedhammer & Weissert, 2015). On the contrary, in AD, activated microglia process and present self-antigen such as amyloid-β (Aβ) and modified Tau proteins, two hallmarks of AD, to the infiltrated T lymphocytes in order to temper neuroinflammation (Das & Chinnathambi, 2019).

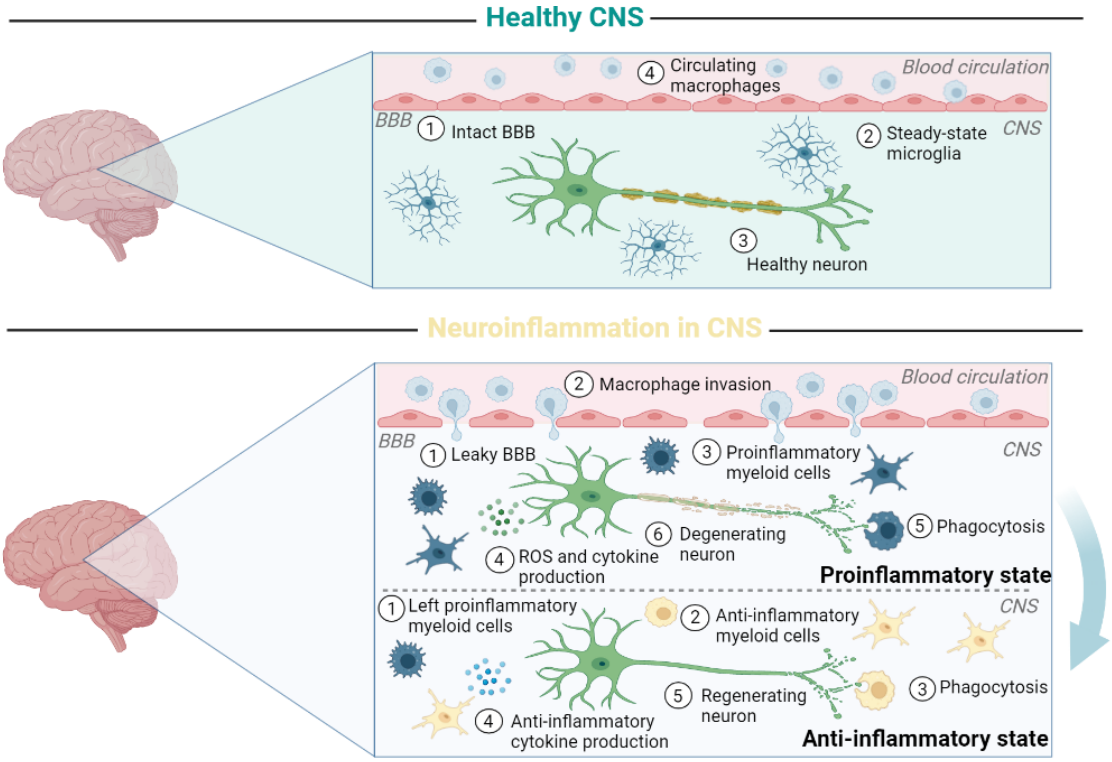

Figure 2. Myeloid cells in a healthy central nervous system (CNS) and during neuroinflammation. In a healthy CNS, macrophages and monocytes are circulating in blood vessels and are not able to cross the intact blood brain barrier (BBB). Microglia are in a steady state and play a role in the maintenance and homeostasis of the CNS to support healthy neurons. During neuroinflammation, monocytes and macrophages are able to cross the leaky BBB, become activated, and adopt a pro-inflammatory state together with microglia. These myeloid cells will secrete pro-inflammatory cytokines to activate and more myeloid cells, consequently amplifying the inflammatory response. In addition, myeloid cells will secrete reactive oxygen species (ROS) which create a cytotoxic environment for neurons and other supportive cells leading to neuron degeneration. The debris of the degenerating neurons will be removed through phagocytosis by the myeloid cells. CNS myeloid cells will also secrete anti-inflammatory cytokines to counteract the neuroinflammation and induce repair and homeostasis. In most of the cases, anti -and pro-inflammatory responses will exist in parallel which prevents full recovery from damage and induce the formation of scar tissue. Figure created with BioRender.

Another important function of myeloid cells during neuroinflammation is the phagocytosis of cellular debris, apoptotic cells, and other macromolecules, in order to dampen inflammation and promote homeostasis and repair (Figure 2)(Sierra et al. 2013).

Indeed, besides displaying a pro-inflammatory signature, myeloid cells have been found to also secrete anti-inflammatory molecules such as IL-4, IL-10, IL-13, and transforming growth factor (TGF)-β (Figure 2) (Gordon, 2003). These molecules work together to promote the development of a protective type 2 T helper (Th2) and regulatory T (Treg) cells response in various neuroinflammatory conditions to induce the resolution of inflammation. However, these latter cells are also one of the most important sources of the anti-inflammatory cytokines which in their turn temper the pro-inflammatory response of myeloid cells (Liston et al., 2022). Furthermore, myeloid cells have important roles in CNS repair following damage. Macrophages and microglia adopt a wound healing phenotype characterized by the production of growth factors such as platelet derived growth factor (PDGF), TGF-β1, insulin growth factor (IGF-1), and vascular endothelial growth factor (VEGF)-α, which promote cellular proliferation and blood vessel development (Berse et al., 1992). They also produce soluble mediators that stimulate tissue fibroblasts to differentiate into myofibroblasts, facilitating wound contraction and closure, as well as the synthesis of extracellular matrix components. In summary, myeloid cells have diverse and important functions in the CNS, ranging from immune surveillance and inflammation to tissue repair and homeostasis (Quarta et al., 2021; Sierra et al., 2013).

1.2.3 Myeloid Subpopulations in the CNS

High-dimensional single-cell sequencing has revealed that different subpopulations of myeloid cells, with their different activated phenotypes, coexist in both healthy and diseased CNS (Mrdjen et al., 2018). The existence of different microglia and macrophage subpopulations in the CNS, known as myeloid cell heterogeneity, is characterized by morphological and transcriptional differences depending on the CNS region (Grabert et al., 2016; Lavin et al., 2014). The cells' response depends on the local microenvironment, which they sense through unique clusters of surface and intracellular proteins, known as the "sensome" (Hickman et al., 2013). By using these sensors, the cells can detect endogenous ligands and microorganisms, and adjust their transcriptome to produce a cell specific response (Gertig & Hanisch, 2014). In pathological conditions, microglia and other CNS macrophages can lose their homeostatic gene signature and undergo changes in both morphology and transcriptional identity, a process known as polarization (Ajami et al., 2018).

Originally, polarization was explained by the M1-M2 dichotomy: classical (M1)-activated macrophages and microglia were thought to be harmful due to the release of destructive pro-inflammatory mediators, while alternative (M2)-activated cells were believed to be involved in resolving inflammation and phagocytosis. However, this classification is outdated and no longer explains the different responses of myeloid cells to different challenges (Ransohoff, 2016a). These innate immune cells exhibit a more dynamic and varied spectrum of activation states between the two extreme M1 and M2 states, with some even overlapping (Ajami et al., 2018; Mathys et al., 2017). Interestingly, a disease/damage-associated microglia (DAM) phenotype develops in neuroinflammatory conditions, and has been documented in diseases such as AD disease and MS (Keren-Shaul et al., 2017; Krasemann et al., 2017), but have also been observed in other neurodegenerative diseases. DAM microglia, for example, lose homeostatic markers such as Cx3cr1 and purinergic receptors P2ry12/P2ry13, and gain

inflammation, as well as phagocytic and lipid metabolism genes such as ApoE, Lpl, Cst7, and CD9. However, it remains unclear whether DAMs are beneficial or rather detrimental, or even both, as research is hindered by difficulties in distinguishing the different myeloid subpopulations. Identifying their specific roles may contribute to a better understanding of the importance of these myeloid cells in homeostasis, development, and disease. Moreover, the molecular regulation underlying these myeloid states and phenotypes during neuroinflammation is crucial to find new therapeutic strategies to intervene and treat patients suffering from neurodegenerative diseases.

1.2.4 Molecular Regulation of Neuroinflammation

As mentioned earlier, the secretion of pro-inflammatory cytokines including TNF, IL-6, and IL-1β by myeloid cells and other immune cells, mediates an inflammatory response, and subsequently a repair process in myeloid cells (Sierra et al., 2013). The NF-κB family of transcription factors crucially controls inflammation by regulating the expression of many genes involved in inflammation, cell survival, death, proliferation, and differentiation (Q. Zhang et al., 2017). Activation of NF-κB occurs by stimulation of specific receptors such as Toll-like receptors (TLRs), TNF receptor (TNFR) , IL-1 receptor, and many others (Hayden & Ghosh, 2008). In the CNS, NF-κB can play a dual role contributing to either neuroprotection or neurodegeneration, depending on the specific cell type and subunits involved (Dresselhaus & Meffert, 2019). Indeed, while NF-κB signalling in reactive microglia and astrocytes has been reported to contribute to AD pathology by increasing accumulation of Aβ plaques, tau protein hyperphosphorylation, and neuroinflammation, it has also been shown to promote synapse growth and enhance synaptic activity under normal physiological conditions (De Strooper & Karran, 2016; Kassed et al., 2002). The tight regulation of NF-κB signalling involves many mediators, such as A20, OTULIN, and CYLD, which negatively regulate NF-κB activation and suppress inflammation through their deubiquitinating activity (Q. Zhang et al., 2017). Knockout of A20 in mice, for instance, induces a spontaneous neuroinflammatory phenotype, making mice more sensitive to neurodegenerative diseases, by affecting microglial regulation of neuronal synaptic function (Voet et al., 2018).

In addition to the NF-κB pathway, other important components of the inflammatory response are inflammasomes, which are cytosolic multiprotein complexes. Inflammasomes activate the pro-inflammatory protease caspase-1, responsible for maturation and secretion of cytokines IL-1β and IL-18, as well as for the cleavage of gasdermin-D (GSDMD) to induce pyroptosis, a form of pro-inflammatory cell death (Rathinam and Fitzgerald 2016). Among the inflammasomes, nod-like receptor protein (Nlrp)-3 is the most widely studied one and responds to a diverse range of activating stimuli, including bacterial, fungal, and viral pathogen-associated molecular patterns (PAMPs), as well as damage-associated molecular patterns (DAMPs) such as ATP and uric acid crystals (Lamkanfi & Dixit, 2012). In the CNS, IL-1β and IL-18 play crucial roles in initiating inflammatory signalling cascades that may contribute to neuronal injury and cell death. Consequently, increased levels of IL-1b and IL-18 are often observed in CNS infection, brain injury, and neurodegenerative diseases (Heneka et al., 2018). On the contrary, IL-1β and IL-18 also have important physiological functions in the CNS and participate in cognitive processes, learning, and memory (Tsai, 2017). Although inflammasome signalling in the CNS is mainly attributed to microglia, other cell types of the CNS, including neurons, astrocytes and endothelial cells, have been reported to involve inflammasome activation (Walsh et al., 2014).

In addition, MAPKs play a pivotal role in modulating myeloid responses and are known to contribute to the initiation of pro-inflammatory reactions after activation due to PAMPS and DAMPS. Studies have demonstrated that the phosphorylation of MAPK proteins leads to the activation of the transcription factor NF-κB and other transcription mediators, ultimately inducing a pro-inflammatory response (Gottschalk et al., 2016). Additionally, the JAK/STAT signalling pathway plays a significant role in the regulation of inflammation, cell proliferation, and cell death, much like NF-κB. Intriguingly, while STAT1 and STAT3 mediate the polarization of pro-inflammatory microglia , the activation of STAT6 by IL-4 promotes the anti-inflammatory polarization of microglia (Z. Yan et al., 2018).

The signalling pathways discussed in this context play crucial roles in regulating inflammation in myeloid cells. It is important to note that certain mediators can exhibit dual functions, having both detrimental pro-inflammatory effects and neuroprotective roles, making their regulation highly complex. Hence, activation of multiple signalling pathways drives myeloid cells towards either a pro-inflammatory or anti-inflammatory response, which has significant implications for CNS homeostasis and disease progression (Butovsky & Weiner, 2018; Z. Jiang et al., 2014). Repression of NF-κB, for instance, is necessary for prevention of neuroinflammation, and upstream regulators such as A20 are involved in this regulation (Zhan et al., 2016). The current hypothesis suggests that NF-κB upregulation due to receptor activation is gradually decreased over time through a negative feedback loop, leading to inflammation resolution. However, this negative feedback loop appears to be impaired in neurodegenerative and neuroinflammatory diseases (Shabab et al., 2017b). Recent studies have shown that inhibiting M1 microglia alone is not sufficient to achieve therapeutic benefits in neurodegenerative diseases, highlighting the importance of understanding the shift to a neuroprotective role for the development of effective therapies (Tian et al., 2022).

Although a significant amount of knowledge exists about the pathways involved in driving and regulating neuroinflammation, most of the focus has been on protein coding genes, overlooking other important factors that could contribute to myeloid polarization. Epigenetics has emerged as a promising field that connects the genomic code with the environment. Specifically, chromatin remodelling plays a critical role in regulating neuroinflammation, and lncRNAs have been identified as key regulators in this process. Despite progress in this field, our understanding of the role of lncRNAs in the context of neuroinflammation remains limited.

1.2.5 LncRNAs in the Regulation of Neuroinflammation

As mentioned earlier, lncRNAs exhibit a diverse array of mechanisms through which they regulate cellular activities (Mercer et al., 2009). Increasing evidence suggests that these transcripts play a significant role in the regulation of neuroinflammation. While certain lncRNAs may be specific to particular diseases, others exert cumulative effects in conjunction with other lncRNAs, influencing broader neuroinflammation pathways (Tripathi et al., 2021a). Furthermore, dysregulation of neuroinflammation-related ncRNAs can disrupt specific signalling pathways (Y. Liu et al., 2022b). The following examples illustrate the aforementioned mechanisms within the context of neuroinflammation.

A significant number of identified lncRNAs involved in neuroinflammation exert their functions through interaction with miRNAs, thereby modulating their activity (Y. Liu et al., 2022b). One well-known lncRNA, Metastasis Associated Lung Adenocarcinoma Transcript 1 (*Malat1*), was initially recognized as a critical regulator of the metastasis phenotype in lung cancer cells (Ji et

al., 2003). In the context of the brain, downregulation of *Malat1* has been observed in AD, leading to neuronal apoptosis, inhibition of neurite outgrowth, and increased levels of the pro-inflammatory cytokines IL-6 and TNF, accompanied by decreased levels of the anti-inflammatory cytokine IL-10. This downregulation of *Malat1* results in the degradation of anti-inflammatory regulators of inflammation, mediated by miR-125b, consequently inducing inflammation in AD. Remarkably, the overexpression of *Malat1* reverses these events (Ma et al., 2019). In contrast, in PD, *Malat1* levels are increased in the 1-Methyl-4-phenyl-1,2,3,6-tetrahydropyridine (MPTP)-induced PD mouse model and in LPS/ATP-treated microglial cells *in vitro*. In this context, the upregulation of *Malat1* promotes apoptosis and enhances the expression of IL-1β, IL-6, and TNF-α. *Malat1* achieves these effects through binding and sequestering miR-212 (Cai et al., 2020). These two studies highlight the context-specific and opposite roles that lncRNAs can play, depending on the binding to different miRNAs. Many other studies have also elucidated the relationship between lncRNAs and miRNAs during neuroinflammation (Y. Liu et al., 2022b; Tripathi et al., 2021a).

Apart from their role as miRNA sponges, lncRNAs are also involved in protein interactions, as demonstrated by studies on another well-known lncRNA, nuclear paraspeckle assembly transcript 1 (*Neat1*). While *Neat1* is primarily recognized for its involvement in nuclear organization, it has also been implicated in regulating inflammation and autophagy responses (Clemson et al., 2009; Tripathi et al., 2021a). Specifically, *Neat1* has been linked to the progression of PD through its interactions with PTEN-induced putative kinase 1 (PINK1), an autophagy regulator, and several microRNAs. *In vivo* experiments have shown that silencing *Neat1* can suppress autophagy induced by MPTP, leading to reduced dopaminergic neuronal injury and mitigated neuroinflammation (W. Yan et al., 2018). In the context of AD, *Neat1* was found to be upregulated in animal models, while PINK1 was downregulated, indicating distinct effects of *Neat1* within the same autophagy pathway in different diseases (Huang et al., 2020). These findings highlight again the diverse and context-dependent roles of lncRNAs in modulating neuroinflammation and autophagy.

Epigenetic modifications and chromatin architecture play a crucial role in the regulation of gene expression, including during neuroinflammation (Saldi et al., 2019). One lncRNA that has been implicated in this process is *HOXA-AS2*. In PD patients, *HOXA-AS2* was found to be upregulated in peripheral blood mononuclear cells (PBMCs) and negatively correlated with the expression of peroxisome proliferator-activated receptor gamma coactivator-1a (PGC-1α), a key regulator of mitochondrial biogenesis and inflammation. Interestingly, knockdown of *HOXA-AS2* was shown to significantly inhibit the microglia pro-inflammatory phenotype and promote the anti-inflammatory phenotype by modulating PGC-1α expression. Mechanistic studies revealed that *HOXA-AS2* directly interacts with PRC2 and regulates the histone methylation status of the PGC-1α promoter, thereby influencing its expression. These findings highlight the role of *HOXA-AS2* in epigenetic regulation of neuroinflammation and microglial polarization through its interaction with PRC2 and modulation of histone methylation (X. Yang et al., 2021).

The studies on molecular regulation of neuroinflammation have not only expanded our understanding of the underlying mechanisms but have also highlighted the therapeutic potential of targeting lncRNAs. One such example is the lncRNA Growth arrest-specific 5 (*Gas5)*, which has been shown to induce microglia polarization towards a pro-inflammatory state and regulate inflammasome activation in PD (Xu et al., 2020). Targeting *Gas5* using a

small molecule called NPC86 has demonstrated promising results in aged mice, where intranasal administration of NPC86 improved cellular functions, reduced neuroinflammation, and increased neuronal survival (Patel et al., 2023). This highlights the therapeutic potential of targeting lncRNAs as a strategy to modulate neuroinflammation.

Furthermore, oligonucleotides have emerged as a promising approach for targeting lncRNAs due to their precise complementarity to their target RNA sequences (Wurster & Ludolph, 2018). They offer advantages over traditional therapies, such as small molecules and antibodies, including the ability to target inaccessible RNAs and reduced potential for side effects (Wurster & Ludolph, 2018; T. Zhou et al., 2016). CRISPR-Cas9, a gene editing tool, has also shown efficacy in modifying gene expression and has been used in the treatment of certain autoimmune diseases (C. Liu et al., 2017). Still, the main challenge in treating CNS pathology is delivering ncRNA-based therapies across the BBB (Min et al., 2020). Several strategies are being explored, including non-viral delivery pathways and lipid or polymer nanoparticle delivery systems (Cullis & Hope, 2017). Focused ultrasound has also shown promise in temporarily disrupting the BBB, enabling targeted therapy delivery to brain tissue. Adeno-associated virus (AAV) vectors are already being used to target ncRNAs in the CNS (Di Ianni et al., 2019; Kimura et al., 2019). In conclusion, lncRNAs exhibit context-specific and often cell-specific functions, providing an opportunity to design therapies with minimal side effects. Targeting lncRNAs holds great potential for developing novel therapeutic strategies for neuroinflammatory diseases.

Furthermore, many other studies have revealed the intriguing involvement of lncRNAs in promoting neuroinflammation not only in AD and PD, but also in a range of other neuroinflammatory conditions. These conditions encompass stroke, spinal cord and brain injury, as well as amyotrophic lateral sclerosis (ALS), where the role of lncRNAs has been elucidated. (Tripathi et al., 2021a). However, little is known of the involvement of lncRNAs in driving neuroinflammation in MS, a complex autoimmune inflammatory disease. Investigating the potential role of inflammatory lncRNAs in MS has the potential to advance our understanding of this disease, and could eventually lead to the development of new effective therapies to treat MS.

1.3 Multiple Sclerosis

MS is an acquired paralyzing neurological disease that usually manifests in young adults, and affect approximately 2.5 million people worldwide. It is the most common non-traumatic disabling disease in young people. Moreover, this condition is an autoimmune disease that causes demyelination of neurons in the CNS, which impairs optimal impulse transmission and leads to disability of the patient (Reich et al., 2018; Walton et al., 2020). However, research is in debate whether MS is really an autoimmune disease or rather a degenerative one (Stys et al., 2012). Still, it is widely accepted that neuroinflammation plays a prominent role in this disease.

1.3.1 MS Symptoms and Types

MS is a complex and unpredictable disease that affects various motor, sensory, visual, and autonomic systems over time (Matveeva et al., 2018). Common symptoms include optic neuritis, brainstem and spinal cord syndromes, and other less common manifestations such as cortical symptoms (Reich et al., 2018). Prior to the manifestation of symptoms, patients may be in an asymptomatic, prodromal phase, which will develop into a phase where one

(monosymptomatic) or several (polysymptomatic) symptoms become noticeable. These symptoms may persist for hours to days and stabilize for several weeks before diminishing in severity. However, complete recovery only occurs during the early stages of MS or, in some patients, it may never occur. Notably, the pathological manifestations of MS encompass a diverse array of symptoms and behaviours that evolve over time, leading to the classification of distinct MS subtypes (Frischer et al., 2015; Lublin, 2014).

The most common type of MS is relapsing-remitting MS (RRMS), which is common in 85%–90% of MS patients between the ages of 20 and 40. After each exacerbation, little damage to neurons remains but eventually, neuronal reserve is lost, and recovery after a relapse is no longer possible, leading to secondary progressive MS (SPMS) (Eriksson et al., 2003). A small proportion of patients develop primary progressive MS (PPMS) from the disease onset, which is more severe and lacks partial recovery after each exacerbation (Lassmann et al., 2012).

To diagnose and categorize MS, patients undergo clinical examination, magnetic resonance imaging (MRI) scans, or tests for oligoclonal bands in the cerebrospinal fluid, which are indicative of CNS inflammation (Eshaghi et al., 2021; Kolb et al., 2021). MRI scans can clearly visualize the lesions, although the spatiotemporal explanation for their formation is still lacking (Kolb et al., 2021). Advances in positron emission tomography imaging have enabled the examination of microglial and astrocyte responses linked to MS progression, which helped to unravel their contribution to the disease mechanism (Bodini et al., 2021).

1.3.2 MS Pathophysiology

Although the etiology of MS is not well understood, its pathophysiology has been extensively studied. This involves the breakdown of the blood-brain barrier, multifocal brain inflammation, loss of oligodendrocytes, reactive gliosis, and axonal demyelination and degeneration in both active and inactive lesions, affecting both grey and white matter (Trapp & Nave, 2008). These features are driven by various immune cells and their associated immune and/or inflammatory response. The onset of the disease involves the activation of autoreactive peripheral T-cells, specifically CD4+ Th1 and Th17 cells as stated by the 'outside-in hypothesis'. These cells cross the BBB and begin to secrete pro-inflammatory cytokines, such as IL-17 and interferon (IFN)-γ, upon reactivation by antigen-presenting cells in the CNS. (Figure 3) (Malpass, 2012; Traugott et al., 1983). Active lesions initiate the activation of these cytokines, which in turn stimulate various innate immune cells such as astrocytes and microglia. Consequently, this activation sets off a cascade of events, including an intensified inflammatory response and increased infiltration of immune cells, ultimately creating a cytotoxic environment (Figure 3)(Lucchinetti et al., 2011). Furthermore, the axonal demyelination results from both the antigen-specific CD8+ T cell response as well as the inflammatory conditions characterized by ROS and RNS secretion (Figure 3) (Martin et al., 2000; Traugott et al., 1983). Remarkably, autoreactive T cells can be found in the peripheral blood of both healthy individuals and those with MS. However, in MS patients, these T cells are observed to be in an active state, indicating their involvement in the disease pathogenesis (Martin et al., 2000). Additionally, B cells also play a role in the autoimmune response, and research has shown that alterations in their activity and abundance correlate with disease activity and treatment response (Figure 3)(R. Li et al., 2018). B-cells derived from MS patients secrete more granulocyte-macrophage colony-stimulating factor (GM-CSF) and reduced secretion of IL-10 compared to B-cells of healthy individuals. Specially, the elevated GM-CSF levels from B cells promote the secretion of myeloid cytokines IL-12 and IL-6, which play a role

in directing the development of the T-cell response and contribution to a cytotoxic environment (Lisak et al., 2017). Consequently, a study demonstrated that anti-CD20 treatment results in a long-term benefit that appears to correlate with the absence of memory B-cells and with reduced B-cell secretion of pro-inflammatory cytokines (Florou et al., 2020). Notably, the regulation of these immune cells can be mediated by specific regulatory immune cells, including CD4+ Th2 cells, Tregs, and regulatory B cells (Bregs) (Figure 3). These regulatory immune cells play a crucial role by secreting anti-inflammatory cytokines such as IL-10 and IL-4, which effectively attenuate the inflammatory immune response and initiate the repair process. Consequently, regulatory immune cells play a significant role in RRMS, although their prominence is comparatively diminished in SPMS and PPMS (Ruiz et al., 2019).

The experimental autoimmune encephalomyelitis (EAE) model is widely used to investigate the pathophysiology of MS in rodents due to its similarities in immune mechanisms with the human disease. EAE can be induced in mice by immunization with myelin-specific antigens in an adjuvant or by the adoptive transfer of activated myelin-specific T cells, causing T cell and monocyte infiltration in the brain, CNS inflammation and axon demyelination, comparable to what is seen in human MS. Moreover, the counter-regulatory mechanisms of resolution of inflammation and remyelination also occur in EAE, which, therefore can also serve as a model for these processes (Constantinescu et al., 2011). Still, the model needs to be appointed to the scientific question being asked due to also the clear differences between this model and humane MS.

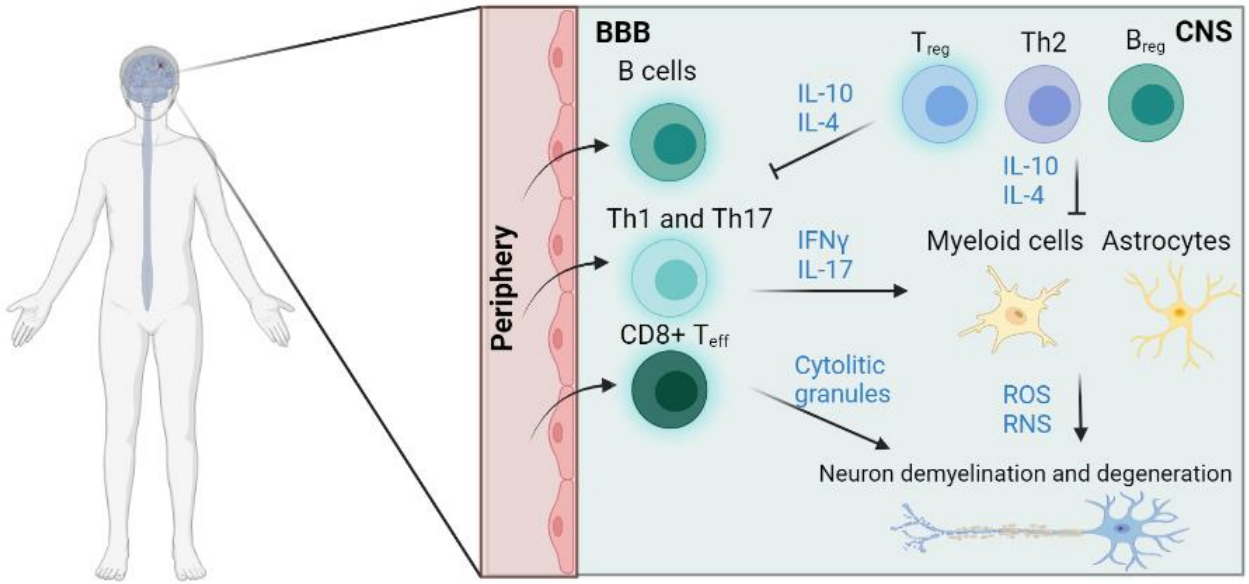

Figure 3. Multiple Sclerosis pathophysiology. Peripheral autoreactive T cells (CD4+ Th1 and Th17) cross the blood-brain barrier (BBB) and enter into the central nervous system (CNS), where they secrete cytokines such as IFNγ and IL-17 to activate innate immune cells. Microglia and astrocytes start producing inflammatory cytokines and reactive oxygen and nitrogen species (ROS and RNS). The myelin targeting of the CD8+ T cells and the cytotoxic inflammatory environment cause neuron demyelination and neurodegeneration. T and B regulatory cells, including Treg, Th2 and Bregs, can suppress the inflammation and induce repair, primarily through the secretion of IL-4 and IL-10. Figure created with BioRender.

1.3.3 MS Prevalence, Incidence and Risk Factors

The incidence of MS is increasing worldwide, along with its socioeconomic consequences. Since 2013, the prevalence of MS has risen by 30% (Walton et al., 2020). While improved reporting and diagnosis may have contributed to this increase, much of its underlying factors remain unknown. MS exhibits a higher prevalence in North America and Europe, while being less prevalent in sub-Saharan Africa and East Asia. This geographical distribution strongly suggests that genetic susceptibility and environmental factors contribute significantly to the etiology of MS (Matveeva et al., 2018; Walton et al., 2020).

Evidence pointing towards the influence of environmental factors on MS was initially observed in a study investigating the impact of latitude and migration (Sabel et al., 2021). This study revealed a distinct latitudinal gradient in MS, whereby the prevalence of the disease increases as one moves farther away from the equator. Moreover, migration studies have demonstrated that individuals who relocate from a high-risk country to a low-risk country before reaching adolescence have a reduced risk of developing MS. Conversely, those who migrate from a low-risk country to a high-risk country exhibit a heightened risk of the disease. These findings strongly suggest that environmental factors play a significant role in the development and incidence of MS (Ostkamp & Schwab, 2022). Indeed, these results led to the hypothesis of a protective effect of sun exposure and ultraviolet (UV) radiation (Vitkova et al., 2022). Consequently, they showed that elevated vitamin D levels, especially before the age of 20, are associated with a reduced risk of MS later in life. In addition, UV radiation also protects against MS, probably through its effects on vitamin D and through independent effects on the immune system (Scazzone et al., 2021) Vitamin D has broad effects on the immune system, including suppression of proliferation of both B and T-cells, down-regulation of inflammatory T cell responses, and promotion of Treg responses and of tolerogenic monocyte and dendritic cell phenotypes, mechanisms all in favour of supressing the auto-inflammatory reaction of MS (Lemke et al. 2021).

Next, cigarette smoking is a known risk factor for MS (Wingerchuk, 2012), while oral tobacco use, cytomegalovirus infection, alcohol and coffee consumption are associated with reduced risk. Smoking appears to exert its effect by stimulating Th17-type responses in the lung, increasing inflammatory responses (Olsson et al., 2017).

Numerous studies have established a significant association between infectious agents, particularly the Epstein-Barr virus (EBV), and MS. The higher prevalence of EBV infection among individuals with MS compared to control groups supports this link. However, the precise mechanism by which EBV may contribute to the development of MS remains unclear, although several hypotheses have been proposed (Bjornevik et al., 2022). One potential explanation involves that EBV could have a specific effect via a mechanism of molecular mimicry. Moreover, a general immune effect of EBV on B cells or other immune regulatory

elements has been proposed. This was based on its effects seen in other autoimmune diseases such as systemic lupus erythematosus (Harley & James, 2006).

Finally, as in many other studies, also a role for the microbiome in MS pathology has been proposed. Recent studies have shown that the gut microbiome participates in immunoregulatory pathways that can both contribute to and protect against disease. Remarkably, in a spontaneous relapsing-remitting EAE model in mice, animals raised under germ-free conditions were shown to be resistant to the disease, while those exposed to commensal bacteria developed EAE (Berer et al., 2017; Cekanaviciute et al., 2017). Moreover, studies examining the gut microbiome of MS patients found that the bacterial species *Methanobrevibacter* and *Akkermansia* were increased, and the bacterium *Butyricimonas* were decreased, in MS patients compared to control subjects (Cekanaviciute et al., 2017).

However, all of these environmental influences also depend on genetic and epigenetic backgrounds (Olsson et al., 2017). For example, the human leukocyte antigen (HLA)-DRB1*15:01 allele in the class II major histocompatibility complex (MHC) most prominent risk factor identified for MS (Baranzini & Oksenberg, 2017). In addition, also the interleukin-2 receptor alpha and the interleukin-7 receptor alpha genes were identified as heritable risk factors. These genes are major immune mediators and consequently specific single nucleotide polymorphisms (SNPs) in these genes could make people more prone to develop an (auto)immune response (International Multiple Sclerosis Genetics Consortium, 2019).

1.3.4 Current Treatments for MS

MS is a complex disease with various subtypes and stages that involve multiple genetic, environmental, and immunological factors (Olsson et al., 2017). Although current therapies have demonstrated some success in treating specific types of MS, they frequently carry notable side effects and do not work for all patients. Additionally, progressive MS continues to present a significant challenge, emphasizing the necessity for improved comprehension of the molecular mechanisms involved in this subtype. Such understanding will aid in the development of more effective treatments (Dangond et al., 2021).

Treatments for MS usually consist of immunosuppressive drugs that target the inflammatory and relapsing stages of MS. Specifically, they target reactions to reduce Th1/Th17 cell reactivity, induce T-reg cells and affect cell transport to the nervous system (Tramacere et al., 2015). The first line of treatment was represented by type 1 IFNs, which are natural antiviral molecules produced with immunoregulatory properties (Comi, 2009). Now, natalizumab serves as an excellent example of an effective treatment for MS. It is an anti-α4 integrin monoclonal antibody that effectively reduces inflammation in the CNS by blocking lymphocyte migration via the BBB (Polman et al., 2006). Yet, the use of this medicine has to be weighed against side-effects such as fatal progressive multifocal leukoencephalopathy. Another notable drug for MS treatment is ocrelizumab, which specifically targets B cells. Interestingly, this monoclonal antibody therapy has also demonstrated efficacy in patients with progressive forms of MS (Hauser et al., 2017). Unfortunately, there have also been immunomodulatory treatments that turned out to exacerbate MS, such as anti-TNF therapy, which was shown to be effective for the treatment of RA (Caminero et al., 2011). Slightly further at the horizon are the future cellular therapies. The only such treatment that has entered clinical practice, albeit not in large controlled studies, is haematopoietic stem cell transplantation. This therapy

thought to represent a drastic form of immunosuppression, which may reset an autoimmune-prone immune system, and has theoretical potential for neurorepair (Muraro & Uccelli, 2010).

Emerging research has emphasized the significance of targeting innate immune cells, including microglia and CNS macrophages, which play a pivotal role in driving chronic inflammation in progressive MS. An intriguing therapeutic approach involves the nasal administration of anti-CD3, which has demonstrated the ability to stimulate the generation of IL-10-secreting Tregs. These Tregs can migrate to the CNS and effectively mitigate the inflammatory responses of microglia and astrocytes, potentially leading to a slowdown in disease progression (Mayo et al., 2016). This line of investigation suggests the importance of identifying novel molecular targets that can be leveraged to develop more effective therapies for progressive MS. Ongoing research in this targeting the innate immune cells such as myeloid cells, holds promise for uncovering new strategies and therapeutic avenues to better manage the disease.

1.3.5 Myeloid Cells in MS

Indeed, studies of MS and EAE reveal highly dynamic communication between CNS-resident cells including microglia, astrocytes, oligodendrocytes, and neurons, as well as CNS-recruited peripheral immune cells, such as T cells and macrophages/monocytes. While myeloid cells are considered the primary drivers of inflammation and immune reactions during MS and EAE, studies have also suggested their involvement in initiating the repair process through mechanisms such as phagocytosis of myelin debris and induction of remyelination (Bogie et al., 2014). It is unclear, however, which response prevails at any particular time in MS, but myeloid cells may possess both properties at the same time, with a greater tendency towards pro-inflammatory responses (Ransohoff, 2016a). The balance and interplay between these responses are complex and may contribute to the diverse clinical manifestations and disease course observed in MS.

Microglia exhibit interesting aspects over time and space during MS and EAE. Focal lesions of active demyelination and neurodegeneration are characterized by inflammation and microgliosis. However, microglial activation is not restricted to these lesion areas only (Zrzavy et al., 2017). The normal-appearing white matter of MS patients also shows pronounced microglial activation compared to healthy individuals. In addition, clusters of activated microglia, called 'microglial nodules,' can be observed in the white matter of MS patients near plaques, and are associated with degenerating axons, stressed oligodendrocytes, or deposits of activated complement pathway products (Ramaglia et al., 2012; Singh et al., 2013). These nodules are considered 'pre-active lesions' and are characterized by a lack of macrophage infiltration and demyelination. Over time, these sites may develop into active demyelinating MS lesions (Singh et al., 2013). A particular microglia population, TMEM119-positive microglia, governs the edge of active lesions and acquires a phagocytic phenotype, suggesting that microglia play an important role in the initial and early stages of tissue damage in MS patients. However, as lesions mature, the proportion of TMEM119-negative macrophages recruited from the periphery increases (Zrzavy et al., 2017).

Both these microglia and recruited macrophages predominantly display a pro-inflammatory phenotype in these early active lesions, expressing molecules involved in inflammation, phagocytosis, oxidative injury, antigen presentation, T cell stimulation, and iron metabolism. Indeed, pro-inflammatory cytokines such as TNF, IFNγ, IL-1β, IL-6, and ROS, which are produced by infiltrating T-cells and various cell types, have the capability to activate microglia

cells. This activation triggers an amplified release of pro-inflammatory cytokines, exacerbating the symptoms of EAE (Merson et al., 2010a). Additionally, myeloid cells and DCs participate in antigen-spreading and presentation, which contributes to MS progression and chronic inflammation (Neumann et al., 2009). However, myeloid cells also play a critical role in removing myelin debris, which is essential for inflammation resolution and tissue repair. Alternatively activated microglia have been found to drive oligodendrocyte differentiation through the TGFβ-dependent signalling pathway, promoting remyelination (Butovsky et al., 2014). Additionally, IFNβ, secreted by microglia, plays also a significant role in myelin phagocytosis. As a result, exogenous IFNβ administration has shown protective effects in EAE by modulating microglia and is used as a treatment for MS (Pennell & Fish, 2017).

While microglia play a crucial role in the pathogenesis of EAE and MS, it has been observed that the early immune response is predominantly driven by infiltrated monocytes and macrophages. However, microglia are responsible for the recruitment of these myeloid cells (Brosnan, Bornstein, and Bloom, 1981). The inflammatory phenotype of these myeloid cells primarily manifests during the active stage of the disease, while later on in the chronic progressive phase of the disease the microglial activity will prevail. Interestingly, the pro-inflammatory polarization of the infiltrating myeloid cells is only induced after CNS entry, while very few microglia adopt this phenotype at this stage (Vainchtein et al., 2014). During later disease stages, these myeloid cells return to an expression profile more similar to circulating macrophages and monocytes. Overall, CNS-infiltrating monocyte-derived cells do not acquire the typical microglia-specific transcriptional signature and reveil a different activation course (Ajami et al., 2011; Yamasaki et al., 2014).

Interesting, studies have also shown that infiltrating monocytes and macrophages are the principal mediators for remyelination and neuroprotection. In a neurotropic JHM coronavirus-induced demyelination mouse model, these cells exhibited a mixed phenotype with both pro- and anti-inflammatory characteristics, similar to the microglia DAM phenotype as mentioned earlier and consequently were important in the resolution of inflammation (Savarin et al., 2018). In addition, another study showed that lenalidomide, an anti-cancer molecule, could promote macrophage M2 polarization and suppress pro-inflammatory Th1 and Th17 cells to prevent the progression of EAE. However, lenalidomide showed no effect in macrophage-depleted EAE mice, suggesting that these macrophages are one of the most important mediators in inducing a repair response (Weng et al., 2018).

In conclusion, the myeloid cells have a complex but interesting role in the initiation and duration of MS. Better understanding of this cell population and their molecular regulation is crucial to understand all the aspects of the disease.

1.3.6 Regulation of Neuroinflammation in MS and EAE

Understanding the intricate molecular regulation of neuroinflammation is of utmost importance in the quest to develop effective therapies for treating MS and other neuroinflammatory diseases. Remarkable progress has already been made through extensive research on MS and its widely utilized mouse model, EAE, leading to valuable insights into the underlying mechanisms that drive and govern neuroinflammation. These significant discoveries hold great promise for the advancement of therapeutic interventions and strategies aimed at tackling these debilitating conditions.

Activation of NF-κB in peripheral immune cells is crucial for inducing EAE pathology. Moreover, its inhibition in the CNS can be protective in EAE by preventing the expression of pro-inflammatory mediators (Hilliard et al., 1999). Additionally, inhibiting upstream mediators of NF-κB activation has also been shown to provide protection in EAE (van Loo et al., 2006). Studies have also shown the importance of inflammasome activation in MS and EAE. Elevated levels of caspase-1, IL-18, and IL-1β are seen in PBMCs and CSF of MS patients and EAE mice due to hyperactivation of NLRP3, leading to increased IL-1β secretion and CNS inflammation (Inoue & Shinohara, 2013). Furthermore, the anti-inflammatory protein A20 negatively regulates NF-κB activation, and its deletion in microglia and CNS macrophages exacerbates EAE in mice due to NLRP3 hyperactivation (Voet et al., 2018). CNS-intrinsic inflammasome activation in MS and EAE has been reported in a study showing caspase-1- and GSDMD-mediated pyroptosis in microglia and myelin-forming oligodendrocytes in the CNS of MS patients and in EAE mice. While TNF has both pro-inflammatory and protective functions, microglial TNF is dispensable for EAE (Wolf et al., 2017). However, a recent study has identified TNFR2 signalling in microglia as an important neuroprotective signal in EAE, as ablation of microglial TNFR2 leads to earlier disease onset, increased demyelination, and leukocyte infiltration (Gao et al., 2017).

Interference in inflammation signalling as described here, proves potential in developing therapies. However this interference on protein levels causes a range of side effects as most of the mediators have multiple functions. On the other hand, lncRNAs have cell and context specific regulation mechanisms, which holds potential in the development of better therapy strategies by reducing side effects.

1.3.7 Inflammatory lncRNAs in MS and EAE

Regrettably, our understanding of the role of lncRNAs in MS and EAE neuroinflammation is limited. While there has been a surge in articles exploring lncRNAs in MS over the past two years, most of these studies have primarily focused on their potential as biomarkers (Akbari et al., 2022; Nociti & Santoro, 2021). Furthermore, the mechanisms of the identified lncRNAs primarily relate to the initiation of T-cell responses, as the scientific community has primarily been interested in the disease onset (Sabaie et al., 2021). Consequently, few studies have delved into the role of lncRNAs in mediating chronic inflammation.

So far, only three studies have highlighted the significance of lncRNAs in myeloid neuroinflammation during EAE. One study demonstrated decreased expression of *Malat1* in the spinal cords of EAE mice, as well as in stimulated splenocytes and primary macrophages. Interestingly, downregulation of *Malat1* using specific siRNAs enhanced the polarization of macrophages toward the pro-inflammatory phenotype (Masoumi et al., 2019). Next, *Linc-Cox2*, located 51 kb upstream of the protein-coding gene *Cox2*, was shown to be implicated in EAE-associated inflammation. *Linc-Cox2* can bind NF-κB subunit p65 and promote its nuclear translocation and transcriptional activity, modulating the expression of the inflammasome sensor NLRP3 and the inflammasome adaptor protein ASC. Knockdown of *linc-Cox2* was shown to inhibit inflammasome activation and prevent the *linc-Cox2*-triggered caspase-1 activation, leading to decreased IL-1β secretion. Interestingly, *linc-Cox2* regulates microglia quiescence in the CNS and during EAE as well as in BMDMs. Hence, *linc-Cox2* knockdown using AAV containing targeting siRNAs, significantly improved the clinical outcome of EAE development by targeting macrophages and microglia (Xue et al., 2019). Another study highlighted the importance of the lncRNAs *Gas5* in myeloid neuroinflammation in EAE, which

is additionally upregulated in microglia of MS patients. Furthermore, *Gas5* was shown to have transcriptional repressive activity on IRF4, peroxisome proliferator-activated receptor γ (PPAR γ) , and STAT6 through binding and recruitment of the PRC2 to their promoter. Interference with *Gas5* in transplanted microglia reduces EAE progression and promotes remyelination in a lysolecithin-induced demyelination model (Sun et al., 2017).

Even though the above studies have shown a potential role for these lncRNAs in EAE and MS it is just the tip of the iceberg as there are more than 100.000 lncRNAs. More studies are needed to understand the role and mechanisms of other lncRNAs in MS and EAE. As targeting of lncRNAs behold potential to reduce neuroinflammation. Investigation in this direction could lead to the development of effective therapies for all types of MS.

Part 2: Aim of Research Project

LncRNAs have emerged as key regulators of cellular processes, yet their role in neuroinflammation, specifically in Multiple Sclerosis (MS), remains relatively understudied compared to other neuroinflammatory pathologies such as Alzheimer's and Parkinson's disease. In order to fill this knowledge gap, further investigation into the involvement of lncRNAs in MS is needed.

Consequently, the main objective of this M.Sc. thesis was to identify and characterize specific lncRNAs that regulate inflammation in the mouse model of MS, experimental autoimmune encephalomyelitis (EAE). By comprehensively examining the landscape of lncRNAs involved in neuroinflammation and their functional significance in the context of MS, this research aimed to shed light on the molecular mechanisms underlying the disease and aid in the development of innovative therapeutic approaches.

2.1 Unbiased Bioinformatics Screening for LncRNAs That Regulate Neuroinflammation and EAE

We started the investigation by conducting an *in silico* bioinformatic analysis on a previously generated dataset in the host lab to gain early insights into the lncRNAs involved in the regulation of general neuroinflammation. We analysed bulk RNA sequencing dataset of microglia isolated from $A20^{Cx3cr1\text{-}KO}$ and control littermate mice non-stimulated or LPS stimulated. Our aim was here to 'mine' for lncRNAs that have previously been identified in literature for their role in (neuro)inflammation.

Next we aimed to investigate lncRNAs in regulating neuroinflammation in the context of EAE. To address this, we have, in collaboration with the OncoRNALab of Prof. Pieter Mestdagh (UGent), performed an unbiased screening for expression of lncRNAs in the spinal cord of non-immunized control mice and EAE mice though total RNA-sequencing. Using the same bioinformatic analyses as before, we aimed to identify lncRNAs that regulate key mediators of inflammation signalling.

These analyses provide us with a preliminary understanding of the lncRNAs that potentially regulate neuroinflammation, particularly in microglia, as well as their roles in the context of EAE. LncRNAs identified through these analyses were selected for further characterization in both *in vivo* studies using EAE-associated neuroinflammation models and *in vitro* experiments using myeloid cells subjected to inflammatory stimuli.

2.2 Characterization of Selected LncRNAs *in vivo*

We further investigated the role of the selected lncRNAs in neuroinflammation and EAE pathology using mice with different genetic backgrounds and immune responses. Our approach involved analysing the expression levels with RT-qPCR of these lncRNAs in specific knockout mouse models which are 'hypersensitive' to EAE: microglia-specific A20 and OTULIN knockout mice ($A20^{Cx3cr1\text{-}KO}$ and $OTULIN^{Cx3cr1\text{-}KO}$, respectively) and control littermate mice. Secondly, we examined the selected lncRNAs in mice that are deficient in Protein Geranyl geranyl transferase Type I Subunit Beta (PGGTB1) specifically in T-cells ($Pggtb1^{CD4\text{-}KO}$), which are highly resistant to EAE (unpublished data van Loo group). By conducting comparative analyses of the expression levels of specific lncRNAs in non-immunized and immunized

knockout and wild-type mice, our objective was to gain further insights into the involvement of these lncRNAs in EAE-associated neuroinflammation.

2.3 Characterization of Selected LncRNAs *in vitro*

Lastly, we aimed to better understand the expression profiles of selected lncRNAs in various aspects of myeloid cell inflammation. By this, we wanted to gain insights in the influence of inflammation signalling pathways on the expression profiles of the lncRNAs and compare these with the observed results from the *in vivo* experiments.

We isolated bone marrow-derived macrophages (BMDMs) from wild-type and myeloid-specific A20 knockout ($A20^{Myel\text{-}KO}$) mice. The latter group shows increased inflammation and proves to be a good model to correlate inflammation with the expression of the lncRNAs (Vande Walle et al., 2014). We aimed to study lncRNA expression in the context of NF-κB signalling and inflammasome activation to monitor their role in an acute inflammatory context. In addition, we wanted to examine their expression after IL-4 stimulation of BMDMs to monitor their role in the context of inflammation resolution and repair. These experiments may demonstrate how different lncRNAs are regulated under different inflammatory conditions.

Finally, in order to know the significance of lncRNAs in mediating inflammation in BMDMs, we aimed to silence specific lncRNAs through the use of antisense oligonucleotides, and assess the impact of such 'knockdown' on the inflammatory cell response after stimulation with the above mentioned stimuli.

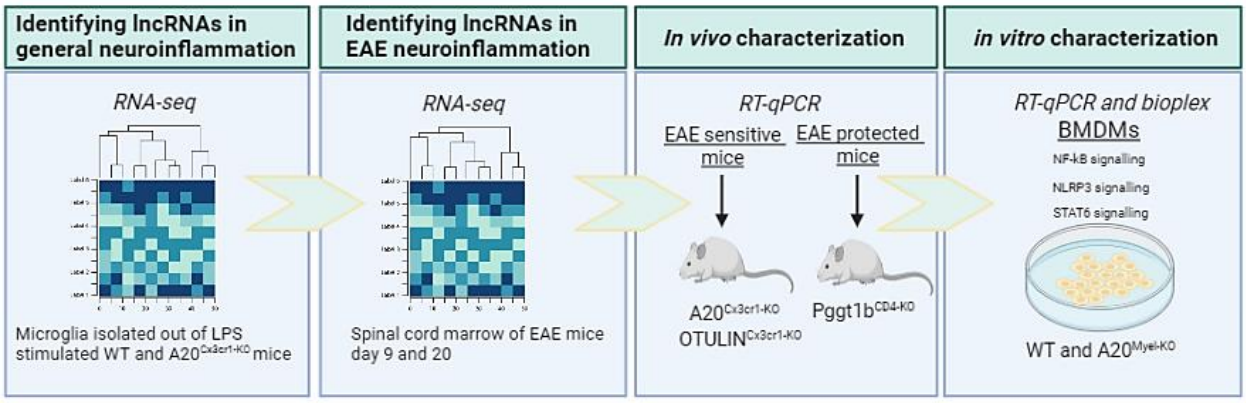

Figure 4. Experimental set-up and aims of the master thesis project. We first aimed to identify long non-coding (lnc)RNAs during general neuroinflammation by analysis of an RNA sequencing dataset of isolated microglia from $A20^{Cx3cr1\text{-}KO}$ and wild-type (WT) mice either or not stimulated with LPS. Next we wanted to identify lncRNAs that are differentially expressed in the spinal cord of mice subjected to experimental autoimmune encephalomyelitis (EAE) at two timepoints (day 9 and 20) post-immunisation, through total RNA sequencing. To further validate their contribution to EAE neuroinflammation we wanted next to characterize a selected number of lncRNAs *in vivo* utilizing EAE-sensitive mice ($A20^{Cx3cr1\text{-}KO}$ and $OTULIN^{Cx3cr1\text{-}KO}$) as well as EAE-protected ($Pggt1b^{Cx3cr1\text{-}KO}$) mice. Finally, we aimed to investigate their expression in inflammatory conditions *in vitro* in bone marrow-derived macrophages (BMDMs).

Part 3: Results

3.1 Identification of lncRNAs During Neuroinflammation and EAE Pathology

Numerous studies have highlighted the importance of lncRNAs in regulating neuroinflammation, particularly in neurodegenerative conditions such as in Alzheimer's disease and Parkinson's disease (Wan et al., 2017). However, the role of lncRNAs has been poorly studied in Multiple Sclerosis (MS), the most prevalent neuroinflammatory disease. Therefore, our study aimed to first identify lncRNAs in both general neuroinflammation and in an mouse model of MS, EAE.

3.1.1 In silico Analysis of Microglia from Untreated and LPS-Treated Wild-type and A20$^{Cx3cr1\text{-}KO}$ mice

The investigation into the underlying mechanisms of neuroinflammation offers valuable insights into the pathophysiology of both neuroinflammatory and neurodegenerative diseases. Although the involvement of lncRNAs has been explored to some extent in microglial neuroinflammation induced by lipopolysaccharide (LPS), a comprehensive understanding of their expression patterns during heightened systemic LPS-induced neuroinflammation is missing (Baek et al., 2022; Tripathi et al., 2021a). We analysed the RNA-sequencing expression profiles of sorted CD45^{int}CD11b^{+} microglia from a previous study conducted by the host laboratory (Voet et al., 2018). The microglia were isolated from the brains of CNS myeloid-specific A20 knockout (A20$^{Cx3Cr1\text{-}KO}$, A20 KO) mice and wild-type control littermates (WT), either or not injected intraperitoneally with a sublethal dose of LPS (3.5 mg/kg body weight). The earlier study demonstrated that A20 KO microglia display a hyperinflammatory phenotype, suggesting a crucial role for A20 in the control of microglia activation under steady-state conditions. Moreover, microglia from LPS-stimulated A20 KO mice exhibit a more pronounced inflammatory signature compared to those from LPS-stimulated control mice (Voet et al., 2018). Thus, exposure to LPS is an appropriate model for investigating general neuroinflammation and identifying lncRNAs involved in this process. Moreover, the hyperactivated microglia phenotype from unchallenged and LPS-stimulated A20 KO mice provides an excellent model for correlating and validating the identified lncRNAs in a context of exacerbated neuroinflammation.

As the prior RNA-sequencing expression analysis, as presented previously, did not yield annotations for lncRNAs, we adopted a manual approach to identify them in the sequencing data. We employed the Integrative Genome Viewer (IGV) tool to obtain expression counts of the target genes by detecting sequenced fragments at their specific genomic locations. Subsequently, we conducted differential expression analysis on these manually retrieved counts utilizing appropriate bioinformatic techniques

First, we validated the previous findings of the study by reanalysing the expression of specific inflammatory mediators in microglia from unchallenged and LPS-challenged WT control and A20 KO mice. To do so, we selected a group of well-established inflammation markers and used the above manual approach to analyse these (Figure 5). Our results confirmed an upregulation of cytokines *Tnf, Il6, Il1β, Il12b, Il1α* and chemokine *Cxcl10* as well as the NF-κB subunit *Relb* in the LPS-stimulated groups, with notably higher expression levels in A20 KO

mice (Figure 5). From this, we concluded that neuroinflammation is induced upon LPS stimulation, and is more pronounced in microglia of A20 KO mice, as previously demonstrated (Voet et al., 2018).

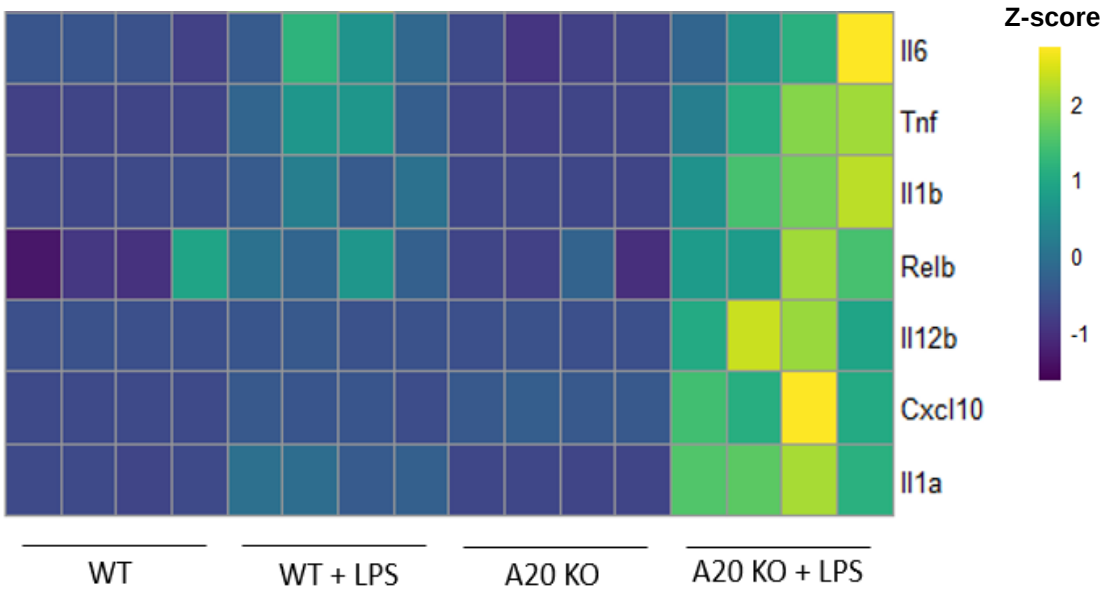

Figure 5. Relative gene expression levels of inflammatory markers in FACS-sorted microglia isolated from wild-type (WT) and A20$^{Cx3cr1\text{-}KO}$ (A20 KO) mice, with or without exposure to LPS. Each row presents normalized expression counts of inflammation markers retrieved from bulk RNA sequencing of CD45^{int}CD11b^{+} isolated microglia from WT and A20 KO mice either or not intraperitoneally injected with a sublethal dose of lipopolysaccharide (LPS). Each column represents expression levels in microglia from one individual mouse, n = 4 per group. Color code presents linear scale.

To investigate the expression of specific lncRNAs in this dataset, we first curated a list of 115 lncRNAs that were previously reported to be involved in inflammatory signalling, out of which 62 were relevant to mice. Employing the same methodology as mentioned above, we identified 11 sequenced lncRNAs from this list in our dataset, namely *Hoxa11-as, Oser-as1, Mirt2, Zfas1, Gm28309, Cdkn2b-as1, Miat, Snhg5, Snhg4, Neat1,* and *Malat1*. We performed a differential expression analysis on these and subsequently generated a heatmap to present the normalized expression patterns of these lncRNAs across the various experimental groups in individual mice, providing a general overview of their expression profiles (Figure 6). Due to the context-specific expression profiles of these lncRNAs, we had no prior expectations. We noted the downregulation of *Miat, Snhg5, Snhg4, Neat1*, and *Malat1* in both LPS-stimulated groups, with a more pronounced decrease observed in the A20 KO group (Figure 6). Furthermore, *Zfas1, Gm28309*, and *Cdkn2b-as1* exhibit a similar pattern of downregulation in the LPS-stimulated A20 KO group (Figure 6). In contrast, *Hoxa11-as*, *Oser-as1*, and *Mirt2* did not display major differences in expression across the different experimental groups (Figure 6).

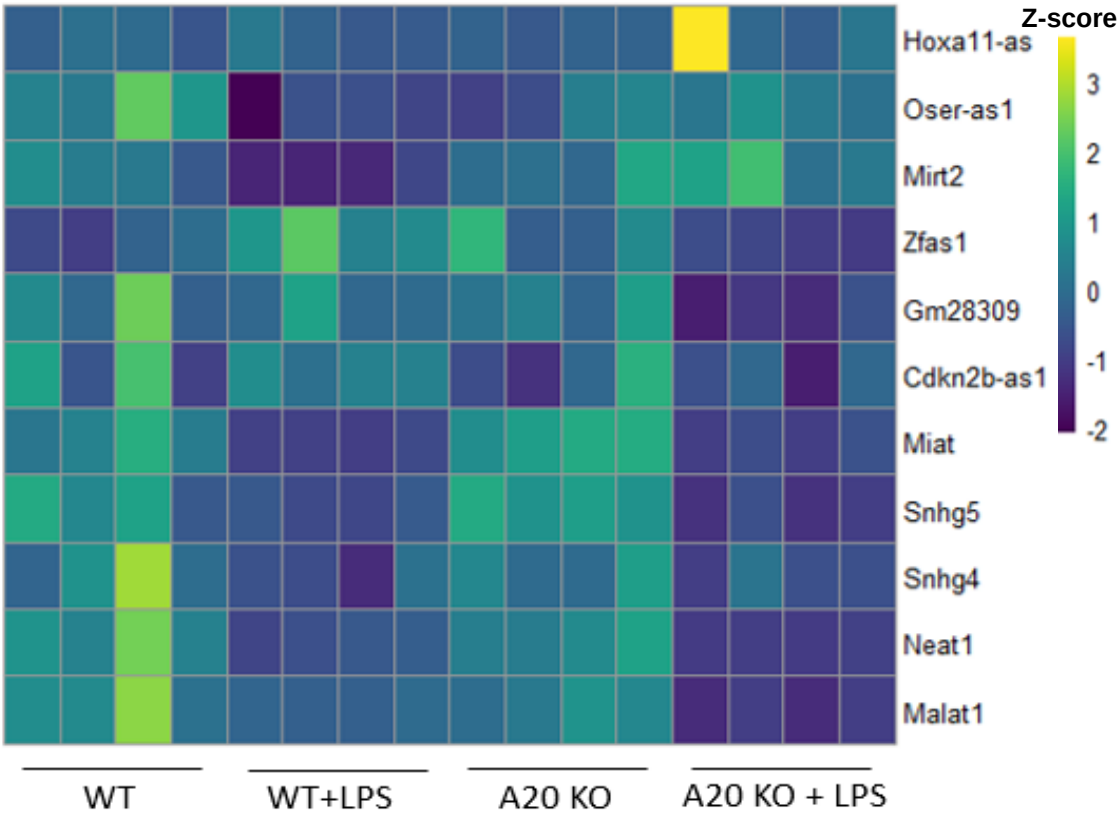

Figure 6. Relative gene expression levels of inflammation-related lncRNAs in FACS-sorted microglia from wild-type (WT) and A20$^{Cx3cr1\text{-}KO}$ (A20 KO) mice, with or without exposure to LPS. Each row presents normalized expression counts of identified inflammation-related long non-coding (lnc)RNAs retrieved from bulk RNA sequencing of CD45^{int}CD11b^{+} isolated microglia from WT and A20 KO mice either or not intraperitoneally injected with a sublethal dose of lipopolysaccharide (LPS). Each column represents microglia from one individual mouse, n = 4 per group. Color code presents linear scale.

To obtain a more accurate and statistically robust assessment of the expression of these lncRNAs, we conducted a one-way ANOVA test with Tukey correction for multiple comparison test for each lncRNA as the data are not normally distributed and do not have equal variance (Figure 7). In agreement with the heatmap shown above, we observed significant downregulation of *Malat1, Neat1*, *Miat, Snhg4, Snhg5,* and *Oser-as1,* in both LPS-stimulated groups compared to the non-stimulated groups (Figure 7a-f). Interesting, these lncRNAs showed a slight trend of further downregulation in the LPS-stimulated A20 KO group together with *Cdkn2b-as1 and Zfas1,* which had significant results. Furthermore, we observed significant downregulation of *Malat1, Neat1, Snhg5* and *Snhg4* in the unstimulated A20 KO group compared to the WT group (Figure 7a-d). We observed similar expression profiles for *Mirt2, Gm28309* and *Cdkn2b-as1*, but not for *Zfas1* that only showed significant downregulation in the LPS-stimulated A20 KO group (Figure 7g-j). Finally, no significant differences were observed in the expression of *Hoxa11-as* between the different experimental groups (Figure 7k).

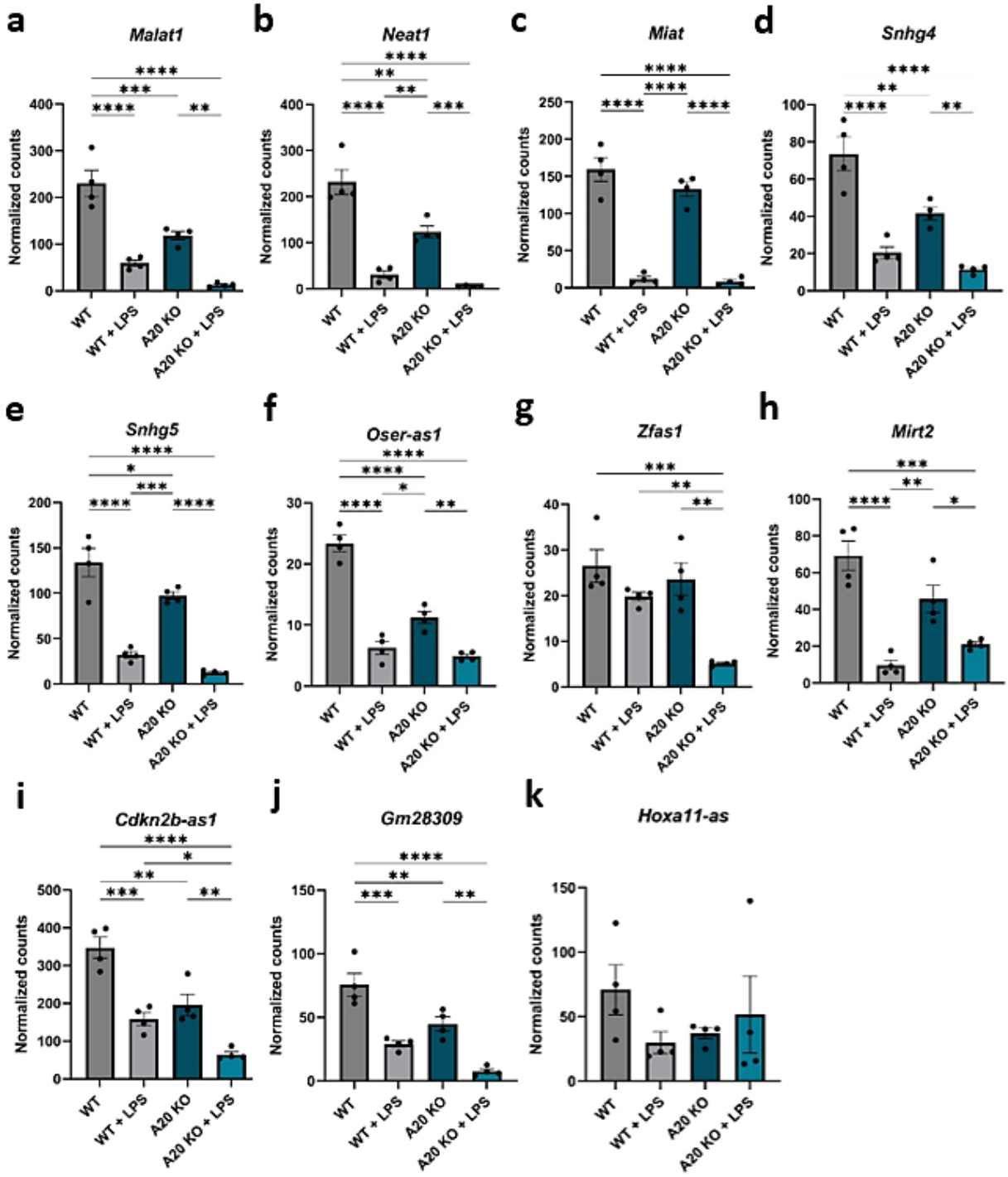

Figure 7. Relative gene expression levels of inflammation-related lncRNAs in FACS sorted microglia from wild-type (WT) or A20$^{Cx3cr1\text{-}KO}$ (A20 KO) mice, with or without exposure to LPS. The y-axis represents the normalized expression counts of identified inflammation-related long non-coding (lnc)RNAs from bulk RNA sequencing of CD45^{int}CD11b^{+} isolated microglia from WT and A20 KO mice either or not intraperitoneally injected with a sublethal dose of lipopolysaccharide (LPS), n = 4 per group. Statistical significance was determined using a one-way ANOVA test with Tukey correction for multiple comparison(*p < 0.05, **p < 0.01, ***p < 0.001, ****p < 0.0001). Results are displayed as mean ± SEM.

In conclusion, this *in silico* analysis, of a previously published dataset, confirmed the presence of hyperactivated microglia in A20$^{Cx3cr1\text{-}KO}$ mice compared to microglia from control littermate mice. We identified several lncRNAs (*Malat1, Neat1, Miat, Snhg5, Snhg4, Zfas1*, *Gm28309* and

Cdkn2b-as1) which showed differential expression in this dataset. Furthermore we observed significant downregulation of *Malat1, Neat1, Miat, Snhg5* and *Snhg4* in microglia from LPS-stimulated mice, and more pronounced decreases in the A20 KO condition. These observations suggest a correlation with increased inflammation.

3.1.2 Identification of LncRNAs in the Regulation of EAE Neuroinflammation

Since little is known of lncRNAs involved in EAE neuroinflammation, we conducted an unbiased RNA sequencing analysis to comprehensively identify lncRNAs involved in the regulation of neuroinflammation within the context of MS and EAE pathology. Our analysis focused on the dynamic expression of lncRNAs in the spinal cord of both control mice and EAE mice, as inflammatory lesions are highly present there. By examining the entire transcriptome, our aim was to uncover lncRNAs that exhibit significant changes in expression during EAE and might play a role in regulating neuroinflammation. Furthermore, we sought to compare these identified lncRNAs with the results of our previous *in silico* analysis.

We immunized eight male wild-type C57BL/6J mice with myelin oligodendrocyte glycoprotein (MOG_{35-55}) peptide and disease progression was monitored by assessing clinical disease symptoms and body weight. All immunized mice developed EAE, whereas the non-immunized control group remained free from clinical pathology (Figure 8). We collected spinal cord tissue from four mice on day 9, when mice had an average clinical score of one, and from four mice on day 20, when mice had an average clinical score of 4 (Figure 8a). These two timepoints reflect an early and a peak disease response, respectively. We also isolated spinal cord tissue from the four non-immunized control mice on day 20. RNA was isolated from all spinal cord samples and both the polyadenylated and non-polyadenylated RNAs were subjected to quantitative total RNA sequencing, performed by the UGent Next Generation Sequencing (NXTGNT) core facility with the help of the lab of prof. Pieter Mestdagh.

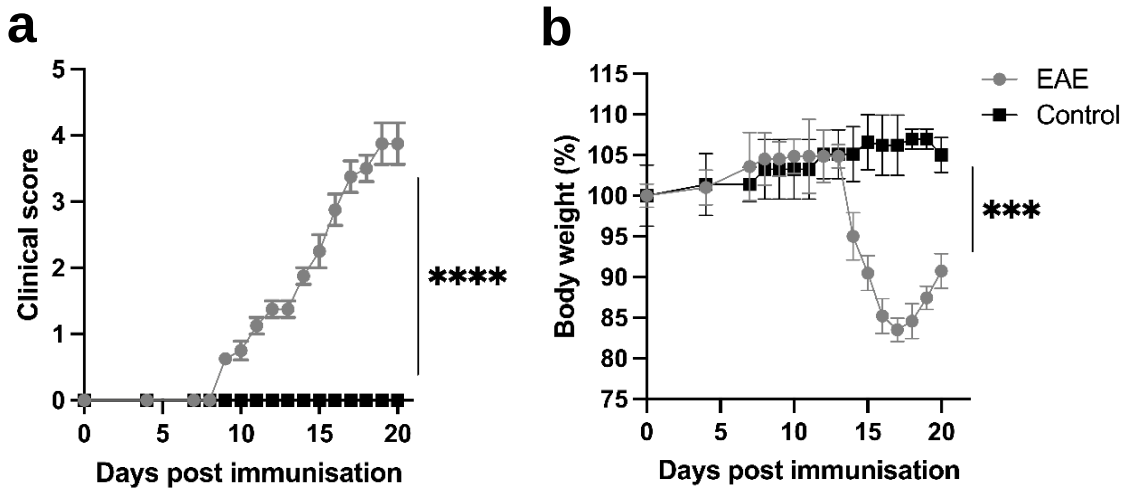

Figure 8. Experimental autoimmune encephalomyelitis (EAE) disease progression. EAE was induced by active immunization of C57BL/6J mice (EAE, n = 8) with myelin oligodendrocyte glycoprotein (MOG_{35-55}) peptide, and clinical score **(a)** and body weight **(b)** was followed over time. Non-immunized C57BL/6J control mice (Control, n = 4) were included in the study. Changes in clinical score and relative body weight differ significantly between groups across the time span, analysed with F-test on repeated measurements (**p < 0.01, ****p < 0.0001).Each data point represents the mean ± SEM as estimated by the REML analysis.

After processing the RNA sequencing data, we found minor changes in gene expression between the EAE group on day 9 and the control group, with 199 genes significantly

upregulated and only 1 gene significantly downregulated. However, on day 20, a significant increase in gene expression could be observed between the EAE group and the control group, with 5837 genes significantly upregulated and 5045 genes significantly downregulated in the EAE mice. These findings were supported by principal component analysis (PCA), which showed low variance between EAE day 9 mice and the control group, but high variance on PC1 in EAE day 20 mice compared to the control group, accounting for 97 % of the variance. One EAE day 20 sample exhibited little variance on PC2 compared to the other samples at day 20, possibly reflecting biological variance between the samples (Figure 9).

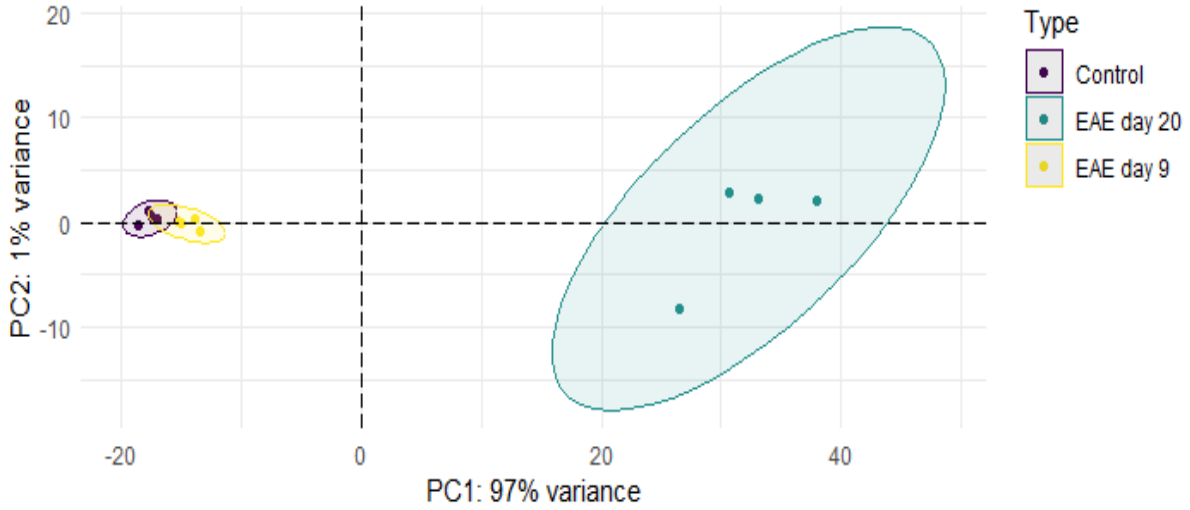

Figure 9. Principal component analysis (PCA) on gene expression data from experimental autoimmune encephalomyelitis (EAE) mice 9 and 20 days post-immunisation, as well as non-immunized control mice. RNA isolated from spinal cord tissue of non-immunised control (n = 4) mice and myelin oligodendrocyte glycoprotein (MOG_{35-55}) immunised EAE mice at day 9 (n = 4) and day 20 (n = 4) post-immunisation, was subjected to total RNA sequencing and processed for PCA analysis. The PCA plot shows the distribution of samples based on the first two principal components, which together account for 98 % of the total variance from the processed RNA sequencing expression data. Each point represents a sample from one of three experimental groups: Control (purple), EAE day 9 (yellow), and EAE day 20 (green). Samples within each group are represented by ellipses, with the ellipse area proportional to the variance of the group.

Next, we used gene ontology enrichment (GOE) analysis to identify the top biological processes enriched among the differentially expressed genes. By employing this approach, we were able to gain further insights into additional pathways that have potentially influenced the observed expression profiles of the lncRNAs. At EAE day 9, the top ten enriched biological processes were mainly involved in immune response initiation, such as *'leukocyte migration', 'regulation of immune effector process', 'myeloid leukocyte activation', and 'cell activation involved in immune response'*, among others (Figure 10a). In contrast, at day 20, we observed a range of different biological processes, including *'synapse organization', 'positive regulation of cell adhesion', 'mononuclear cell differentiation'*, and *'regulation of cell-cell adhesion'*, which could indicate the process of tissue repair initiation (Figure 10b).

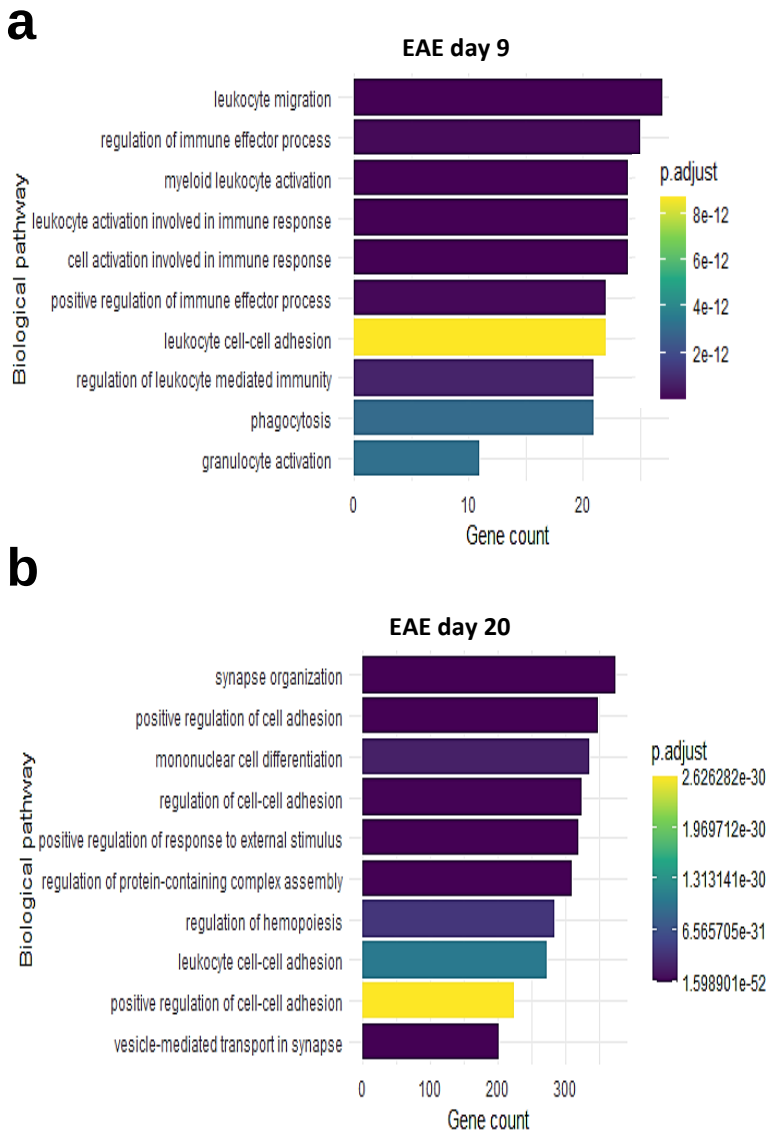

Figure 10. Top 10 biological pathways based on gene ontology enrichment (GOE) analysis of differentially expressed genes in spinal cord tissue of experimental autoimmune encephalomyelitis (EAE) mice at day 9 and 20 post-immunization. RNA isolated from spinal cord tissue of non-immunised control (n = 4) mice and myelin oligodendrocyte glycoprotein (MOG_{35-55}) immunised EAE mice at day 9 (n = 4) and day 20 (n = 4) post-immunisation, was subjected to total RNA sequencing and downstream processing. Transcripts with an adjusted p-value < 0.05 and log_2 fold change greater or smaller than 0.5 compared to the control, were subjected to GOE. The x-axis displays the number of differentially expressed genes belonging to each biological pathway, while the color gradient indicates the corresponding adjusted p-value (p.adjust). The lower the p-value the more significant the pathway is enriched (more identified differential expressed genes on the total amount of genes belonging to the pathway). The top 10 biological pathways are visualized for both EAE day 9 **(a)** and EAE day 20 **(b).**

Because of our prior interest in neuroinflammation, we also examined and highlighted the biological pathways related to inflammation, such as '*NF-kB signalling', 'cytokine production', 'interferon signalling', 'macrophage activation', 'microglia activation'*, and *'inflammasome complex'*, which were highly present and significant at EAE day 20 and to a lesser extent at day 9 (Figure 11). Notably, at day 9, we observed no '*macrophage activation', 'microglia activation'*, or '*inflammasome complex signalling'* pathways, and the significant gene counts for the enriched biological pathways were lower at day 9, together with higher adjusted p-values (Figure11a). Furthermore, the limited number of significant genes associated with the pathways did not entirely confirm the presence of neuroinflammation. These transcripts may provide less informative insights compared to other genes that are more robustly associated with neuroinflammatory processes. Consequently, we suggested that neuroinflammation is less or not prominent at this time point.

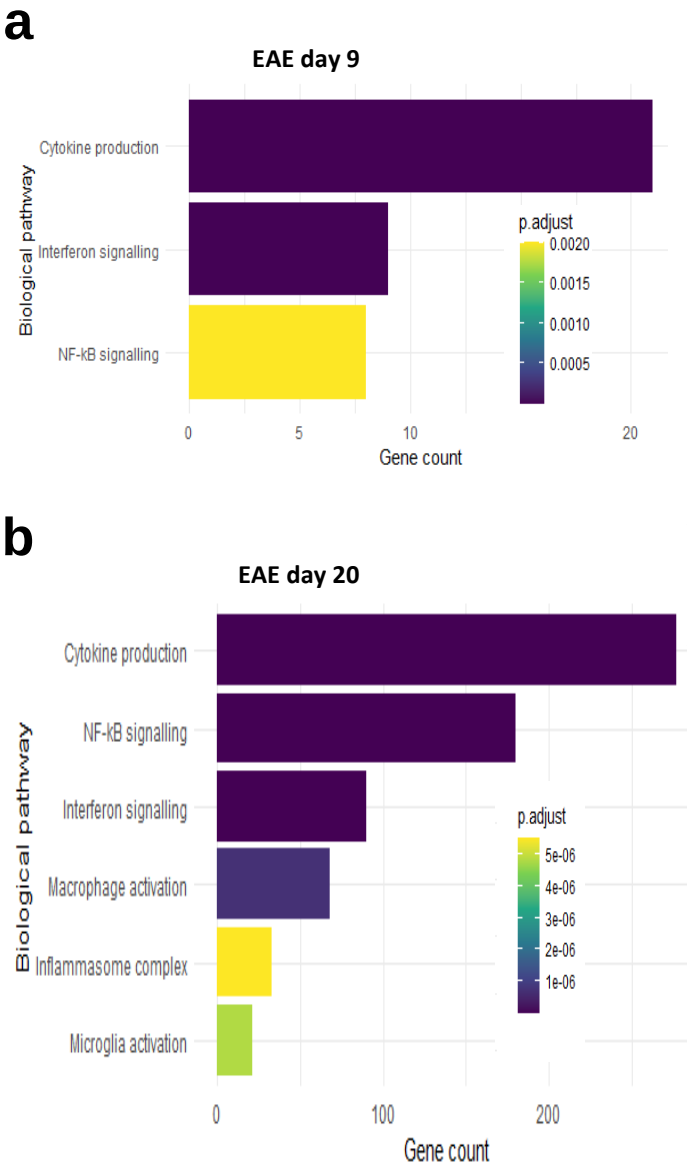

Figure 11. Enriched biological pathways related to inflammation based on gene ontology enrichment (GOE) analysis of differentially expressed genes in spinal cord tissue of experimental autoimmune encephalomyelitis (EAE) mice at day 9 and 20 post-immunization. RNA isolated from spinal cord tissue of non-immunised control (n = 4) mice and myelin oligodendrocyte glycoprotein (MOG_{35-55}) immunised EAE mice at day 9 (n = 4) and day 20 (n = 4) post-immunisation, was subjected to total RNA sequencing and downstream processing. Transcripts with an adjusted p-value < 0.05 and log_2 fold change greater or smaller than 0.5 compared to the control, were subjected to GOE. The x-axis displays the number of differentially expressed genes belonging to each biological pathway, while the color gradient indicates the corresponding adjusted p-value (p.adjust). The lower the p-value the more significant the pathway is enriched (more identified differential expressed genes on the total amount of genes belonging to the pathway). To investigate the presence of neuroinflammation we selected the pathways *'cytokine production', 'NF-kB signalling', 'interferon signalling', 'macrophage activation', 'microglia activation'* and *'inflammasome complex',* and visualized these for EAE day 9 **(a)** and EAE day 20 **(b).**

In order to more comprehensively compare inflammation signalling between control samples, EAE day 9, and day 20 samples, we generated a heatmap to visualize expression of prominent transcripts identified through gene ontology pathway analysis (Figure 12). In addition we also evaluated expression of 'M2' markers (*Tgfb1, Il4ra, Stat6, Igf1, Arg1, Il13ra1, Cd163, Cd200r1*) representative for the presence of anti-inflammatory responses (Figure 12). Despite the significant presence for '*NF-κB signalling'*, '*interferon signalling'*, and '*cytokine production'* at day 9 of EAE of the gene ontology analysis, we did not observe any differences in the inflammation transcripts compared to control (Figure 12), which confirmed our above mentioned statements. Additionally, we found no enrichment of inflammasome signalling, chemokine production, or the presence of M1 or M2 markers (Figure 12). The heatmap did perfectly visualize the significant presence of neuroinflammation of EAE at day 20 (Figure 12).

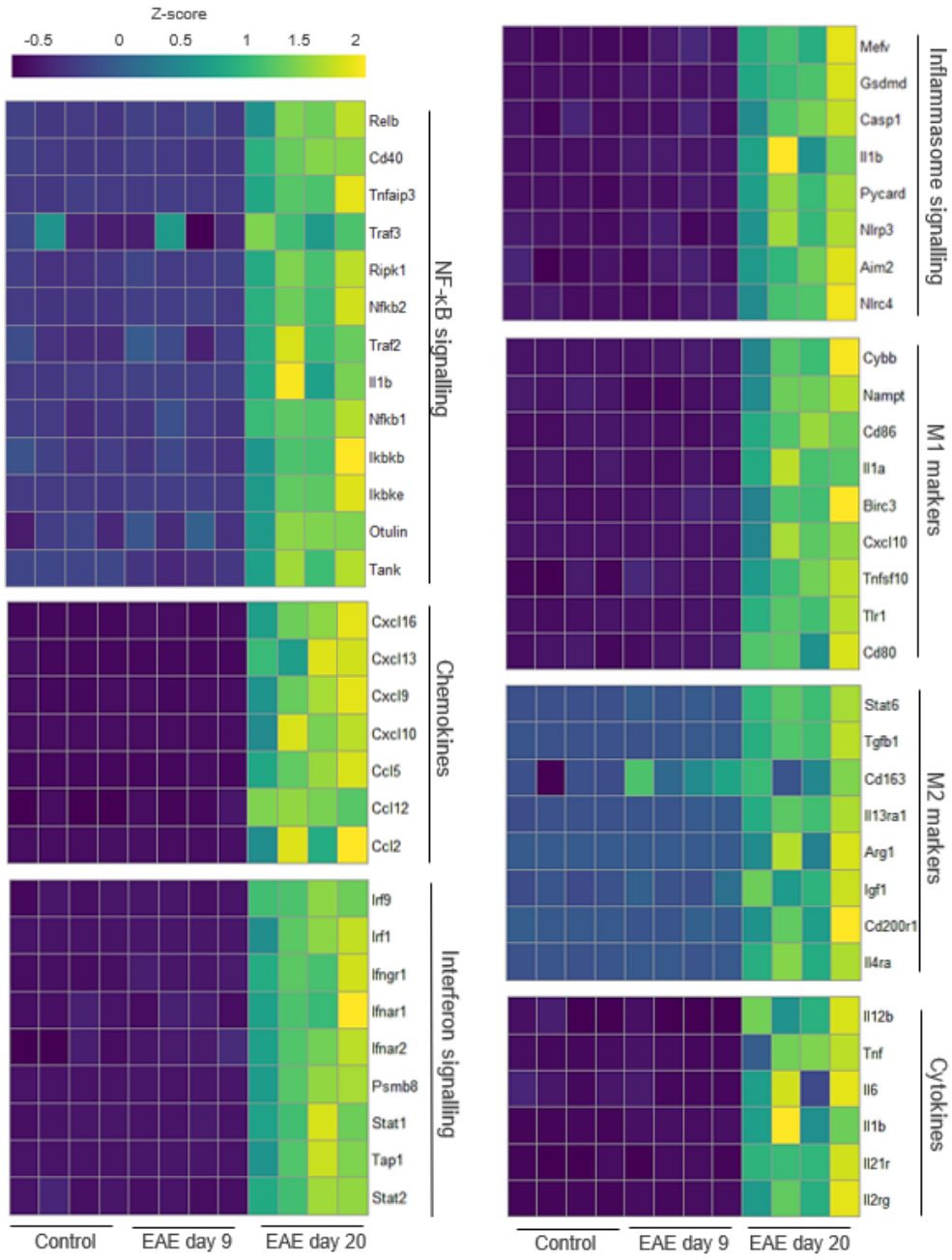

Figure 12. Relative gene expression levels of inflammation markers in spinal cord tissue of non-immunized control and experimental autoimmune encephalomyelitis (EAE) mice at day 9 and 20 post-immunization. RNA isolated from spinal cord tissue of non-immunised control (n = 4) mice and myelin oligodendrocyte glycoprotein (MOG_{35-55}) immunised EAE mice at day 9 (n = 4) and day 20 (n = 4) post-immunisation, was subjected to total RNA sequencing. Each row presents normalized expression counts of inflammation markers belonging to 'NF-κB signalling, 'Chemokines', 'Interferon signalling', 'Inflammasome signalling', 'M1 markers', 'M2 markers', and 'Cytokines' pathways retrieved from the RNA-sequencing dataset. Each column represents data from one individual mouse, n = 4 per group. Color code presents linear scale.

We next aimed to identify differential expression of lncRNAs during this process. Our dataset revealed a difference in the number of expressed lncRNAs between EAE day 9 and day 20 compared to the control group, with only two lncRNAs significantly expressed at day 9 and 557 at day 20. However, due to the lack of pathway annotations for most lncRNAs, GOE analysis only provided limited information on the biological pathways involving lncRNAs, such

as *'DNA methylation'*, *'regulation of DNA methylation'*, *'DNA alkylation'*, *'chromatin remodelling'* and *'gene silencing by RNA'* (Supplementary figure 1). In addition, the GOE analysis yielded non-significant results with adjusted p-values greater than 0,3 and low gene counts of lncRNAs enriched in those pathways (Supplementary figure 1).

Since we could not automatically retrieve differentially expressed lncRNAs using gene enrichment analysis, we employed a manual analysis approach based on the scientific literature and available databases to look at the involvement of specific lncRNA in our neuroinflammation model. This resulted in the identification of 50 significantly differentially expressed lncRNAs that have been implicated in inflammation (Figure 13). Additionally, we included *Malat1* in our analysis, since *Malat1* has previously been associated with MS and EAE (Eftekharian et al., 2019; Masoumi et al., 2019), thus increasing the total number to 51 lncRNAs. Our analysis identified both upregulated and downregulated lncRNAs (Figure 13). Furthermore, in order to compare differential expression of lncRNAs between the three different groups (control, EAE day 9 and EAE day 20), we conducted a clustering analysis within the heatmap (Figure 13). The results of the clustering analysis showed that the four samples from EAE day 20 were grouped together, whereas the EAE day 9 group together with the control samples (Figure 13).

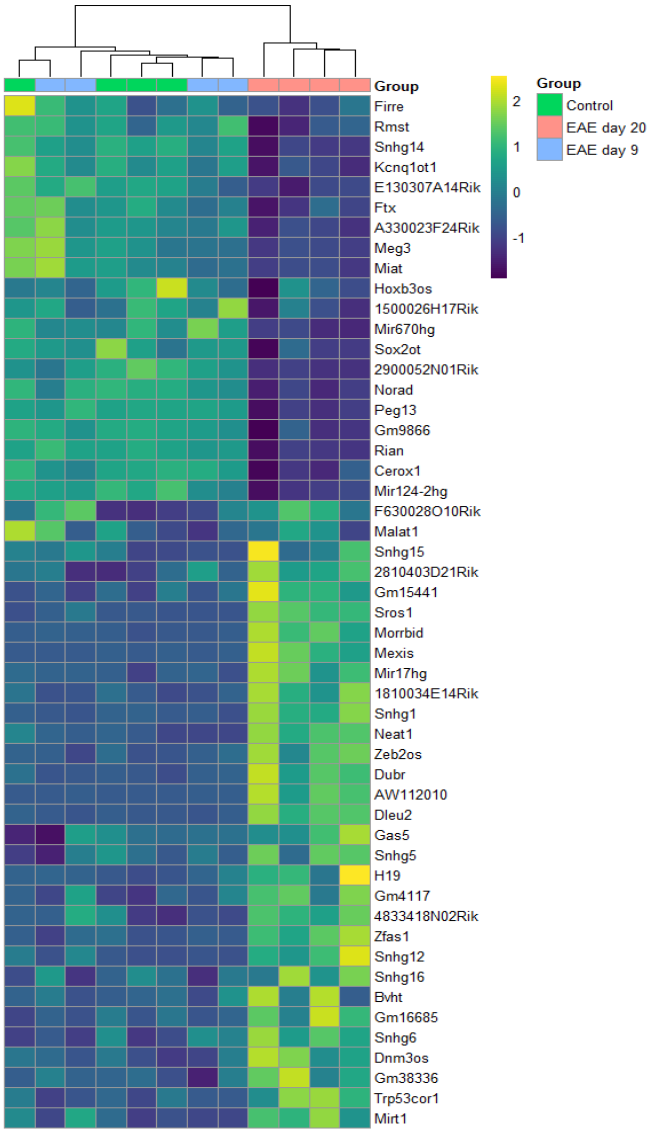

Figure 13. Relative gene expression levels of inflammation-associated lncRNAs in spinal cord tissue of non-immunized control and experimental autoimmune encephalomyelitis (EAE) mice at day 9 and 20 post-immunization. RNA isolated from spinal cord tissue of non-immunised control (n = 4) mice and myelin oligodendrocyte glycoprotein (MOG_{35-55}) immunised EAE mice at day 9 (n=4) and day 20 (n = 4) post-immunisation, was subjected to total RNA sequencing. The 557 significantly differentially (p-value < 0,05) expressed long non-coding (lnc)RNAs in the spinal cord tissue of EAE mice at day 20 compared to the control group and EAE day 9 were individually evaluated for their involvement in inflammation. Each row represents normalized expression counts of inflammation-related lncRNAs. Each column represents one individual mouse, n = 4 per group. Color code presents linear scale. Column clustering was included to highlight significance.

To enhance our analysis, we conducted a coding-noncoding coexpression network analysis to investigate the relationship between NF-κB signaling mediators and cytokines (TNF, IL-6, and IL-1β) with the expression of lncRNAs in the dataset. This analysis enabled us to identify regulatory relationships of lncRNAs during neuroinflammation and potentially validate our previous findings. Furthermore, it serves as a starting point for discovering novel lncRNAs. We visualised the network of transcripts with a Pearson correlation coefficient r > 0.55 and a direct association with inflammation markers (Figure 14). Our findings revealed the presence of characterized lncRNAs such as *Neat1, Zeb2os, Dleu2, Dubr, Peg13*, and *Morrbid* which we previously identified, alongside unidentified lncRNAs (Figure 14). Notably, *Nfkb2* and *Stat3* exhibited the highest number of connections in the network (Figure 14).

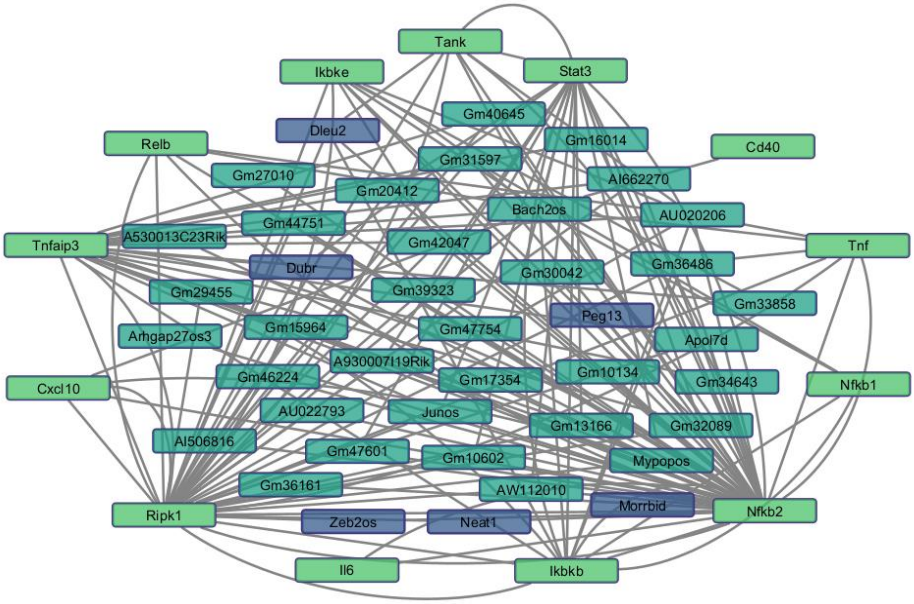

Figure 14. Coding non-coding coexpression network analysis of spinal cord tissue from experimental autoimmune encephalomyelitis (EAE). RNA isolated from spinal cord tissue of non-immunised control (n = 4) mice and myelin oligodendrocyte glycoprotein (MOG_{35-55}) peptide immunised EAE mice at day 9 (n=4) and day 20 (n = 4) post-immunisation, was subjected to total RNA sequencing. The 2208 annotated long non-coding (lnc)RNAs with inflammation related transcripts were subjected to a Pearson correlation analysis. Corelations of lncRNAs (dark green) r > 0.55 and a direct link (grey) with the inflammation transcripts (light green) were visualised using the Cytoscape tool. Previously identified inflammation-related lncRNAs were highlighted (blue).

Taken together, both bioinformatic analyses allowed us to select lncRNAs that showed significant changes in expression in conditions of neuroinflammation. The lncRNAs *Malat1, Neat1, Miat, Snhg5, Snhg4, Zfas1 and Cdk2nb-as1* demonstrated downregulation after LPS exposure and correlated with increased expression of inflammatory markers. ***Malat1*** and ***Miat*** also showed downregulation during EAE. While *Malat1* has been studied in EAE neuroinflammation (Masoumi et al., 2019), the role of *Miat* in this context has not been investigated. Moreover, we observed upregulation of lncRNAs *Snhhg5, Neat1* and *Zfas1,* but no significant changes in expression of *Snhg4* and *Cdk2nb-as1* in the EAE dataset. Because ***Neat1*** showed interesting results in our analyses and published studies investigating neuroinflammation, we also included this lncRNA for further analysis (Tripathi et al., 2021b). Similarly, ***Zfas1*** was previously shown to exhibit context-specific responses, requiring further characterization (Zhu et al., 2022). Hence, qPCR primers were designed for these four lncRNAs allowing to assess their expression in both *in vivo* and *in vitro* experiments.

3.2 Characterization of Selected LncRNAs *in vivo*

To enhance our understanding of the involvement of the above selected lncRNAs *Malat1, Neat1, Miat* and *Zfas1* in EAE neuroinflammation, we made use of different transgenic mouse lines exhibiting differential immune responses in EAE. This approach enabled us to determine the extent to which the identified lncRNAs positively or negatively impact EAE pathology and neuroinflammation.

3.2.1 *Investigating LncRNAs in EAE 'hypersensitive' Mice: A20$^{Cx3cr1\text{-}KO}$ and OTULIN$^{Cx3cr1\text{-}KO}$*

The host lab previously demonstrated that A20$^{Cx3cr1\text{-}KO}$ (A20 KO) mice, which lack A20 expression in CNS myeloid cells, display hyperactive microglia and exhibit worsened EAE disease. This effect is attributed to the hyperactivation of the Nlrp3 inflammasome in microglia, resulting in increased secretion of IL-1β. (Voet et al., 2018). Therefore, because of their increased susceptibility to neuroinflammation and EAE, we aimed to examine the expression pattern of our selected lncRNAs in these mice.

We immunized eight A20 KO mice and eight wild-type littermate (WT) mice with $MOG_{35–55}$ peptide to induce EAE. Consistent with previous findings from the host lab (Voet et al., 2018), A20 KO mice exhibited a more severe disease course as compared to WT mice (Figure 15). Once a clear difference in clinical scores became apparent between the two mouse groups, we collected spinal cord tissue for RNA isolation and performed RT-qPCR to analyse gene expression. We also isolated spinal cord tissue from four non-immunized A20 KO and WT mice as controls.

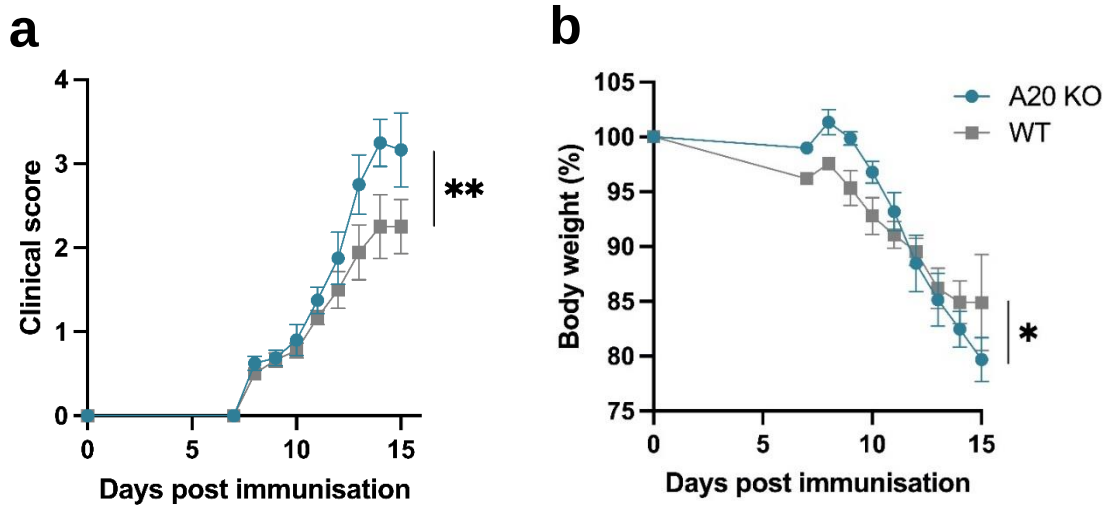

Figure 15. Experimental autoimmune encephalomyelitis (EAE) disease progression in A20$^{Cx3cr1\text{-}KO}$ (A20 KO) mice. EAE was induced by active immunization of wild-type (WT, n = 8) and A20 KO (n = 8), mice with myelin oligodendrocyte glycoprotein ($MOG_{35\text{-}55}$) peptide and clinical score **(a)** and body weight **(b)** was followed over time. Changes in clinical score and body weight differ significantly between genotype groups across the time span, analysed with F-test on repeated measurements (*p < 0.05, **p < 0.01). Each data point represents the mean ± SEM as estimated by the REML analysis.

In order to establish a role for the selected lncRNAs in neuroinflammation, we examined the expression levels of the pro-inflammatory cytokines TNF, IL-1β, and IL-6 in the spinal cord of these mice (Figure 16). Our analysis revealed spinal cord neuroinflammation in both groups of EAE mice, shown by a significant upregulation of *Tnf, Il1-β,* and *Il6* (Figure 16a-c). Moreover,

the non-immunized A20 KO group exhibits higher expression levels of *Il1β* (Figure 16c), although not statistically significant, which is consistent with previous findings from the host lab, showing enhanced interleukin-1β secretion by A20 deficient microglia (Voet et al., 2018). We also plotted the expression levels of these cytokines against the clinical score, disregarding the genetic background, and observed a significant increase in expression with an increase in clinical score, reaching maximum expression at score 3 or 4 (Figure 16d-f).

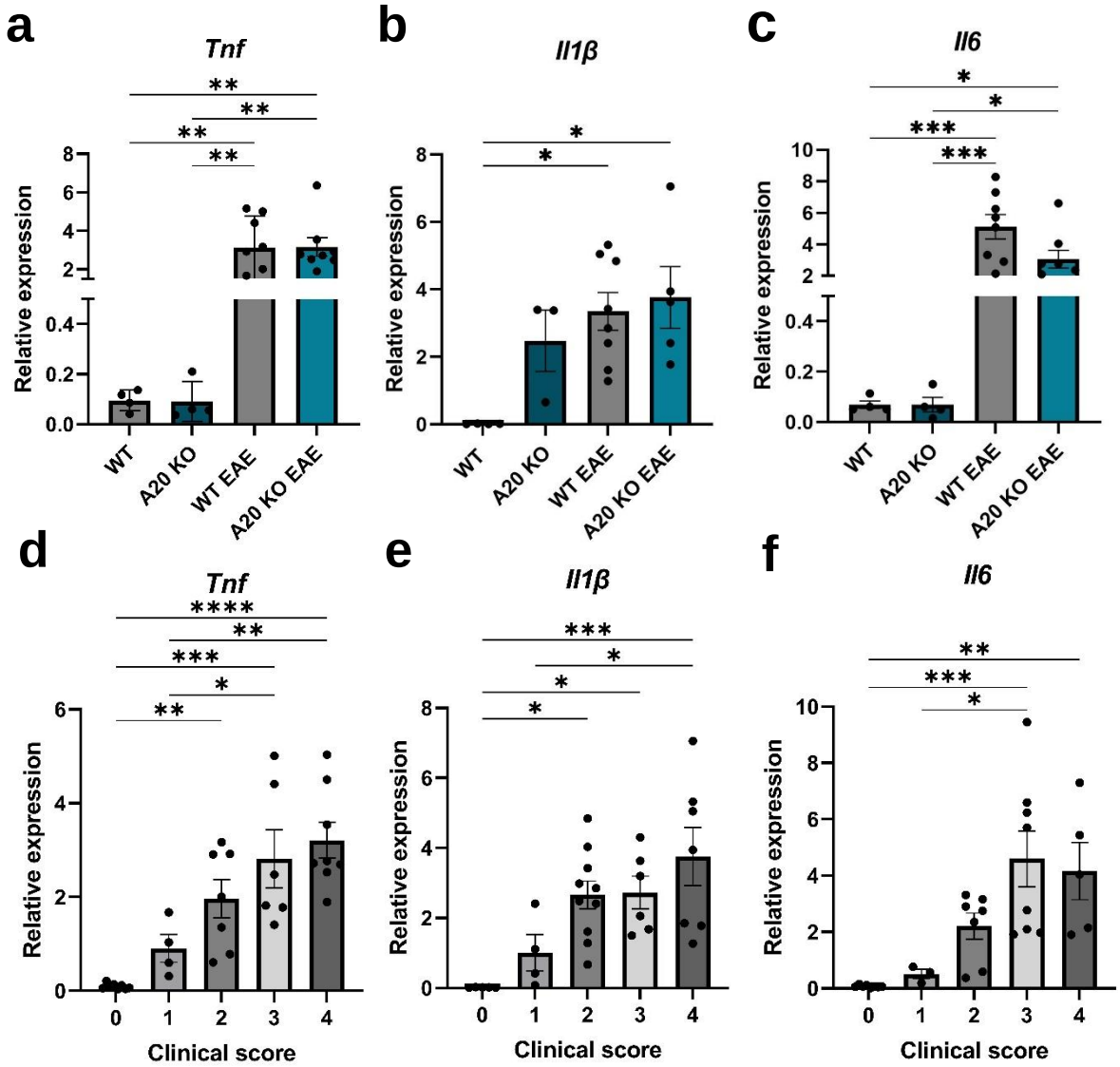

Figure 16. Relative gene expression levels of inflammatory cytokines in the spinal cord of wild-type (WT) and A20$^{Cx3cr1\text{-}KO}$ (A20 KO) mice during experimental autoimmune encephalomyelitis (EAE) pathology. RT-qPCR was performed on RNA from spinal cord tissue of myelin oligodendrocyte glycoprotein ($MOG_{35\text{-}55}$) immunized WT (WT EAE, n = 8) and A20 KO (A20 KO EAE, n = 8), and non-immunised WT (n = 4) and A20 KO (n = 4) mice 15 days post-immunisation. The y-axis represents the relative gene expression of *Tnf, Il1β* and *Il6*, while the x-axis represents the different experimental groups (**a-c**) or the clinical score at end stage (**d-e**). All groups were normalised to the expression of the housekeeping genes *Gapdh* and *Hprt*. Statistical significance was determined using one-way ANOVA test with Tukey correction for multiple comparison (*p < 0.05, **p < 0.01, ***p < 0.001, ****p < 0.0001). Results are displayed as mean ± SEM.

Having confirmed enhanced neuroinflammation in A20 KO and EAE mice, we next explored the expression profiles of our selected lncRNAs - *Malat1, Neat1, Zfas1,* and *Miat* - using qPCR (Figure 17). Our results revealed significant downregulation of *Malat1, Miat* and *Neat1* in in the non-immunised A20 KO group, when compared to the non-immunised WT control group (Figure 17a-c). Also *Zfas1* showed reduced expression, although not significant, in the non-immunised A20 KO mice compared to WT mice (Figure 17d). In the inflammatory EAE condition, however, *Malat1, Miat* and *Neat1* showed lower expression in both WT and A20 KO mice compared to non-immunized WT mice, while *Zfas1* was significantly upregulated compared to the non-immunized condition, and even higher in the A20 KO EAE group compared to the WT EAE group (Figure 17d). Additionally we plotted the lncRNAs to the clinical score of EAE mice and observed a trend of downregulation with higher clinical score for *Malat1, Neat1* and *Miat* as well as upregulation of *Zfas1* (Supplementary figure 2). The results correlated with the trend of pro-inflammatory cytokine expression (Supplementary figure 2).

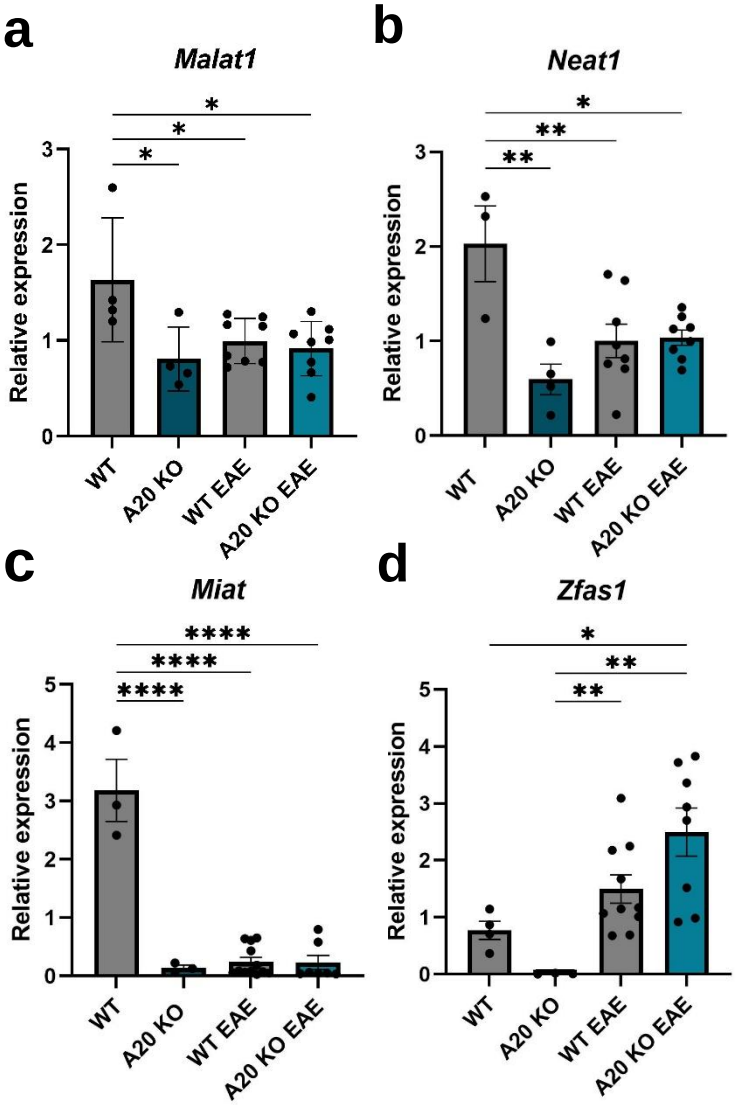

Figure 17.Relative gene expression levels of lncRNAs in the spinal cord of wild-type (WT) and A20$^{Cx3cr1\text{-}KO}$ (A20 KO) mice during experimental autoimmune encephalomyelitis (EAE) pathology. RT-qPCR was performed on RNA from spinal cord tissue of myelin oligodendrocyte glycoprotein ($MOG_{35\text{-}55}$) peptide immunized WT (WT EAE, n = 8) and A20 KO (A20 KO EAE, n = 8) mice, and non-immunised WT (n = 4) and A20 KO (n = 4) mice 15 days post-immunisation. The y-axis represents the relative gene expression of long non-coding (lnc)RNAs *Malat1* (***a***), *Neat1* (***b***), *Miat* (***c***) and *Zfas1* (***d***), while the x-axis represents the different experimental groups. All groups were normalised to the expression of the housekeeping genes *Gapdh* and *Hprt*. Statistical significance was determined using one-way ANOVA test with Tukey correction for multiple comparison (*p < 0.05, **p < 0.01, ***p < 0.001, ****p < 0.0001). Results are displayed as mean ± SEM.

Next to A20, OTULIN also acts as a brake on inflammation, and has also been shown to regulate microglia activation. Indeed, the host lab recently demonstrated that OTULIN$^{Cx3cr1\text{-}KO}$ (OTU KO) mice display a hyperactivated state of microglia, comparable to what is seen in A20$^{Cx3cr1\text{-}KO}$ mice (unpublished data van Loo group). Moreover, OTU KO mice were also shown to be hypersensitive to EAE (unpublished data by van Loo group). Therefore, we also aimed to validate our findings in the OTU KO mouse model to observe possible similarities or differences in the expression of the lncRNAs in this EAE hypersensitive model compared to the previous findings.

We immunized four OTU KO mice and four wild-type littermate (WT) mice with $MOG_{35–55}$ peptide to induce EAE. Consistent with previous findings from the host lab (unpublished data van Loo group), we observed an exacerbated EAE disease course with higher clinical scores in OTU KO mice relative to WT mice (Figure 18). Once a clear difference in clinical scores became apparent between the two mouse groups, at day 16 post-immunization, we collected spinal cord tissue for RNA isolation and performed RT-qPCR to analyse gene expression. We also isolated spinal cord samples from four non-immunized OTU KO and WT mice as controls.

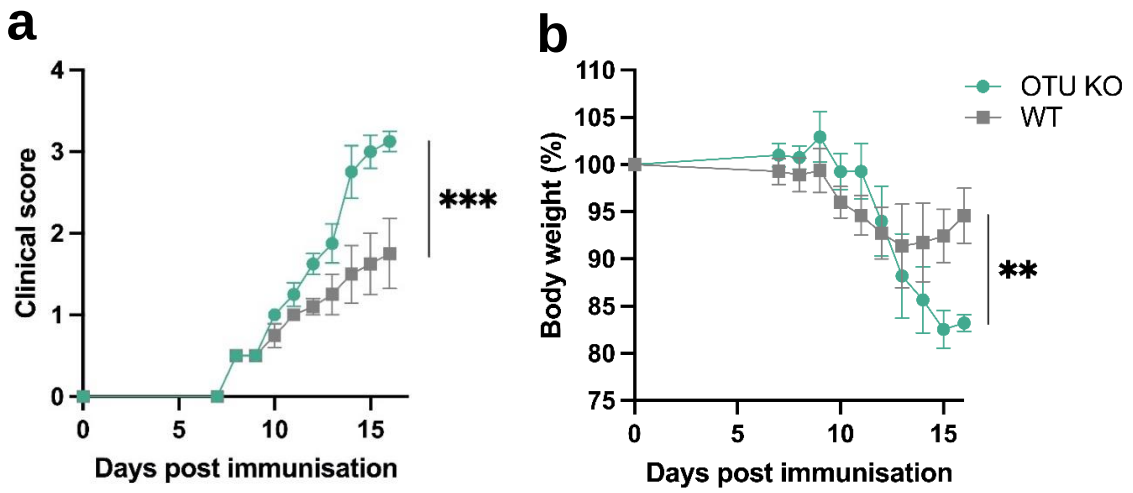

Figure 18. Experimental autoimmune encephalomyelitis (EAE) disease progression in OTULIN$^{Cx3cr1\text{-}KO}$ (OTU KO) mice. EAE was induced by immunization of wild-type (WT, n = 4) and OTU KO (n = 4), mice with myelin oligodendrocyte glycoprotein ($MOG_{35\text{-}55}$) peptide and clinical score **(a)** and body weight **(b)** was followed over time. Changes in clinical score significantly between genotype groups across the time span, analysed with F-test on repeated measurements (**p < 0.01, ***p < 0.001). Each data point represents the mean ± SEM as estimated by the REML analysis.

We next examined the expression levels of the pro-inflammatory cytokines TNF, IL-1β, and IL-6 in the spinal cord using qPCR. Our results revealed a significant upregulation of *Tnf*, and a clear trend towards higher expression of *Il1β* and *Il6* in both EAE groups, which validated the presence of neuroinflammation in these EAE mice (Figure 19).

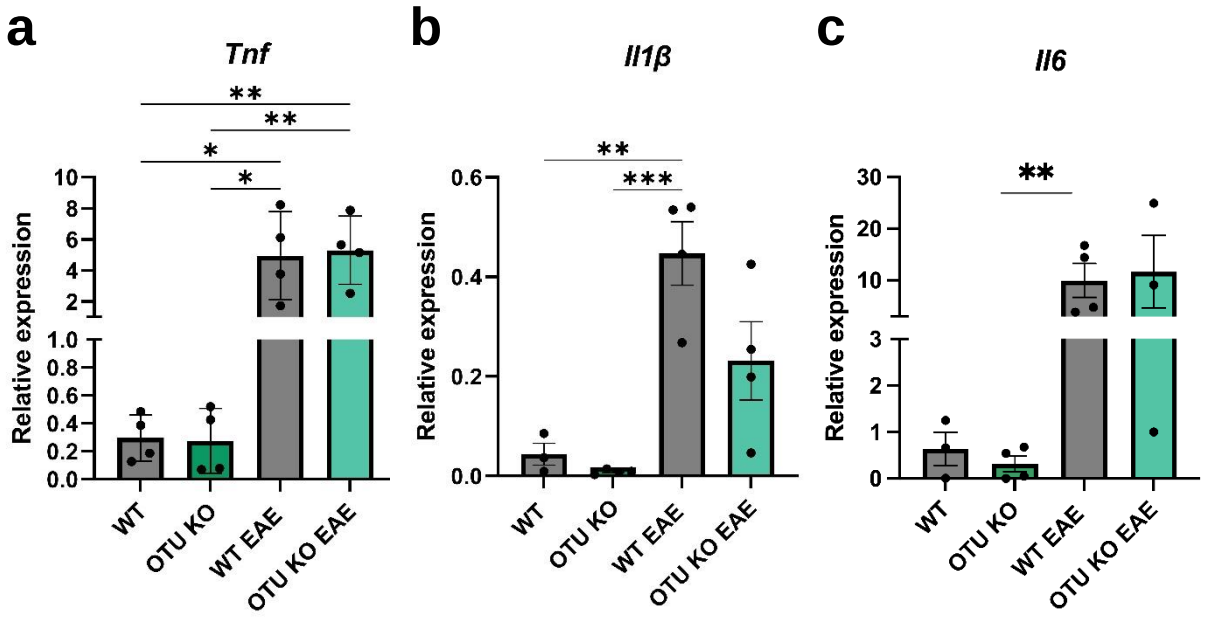

Figure 19. Relative gene expression levels of inflammatory cytokines in spinal cord tissue of wild-type (WT) and OTULIN$^{Cx3cr1\text{-}KO}$ (OTU KO) mice during experimental autoimmune encephalomyelitis (EAE) pathology. RT-qPCR was performed on RNA from spinal cord tissue of myelin oligodendrocyte glycoprotein ($MOG_{35\text{-}55}$) peptide immunised WT (WT EAE, n = 4) and OTU KO (OTU KO EAE, n = 4) mice, and non-immunised WT (n = 4) and OTU KO (n = 4) mice 16 days post-immunisation. The y-axis represents the relative gene expression of *Tnf* **(a),** *Il6* (**b**) and *Il1β* (**c**), while the x-axis represents the different experimental groups. All groups were normalised to the expression of the housekeeping genes *Gapdh* and *Hprt*. Statistical significance was determined using one-way ANOVA test with Tukey correction for multiple comparison (*p < 0.05, **p < 0.01, ***p < 0.001, ****p < 0.0001). Results are displayed as mean ± SEM.

We next analysed the expression profile of our selected lncRNAs using qPCR (Figure 20). Given that OTULIN and A20 have similar effects on the inflammation signalling pathway by destabilizing the signalling pathway to NF-κB, we hypothesized that the expression profiles of the lncRNAs in OTU KO would be similar to the findings described above (unpublished data by van Loo group). *Malat1*, *Neat1*, and *Miat* showed downregulated expression in conditions of EAE, in contrast to *Zfas1* that was upregulated after EAE mice, compared to their expression in non-immunised mice (Figure 20). However, these were mostly trends since statistical analysis could not confirm statistical significance for most of the differences (Figure 20). Interestingly, in non-immunized mice, we observed an upregulation in expression of *Malat1*, *Neat1* (non-significant), and *Miat* (significant) in OTU KO mice compared to WT (Figure 20a-c), which is the opposite of what was observed in non-immunized A20 mice (Figure 17).

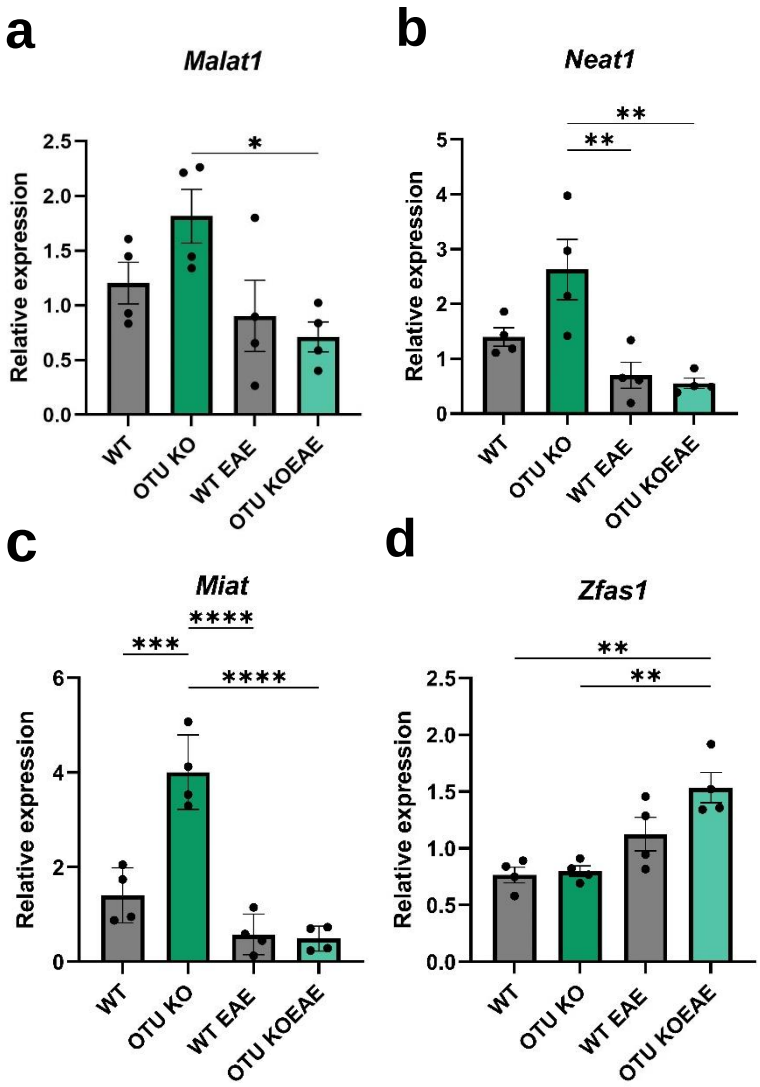

Figure 20. Relative gene expression levels of lncRNAs in spinal cord of wild-type (WT) and OTULIN$^{Cx3cr1\text{-}KO}$ (OTU KO) mice 16 days post-immunization with MOG peptide. RT-qPCR was performed on RNA isolated from the spinal cord tissue of myelin oligodendrocyte glycoprotein ($MOG_{35\text{-}55}$) peptide immunized WT (WT EAE, n = 4) and OUT KO (OTU KO EAE, n = 4), and non-immunised WT (n = 4) and OTU KO (n = 4) mice 16 days post-immunisation. The y-axis represents the relative gene expression of long non-coding (lnc)RNAs *Malat1* (**a**), *Neat1* (**b**), *Miat* (**c**) and *Zfas1* (**d**), while the x-axis represents the different experimental groups. All groups were normalised to the expression of the housekeeping genes *Gapdh* and *Hprt*. Statistical significance was determined using one-way ANOVA test with Tukey correction for multiple comparison. *p < 0.05, **p < 0.01, ***p < 0.001, ****p < 0.0001. Results are displayed as mean ± SEM.

3.2.2 *Investigating LncRNAs in EAE Protected Mice: Pggt1b$^{CD4\text{-}KO}$*

Now that we have characterized the expression profiles of our selected lncRNAs in mice with a hyperactivated microglia state and EAE 'hypersensitivity', we aimed to investigate their expression in a model where mice are protected from EAE. Pggt1b$^{CD4\text{-}KO}$ (Pggt KO) mice lack the β subunit of protein geranylgeranyl transferase-I (GGTase-I) and have been shown to be fully protected from EAE and inflammation (unpublished data van Loo group). GGTase-I is essential for the lipidation of RHO family proteins, which are involved in many intracellular signalling pathways, including inflammation (Khan et al., 2013) (Akula et al., 2016, 2019). We aimed to uncover the neuroprotective role of lncRNAs in this model and expected to observe a reverse expression profile compared to what is seen in A20 and OTU KO EAE 'hypersensitive' mice. In this way, we intended to correlate the expression of the lncRNAs with the process of neuroinflammation, independent of the immunization process.

We immunized four Pggt KO mice and four wild-type littermate (WT) mice with $MOG_{35–55}$ peptide to induce EAE. Consistent with previous findings from the host lab, no clinical disease could be observed in Pggt KO mice, in contrast to WT mice that all develop severe clinical pathology with time (Figure 21). We collected spinal cord tissue 20 days post-immunization,

and isolated RNA for RT-qPCR gene expression analysis. We did not include non-immunised mice in this study due to a shortage in mice.

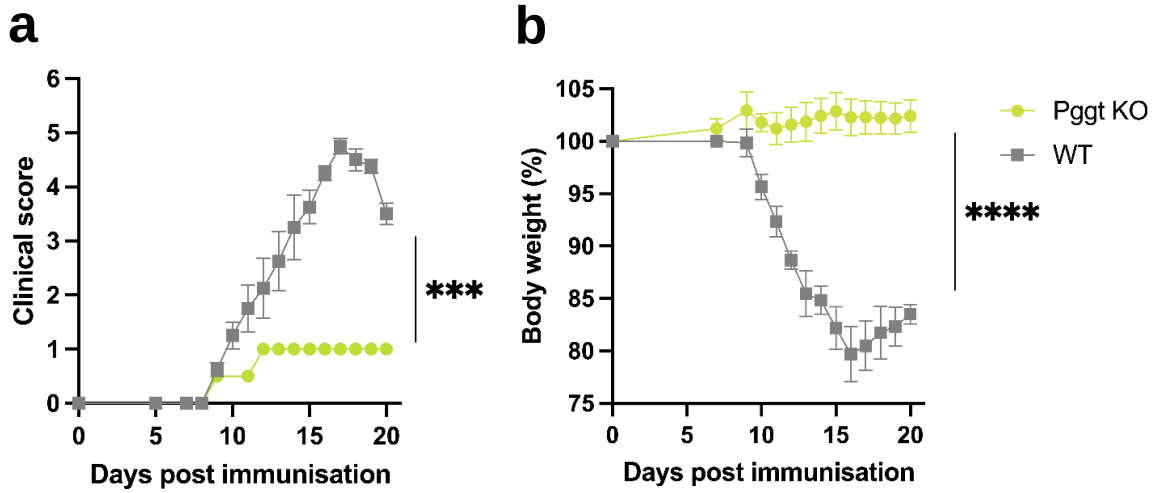

Figure 21. Experimental autoimmune encephalomyelitis (EAE) disease progression in Pggt1b$^{CD4\text{-}KO}$ (Pggt KO) mice. EAE was induced by active immunization of wild-type (WT, n = 4) and GGTase-I KO (Pggt KO, n = 4) mice with myelin oligodendrocyte glycoprotein ($MOG_{35\text{-}55}$) peptide, and clinical score **(a)** and body weight **(b)** was followed over time. Changes in clinical score significantly between genotype groups across the time span, analysed with F-test on repeated measurements (***p < 0.005, ****p < 0.0001). Each data point represents the mean ± SEM as estimated by the REML analysis.

The presence of neuroinflammation is prominent following $MOG_{35\text{-}55}$ immunisation of mice as demonstrated above (Figure 16 & 19). However, since Pggtb KO mice did not display EAE symptoms, we investigated whether there was still an upregulation of pro-inflammatory cytokines. The gene expression analysis revealed significant downregulation of *Tnf* and *Il1β* in Pggt KO EAE mice compared to the WT EAE mice, and a trend in downregulated expression of *Il6* (Figure 21). These findings agreed with the observation that Pggtb KO mice are protected in EAE.

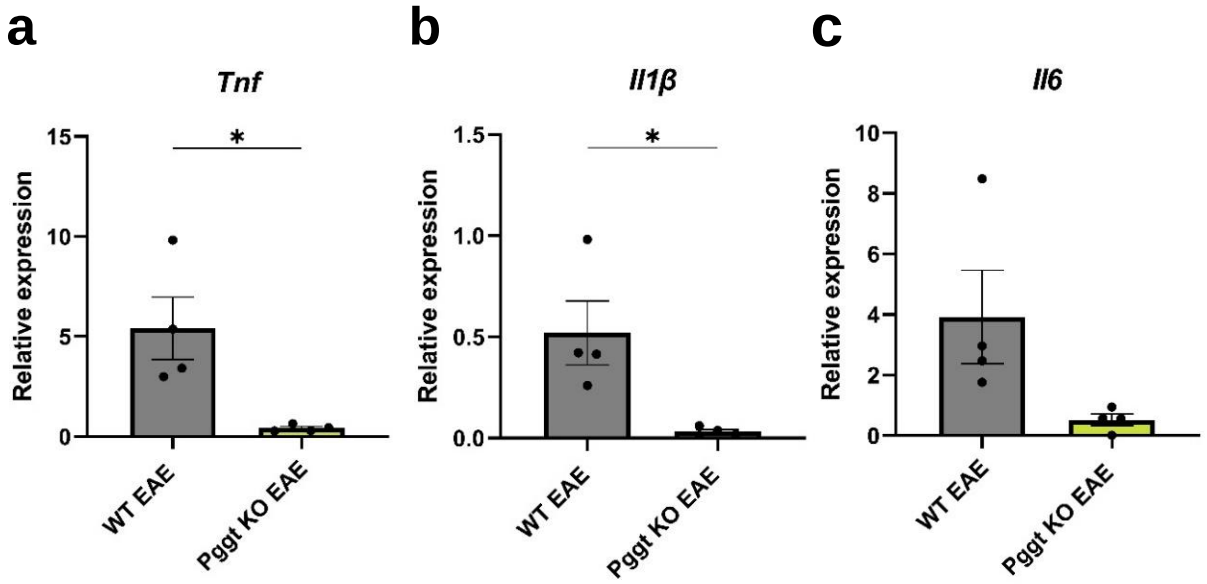

Figure 22. Relative gene expression levels of inflammatory cytokines in spinal cord tissue of wild-type (WT) and Pggt1b$^{CD4\text{-}KO}$ (Pggt KO) mice during experimental autoimmune encephalomyelitis (EAE) pathology. RT-qPCR was performed on RNA isolated from spinal cord of myelin oligodendrocyte glycoprotein ($MOG_{35\text{-}55}$) peptide immunised WT EAE (n = 4) and Pggt KO EAE (n = 4) mice, 20 days post-immunisation. The y-axis represents the relative gene expression of the proinflammatory cytokines *Tnf* **(a),** *Il1β* (**b)** and *Il6* (**c**). Values were normalised to the expression of the housekeeping genes *Gapdh* and *Hprt*. Statistical significance was determined using unpaired t-test with Welsh-correction (*p < 0.05, **p < 0.01, ***p < 0.001, ****p < 0.0001). Results are displayed as mean ± SEM.

Next, we examined the expression profiles of the selected lncRNAs in both immunized mice groups to investigate any differences between them (Figure 23). Since there was no neuroinflammation in Pggtb KO EAE mice, we could partially anticipate that any observed difference in the expression of the lncRNAs in the previous experiments could be attributed to neuroinflammation rather than the immunization process. The analysis did not reveal statistically significant results for *Malat1*, *Neat1*, and *Miat* (Figure 23a-c), although we observed a clear upregulation of these lncRNAs in Pggt KO EAE mice, as expected (Figure 23a-c). *Zfas1* on the other hand showed significant downregulation in Pggt KO EAE mice (Figure 23d). Together, and based on our previous findings in the EAE 'hypersensitive' mice, these results suggested a correlation between the expression of these lncRNAs and the presence of neuroinflammation.

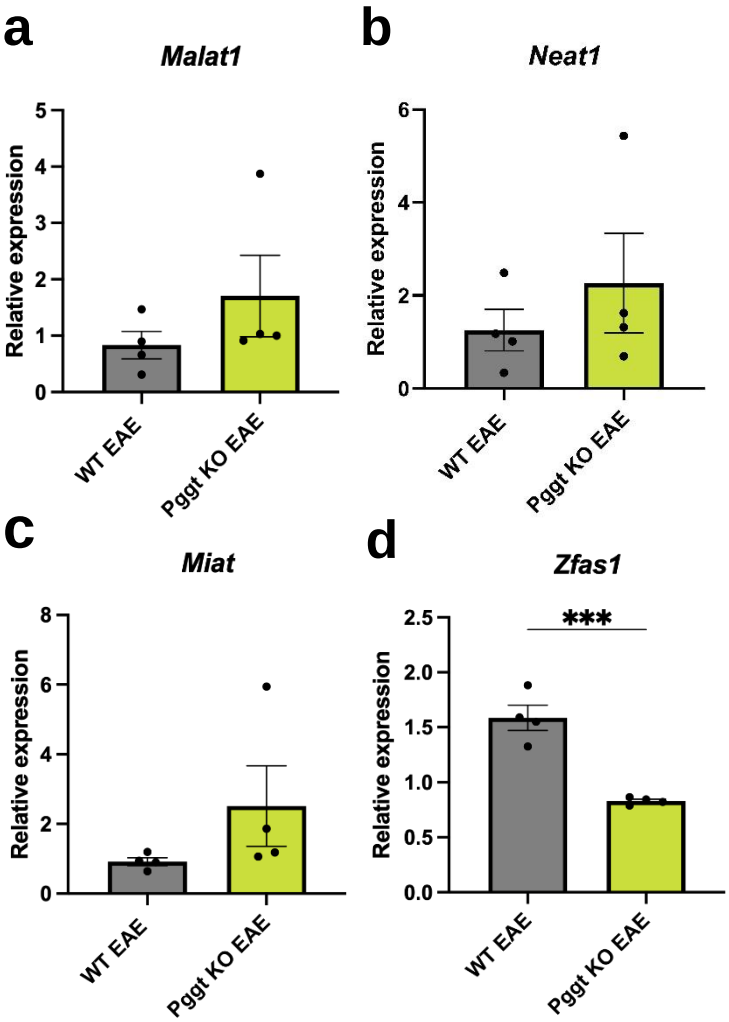

Figure 23. Relative gene expression levels of in spinal cord tissue of wild-type (WT) and Pggtb$^{CD4\text{-}KO}$ (Pggtb KO) mice during experimental autoimmune encephalomyelitis (EAE) pathology. RT-qPCR was performed on RNA isolated from spinal cord tissue of myelin oligodendrocyte glycoprotein ($MOG_{35\text{-}55}$) peptide immunized WT EAE (n = 4) and Pggtb KO EAE (n = 4) mice, 20 days post-immunisation. The y-axis represents the relative gene expression of long non-coding (lnc)RNAs *Malat1 (**a**), Neat1 (**b**), Miat (**c**)* and *Zfas1 (**d**)*, while the x-axis represents the two experimental groups. All values were normalised to the expression of the housekeeping genes *Gapdh* and *Hprt*. Statistical significance was determined using unpaired t-test with Welsh-correction (*p < 0.05, **p < 0.01, ***p < 0.001, ****p < 0.0001) Results are displayed as mean ± SEM.

In conclusion, the *in vivo* studies in mice subjected to EAE suggested that the downregulated expression of *Malat1, Neat1*, and *Miat* is associated with the induction of neuroinflammation. Indeed, these lncRNAs are downregulated during EAE in WT, A20 KO and OTU KO mice, but also in non-immunised mice A20 KO. In contrast, *Zfas1* was shown to be upregulated in these conditions, yet revealed downregulation in non-immunised A20 KO. Moreover, in Pggt KO mice that are protected to EAE, an opposite trend in expression was observed, suggesting a correlation between the expression of these specific lncRNAs and the process of neuroinflammation.

3.3 Characterization of Selected LncRNA *in vitro*

Our previous *in vivo* results provided insights into a possible role of *Malat1, Neat1, Miat*, and *Zfas1* in neuroinflammation during EAE pathology. To further validate their role in the regulation of inflammation, and exclude the complexity of *in vivo* signalling, we performed *in vitro* experiments to correlate the expression profiles of the four lncRNAs to specific molecular responses. To do this, we used bone marrow-derived macrophages (BMDMs) in order to further characterize the role of lncRNAs specifically in myeloid cells in conditions of inflammation.

3.3.1 Activation of the NF-kB Signalling Pathway

NF-κB is a central regulator of inflammation as it controls the activation of hundreds of pro-inflammatory mediators (Dresselhaus & Meffert, 2019; Q. Zhang et al., 2017). We previously observed the upregulation of several NF-κB marker genes in neuroinflammation and EAE, prompting us to investigate the involvement of the lncRNAs *Malat1, Neat1*, *Miat, and Zfas1* in NF-κB signalling after stimulation of BMDMs with LPS. While previous studies have described the involvement of these lncRNAs in NF-κB signalling (Cui et al., 2019; Y. Jiang & Zhang, 2021; Wang et al., 2021; P. Zhang et al., 2019), they have been conducted using different cell lines and conditions. Therefore, we aimed to re-examine their role. We performed our study in BMDMs from wild-type littermate (WT) mice but additionally also in BMDMs isolated from $A20^{Myel\text{-}KO}$ (A20 KO) mice. These latter have been shown to produce increased levels of inflammatory mediators such as TNF and IL-6 due to NF-κB hyperactivation (Matmati et al., Nat. Genet., 2011; Vande Walle et al., 2014). Consequently, we were able to correlate the expression of the lncRNAs with this increased inflammatory signature.

After isolating and culturing BMDMs from A20 KO and WT mice, we stimulated them with LPS for two, four and six hours, after which we analysed the expression of the pro-inflammatory cytokines TNF, IL-6 and IL-1β through a multiplex immunoassay (Figure 23a-c) as well as their transcripts using qPCR (Figure 24d-f). We observed a gradual increase in time of all 3 cytokines in BMDMs after stimulation with LPS, which is more pronounced in the A20 deficient condition (Figure 24a-c), as expected since A20 acts as a negative regulator of NF-kB activation (Martens and van Loo, 2019). The increased cytokine production was also confirmed on transcript level (Figure 24d-f). These results, indicate the successful induction of NF-κB activation in BMDMs.

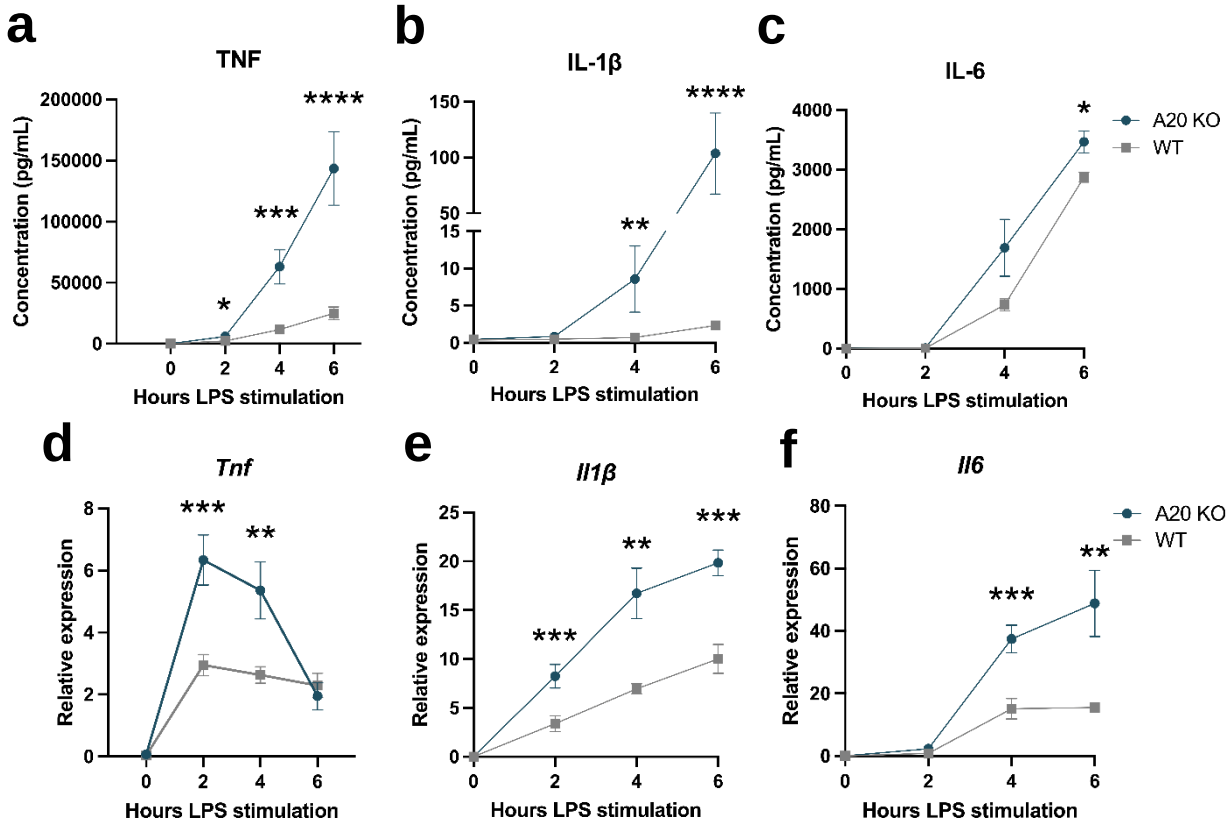

Figure 24. Protein and RNA expression of proinflammatory cytokines in bone marrow derived macrophages (BMDMs) from wild-type (WT) and A20$^{Myel-KO}$ (A20 KO) mice, after LPS stimulation. BMDMs were isolated from WT (n = 3) and A20 KO (n = 3) mice, cultured at 1 x 10^6 cells per replicate and stimulated with lipopolysaccharide (LPS) for 2, 4 and 6 hours. Concentration (pg/mL) of cytokines TNF, IL-1β and IL-6 in the supernatant was determined using a multiplex immunoassay (**a-c**), and relative expression levels of these cytokines were determined by RT-qPCR (**d-f**). All groups were normalised to the expression of the housekeeping genes *Gapdh* and *Hprt*. The two genotypes were statistically compared with each other at every time point using a Wilcoxon-sum rank test (*p < 0.05, **p < 0.01, ***p < 0.001, ****p < 0.0001). Results are displayed as mean ± SEM.

We next analysed the expression levels of our four selected lncRNAs in WT and A20 KO BMDMs using qPCR (Figure 25). Unfortunately, no significant differences were observed between the different genotypes and conditions (Figure 25). Although, we revealed a slight trend of downregulation for the lncRNA *Malat1* with significance between six hours LPS and control in WT BMDMs (Figure 25a). Yet, the only clear trend that could be observed was the upregulation of *Zfas1* in both WT and A20 KO BMDMs overtime (Figure 25d).

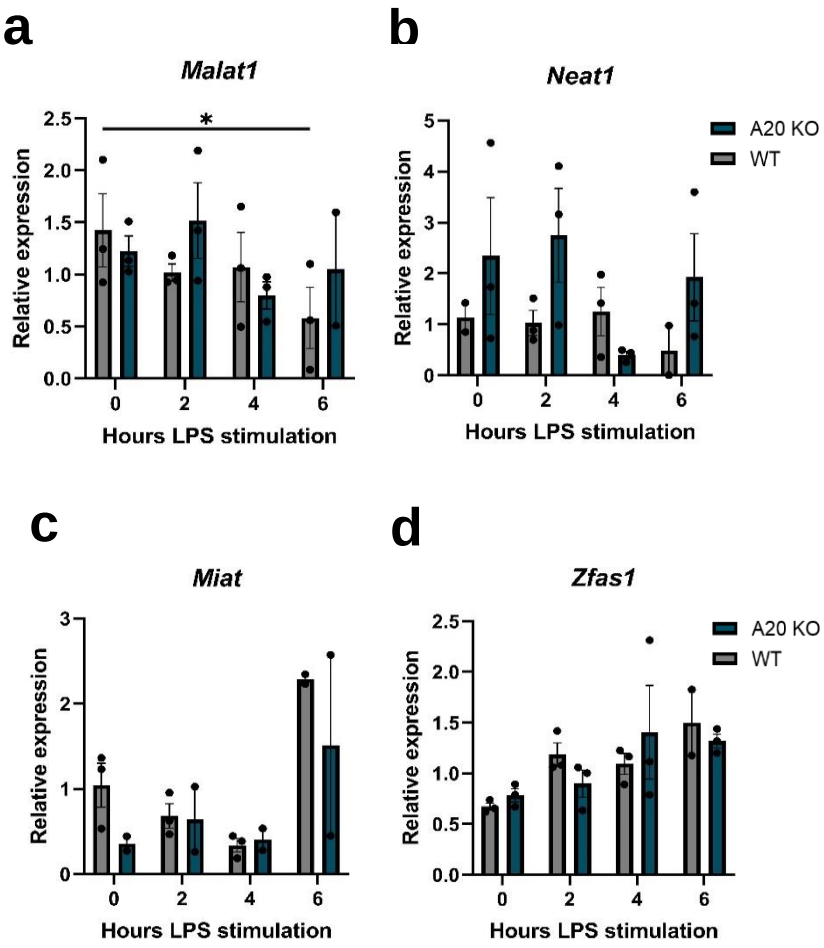

Figure 25. Relative gene expression levels of lncRNAs in bone marrow derived macrophages (BMDMs) from wild-type (WT) and A20$^{Myel\text{-}KO}$ (A20 KO) mice, after LPS stimulation. BMDMs were isolated from WT (n = 3) and A20 KO (n = 3) mice, cultured *at* 1 x 10^6 cells per replicate and stimulated with lipopolysaccharide (LPS) for 2, 4 and 6 hours. RT-qPCR was performed on RNA, isolated from these. The y-axis presents the relative expression levels of long non-coding (lnc)RNAs *Malat1* (***a***), *Neat1* (***b***), *Miat* (***c***) and *Zfas1* (***d***). All values were normalised to the expression of the housekeeping genes *Gapdh* and *Hprt*. Statistical significance was determined using two-way ANOVA with Sidak's multiple comparison test (*p < 0.05, **p < 0.01, ***p < 0.001, ****p < 0.0001). Results are displayed as mean ± SEM.

3.3.2 Activation of the Nlrp3 Inflammasome Signalling Pathway

Inflammasomes are multiprotein complexes that play a crucial role in establishing immune responses by inducing the secretion of the cytokines IL-1β and IL-18, as well as by inducing pyroptosis through release of gasdermin-D (GSDMD) (Lamkanfi & Dixit, 2012). In light of the observed upregulation of *Il1ß* in our bioinformatics and EAE analysis, we aimed to investigate the expression behaviour of our lncRNAs in the process of inflammasome activation. Interestingly, our previous findings indicate that these lncRNAs are downregulated in spinal cord tissue of non-immunised A20$^{Cx3cr1\text{-}KO}$ mice, which were previously shown to produce high levels of IL-1β due to hyperactivation of the NLRP3 inflammasome (Voet el at., 2018). Consequently, these results suggest a possible role for these lncRNAs in NLRP3 inflammasome activation. In addition, BMDMs from A20$^{Myel\text{-}KO}$ (A20 KO) mice produce high levels of IL-1β due to increased NF-κB activity and hyperactivation of the NLRP3 inflammasome (Matmati et al., 2011; Vande Walle et al., 2014). To further explore the role of lncRNAs in the regulation of NLRP3 activation and correlate their expression with increased inflammasome activation, we made use of BMDMs from and wild-type littermate (WT) controls as well as A20 KO mice.

BMDMs from A20 KO and wild-type (WT) littermate mice, were cultured and stimulated with LPS for four hours, followed by treatment with ATP for 45 minutes to activate the NLRP3 inflammasome. Supernatant was collected and IL-1β levels were measured using a multiplex immunoassay (Figure 25). Additionally, we investigated cell death after ATP treatment during 1 hour by staining of cells with sytox green (that stains dying cells) and Draq5 (that stains all cells). The percentage of cell death was calculated by dividing the number of sytox-stained cells by the total number of Draq5-stained cells (Figure 25). Our analysis confirmed the activation of the NLRP3 inflammasome in both groups of cells. We observed a significant increase in the level of IL-1β in A20 KO BMDMs in response to LPS alone, and higher levels of IL-1β in response to LPS + ATP, as previously shown (Vande Walle et al., 2014). Additionally, we observed a logarithmic increase in cell death over a one hour time period after LPS + ATP stimulation, reaching 65% in WT BMDMs and 77% in A20 KO BMDMs.

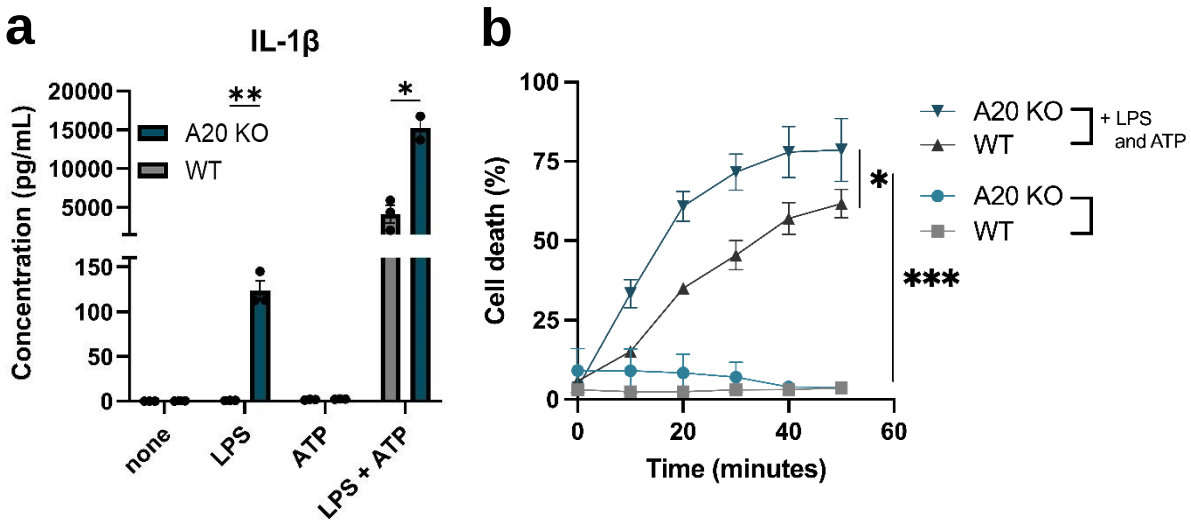

Figure 26. IL-1β levels and cell death percentage after NLRP3 inflammasome activation in bone marrow derived marcophages (BMDMs) from wild-type (WT) and A20$^{Myel-KO}$ (A20 KO) mice. BMDMs were isolated from WT (n = 3) and A20 KO (n = 3) mice, cultured at 1 x 10^6 cells per replicate and stimulated with lipopolysaccharide (LPS) 4 hours and/or ATP to activate the NLRP3 inflammasome. IL-1β concentration (pg/mL) was measured with multiplex immunoassay **(a)**. Statistical significance was determined using multiple non-parametric t-tests,*p < 0.05, **p < 0.01, ***p < 0.001, ****p < 0.0001.Cell death was assessed as the ratio of the number of sytox green stained cells (dying cells) and Draq5 stained cells (all cells) (**b**). For the cell-death data, an F-test on fixed-effects data was performed (*p < 0.05, ***p < 0,001). Results are displayed as mean ± SEM.

We next characterized the expression of *Malat1, Neat1, Miat*, and *Zfas1* under conditions of NLRP3 inflammasome activation using qPCR (Figure 27). The expression analysis revealed no significant results or trends for *Malat1*, *Neat1* and *Miat* (Figure 27a&b). We observed an upregulated trend of Zfas1 under LPS stimulation and under NLRP3 activation. Furthermore, significant differences between the different genotypes and stimulations were observed for *Miat* (Figure 26d), no further conclusions were drawn from these results.

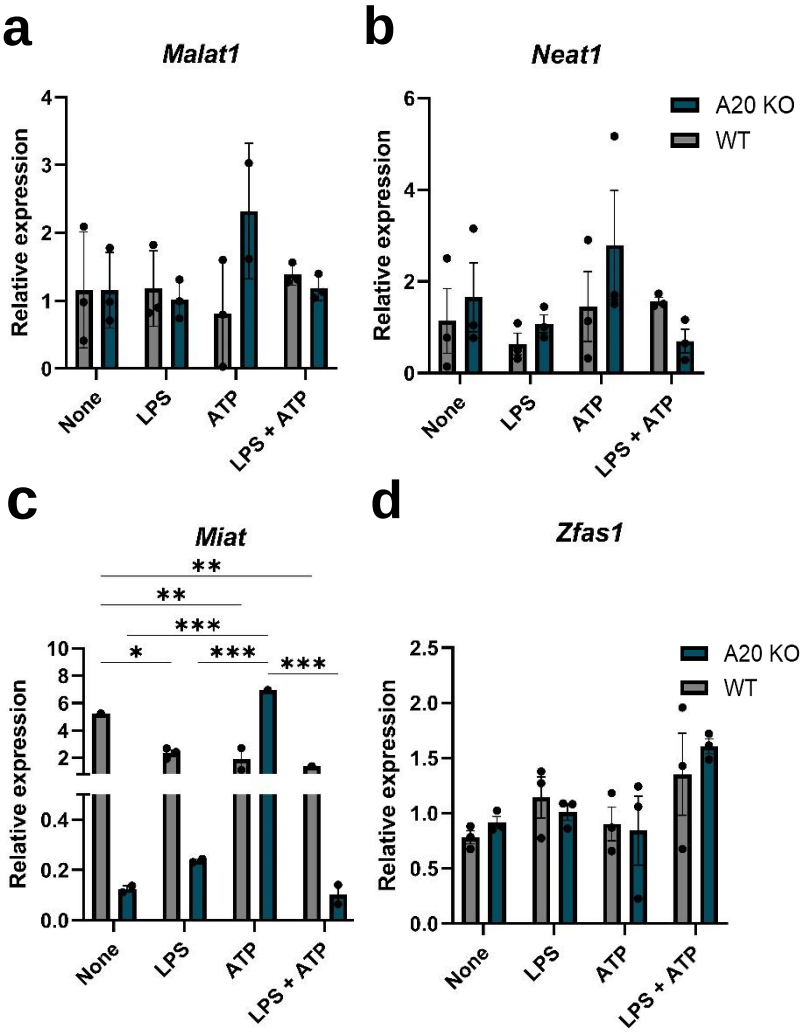

Figure 27. Relative gene expression levels of lncRNAs in bone marrow derived macrophages (BMDMs) from wild-type (WT) and A20$^{Myel-KO}$ (A20 KO) mice, after NLRP3 activation. BMDMs were isolated from WT (n = 3) and A20 KO (n = 3) mice, cultured at 1 x 10^6 cells and stimulated with lipopolysaccharide (LPS) 4 hours and/or ATP to activate the NLRP3 inflammasome. RT-qPCR was performed on RNA, isolated from these. The y-axis presents the relative expression levels of long non-coding (lnc)RNAs *Malat1* (***a***), *Neat1* (***b***), *Miat* (***c***) and *Zfas1* (***d***). All values were normalised to the expression of the housekeeping genes *Gapdh* and *Hprt*. Statistical significance was determined using two-way ANOVA with Sidak's multiple comparisons test, *p < 0.05, **p < 0.01, ***p < 0.001, ****p < 0.0001. Results are displayed as mean ± SEM .

3.3.3 STAT6 Signalling Pathway

An important aspect of resolving inflammation and inducing homeostasis is the promotion of an anti-inflammatory and alternative state of myeloid cells. Cytokines such as IL-4 and IL-10 play crucial roles in regulating this process. The binding of IL-4 to its cognate receptor on T-cells leads to the differentiation to Th2 cells, which are important in reducing neuroinflammation in EAE (Moulder et al., 2010). In macrophages, activation of the STAT6 pathway via the IL-4 receptor induces an alternative activated state that suppresses their pro-inflammatory profile (Yu et al., 2019). Therefore, we aimed to investigate the behaviour of the selected lncRNAs under STAT6 activation for their possible contribution to the resolution of inflammation.

After isolating and culturing BMDMs from A20$^{Myel\text{-}Ko}$ (A20 KO) and wild-type littermate (WT) mice, we stimulated them for four, eight and 24 hours with IL-4 or LPS. First, we examined the expression of Arginase-1 (*Arg1),* a well-known marker for the alternative activated macrophage state after IL-4 stimulation (Figure 28). The *Arg1* expression revealed a strong upregulation at four and eight hours of IL-4 stimulation, which declined at 24 hours in WT cells. A20 KO cells, however showed highest expression at 24 hours of IL-4 stimulation. *Arg1* expression was much lower in cells stimulated with LPS compared to the IL-4 stimulated cells. However they did show a trend of upregulation after 24 hours of LPS with higher levels of expression in the A20 KO BMDMs. These findings support the state of alternative macrophage activation after stimulation with IL-4.

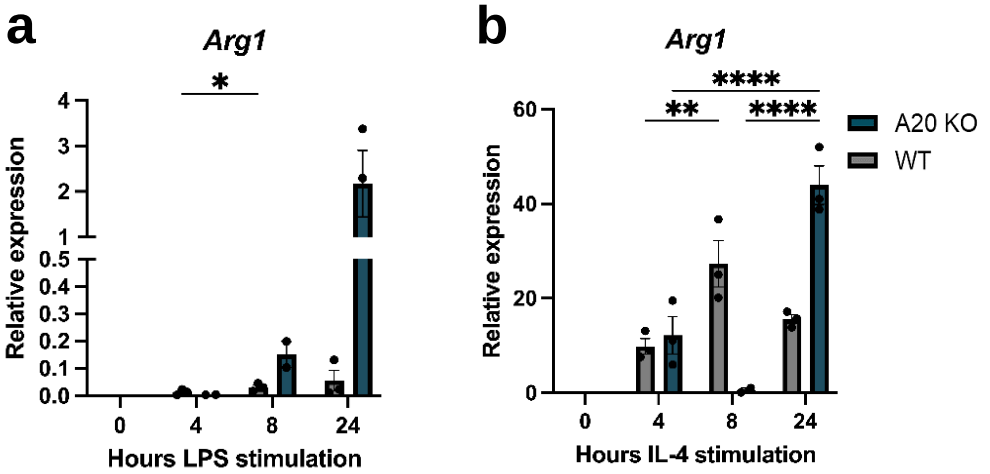

Figure 28. Relative gene expression levels of arginase-1 (*Arg1*) in bone marrow derived macrophages (BMDMs) from wild-type (WT) and A20$^{Myel\text{-}KO}$ (A20 KO) mice, after stimulation with either IL-4 or LPS. BMDMs were isolated from WT (n = 3) and A20 KO (n = 3) mice, cultured at 1 x 10^6 cells and stimulated with lipopolysaccharide (LPS) or interleukin (IL)-4 for 4, 8 and 24 hours. Here, the y-axis represents the relative expression of *Arg1,,* while the x-axis presents the hours of IL4 (**a**) or LPS (**b**) stimulation. All groups were normalised to the expression of the housekeeping genes *Gapdh* and *Hprt*. The values were statistically analysed using a two-way ANOVA analysis with Sidaks multiple comparison (*p < 0.05, **p < 0.01, ***p < 0.001, ****p < 0.0001). Results are displayed as mean ± SEM.

Next, we analysed the supernatant to measure the levels of TNF, IL-1β, IL-6, and IL-10 using a multiplex immunoassay assay (Figure 29). Our analysis confirmed the elevated expression of TNF, IL-1β and IL-6 levels under conditions of LPS stimulation, with higher levels of these pro-inflammatory cytokines in A20 KO cells (Figure 29a-c), as previously shown, but also showed upregulated expression of the anti-inflammatory cytokine IL-10 (Figure 29d). In contrast, IL-4-stimulated cells showed no detectable cytokine levels, except for IL-6, which increased after stimulation in the A20 KO group (Figure 29e-g). A20 KO cells also showed elevated expression of IL-10 after IL-4 stimulation (Figure 29h).

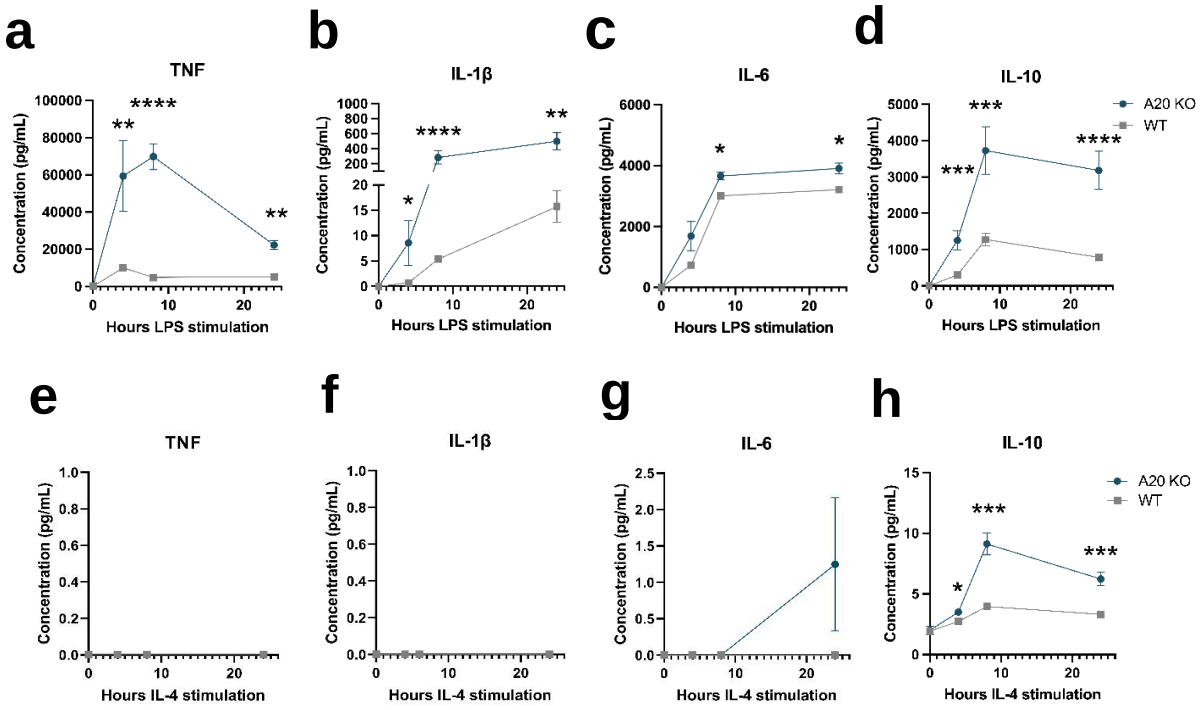

Figure 29. Cytokine levels in bone marrow derived macrophages (BMDMs) from wildtype (WT) and A20$^{Myel-KO}$ (A20 KO) mice, after stimulation with either IL-4 or LPS. BMDMs were isolated from WT (n = 3) and A20 KO (n = 3) mice, cultured at 1 x 10^6 cells and stimulated with lipopolysaccharide (LPS) or interleukin (IL)-4 for 4, 8 and 24 hours. Concentration(pg/mL) of cytokines TNF (**a&e**), IL1β (**b&f**), IL-6 (**c&g**) and IL-10 (**d&h**) in the supernatant was determined with a multiplex immunoassay The two genotypes were compared with each other at every time point using a Wilcoxon rank-sum test (*p < 0.05, **p < 0.01, ***p < 0.001, ****p < 0.0001). Results are displayed as mean ± SEM.

Subsequently, we examined the expression profiles of the four lncRNAs using qPCR (Figure 30). However, the analysis did not yield statistically significant results (Figure 30). Yet, we did observe a slight trend of downregulation for the lncRNAs *Malat1* and *Neat1* at four and eight hours of IL-4 stimulation (Figure 30e-f). Furthermore the previous trends were confirmed in conditions of LPS stimulation (Figure a-d). Moreover, *Zfas1* showed increased expression at 24 hours of LPS stimulation.

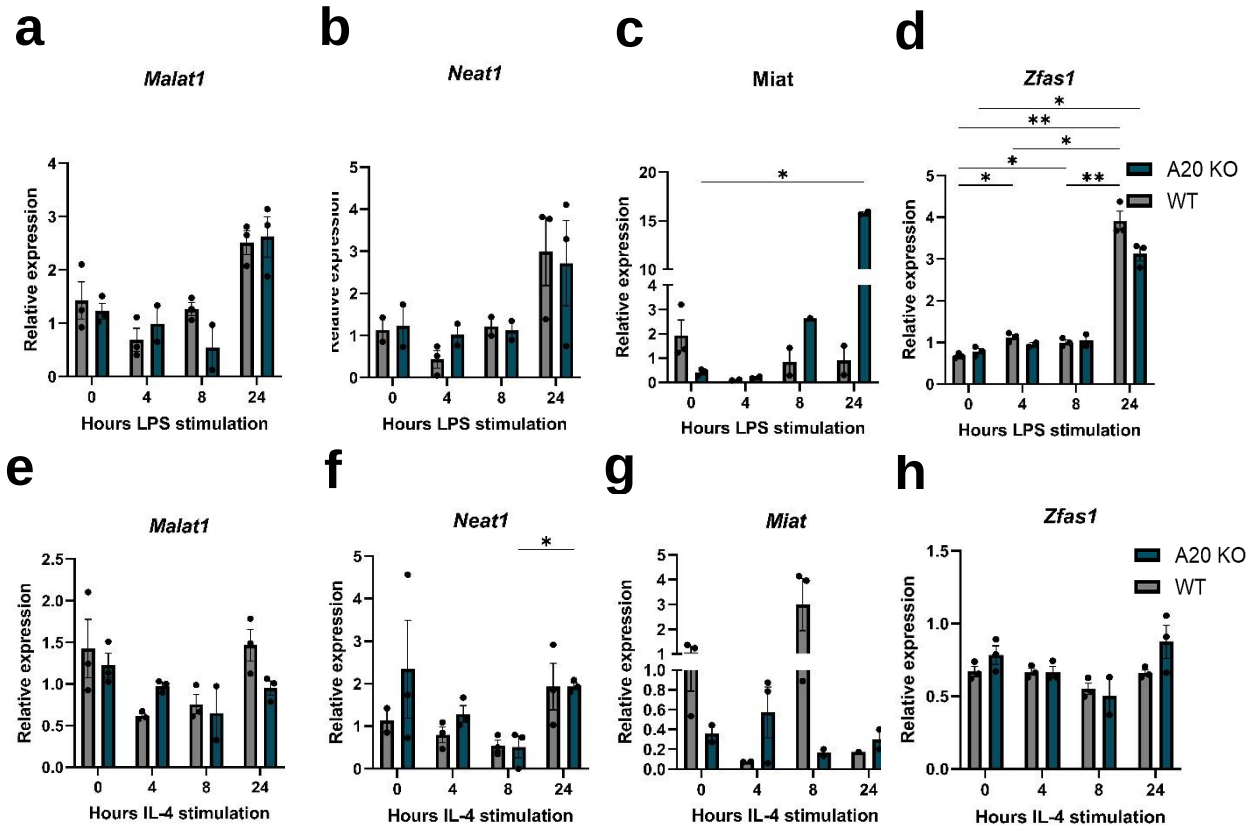

Figure 30. Relative gene expression levels of lncRNAs in bone marrow derived macrophages (BMDMs) from wild-type (WT) and A20$^{Myel-KO}$ (A20 KO) mice, after stimulation with either IL-4 or LPS. BMDMs were isolated from WT (n = 3) and A20 KO (n = 3) mice, cultured at 1 x 10^6 cells and stimulated with lipopolysaccharide (LPS) or interleukin (IL)-4 for 4, 8 and 24 hours. Furthermore RT-qPCR was performed on isolated RNA of the BMDMs. The y-axis represents the relative expression of long non-coding (lnc)RNAs *Malat1 (**a&e**), Neat1 (**b&f**), Miat (**c&g**)* and *Zfas1 (**d&h**),* while the x-axis presents the hours of IL-4 (**e-h**) or LPS (**a-d**) stimulation. All groups were normalised to the expression of the housekeeping genes *Gapdh* and *Hprt*. Statistical significance was determined using two-way ANOVA with multiple comparisons test, *p < 0.05, **p < 0.01, ***p < 0.001, ****p < 0.0001. Results are displayed as mean ± SEM.

3.3.4 Knockdown of Miat by Gapmers

Given *Miat's* putative role in regulating inflammatory signalling and neuroinflammation, based on our *in silico* analyses and our *in vivo* and *in vitro* characterization, we aimed to confirm its importance by neutralization studies using LNA-gapmers to suppress *Miat* expression and evaluate the consequential inflammatory response in BMDMs.

Gapmers are a type of antisense oligonucleotides (ASOs) that can target and degrade complementary RNA molecules through RNAse-H mediated degradation (Ward et al., 2014). ASOs are typically composed of 15 to 22 nucleotides (nt) and have RNA wings on both ends, with a central DNA sequence. To improve their efficacy, the RNA wings are mostly chemically modified, with common modifications including locked-nucleic acids (LNA), 2'-O-methoxyethyl, and phosphorodiamidate morpholino oligomer, and a phosphorothioate backbone (Kurreck et al., 2002). ASOs are a powerful tool for gene knockdown in both the cytosol and nucleus of cells, and have been extensively used in research because of their potential to be used as therapeutics (C. F. Bennett & Swayze, 2010).

To achieve knockdown of *Miat* in BMDMs without the need for transfection reagents, we opted to design gapmers with LNA wings and a phosphorothioate backbone. This approach is expected to increase the likelihood of successful knockdown of *Miat* while minimizing off-target effects.

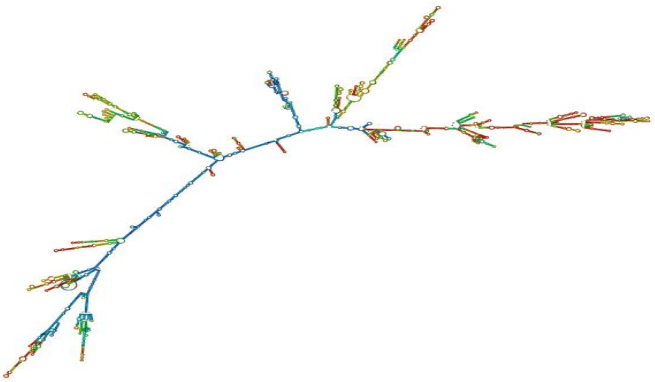

Figure 31. A possible secondary structure of the long non-coding RNA *Miat,* generated by the program mFOLD.

To design the gapmer, we first searched for open single-stranded sequences in the target transcript using the mFOLD online bioinformatic tool. The tool mFOLD is an integrated collection of programs that simulate nucleic acid folding and hybridization, based on the thermodynamic properties of intra-molecular connections, and presents all possible folding possibilities of a given transcript (Zuker, 2003). *Miat* is a transcript of 8716 nt that showed a lot of secondary structures (Figure 31). Since mFOLD is only able to process transcript of 2400 nt, we used a step-wise approach by taking intervals of 1000, 1500, and 2000 nt and looking for sequences of at least 15 nt in which every nucleotide was unbound, approximately 70% of the time out of all possible folding structures. We repeated this process to ensure the selected sequences were open in all possible secondary structures. Using this method, we identified eight potential sequences (number 1-8), which we converted to the complementary ASO sequences (Table 1).

Table 1. Candidate antisense oligonucleotides (ASOs) sequences for *Miat* knockdown. Potential target nucleotide (nt) sequences in *Miat* were obtained by looking for non-bound regions using the mFOLD bioinformatic tool. This analysis revealed 8 potential sequences of which we took the complementary sequence for antisense oligonucleotide (ASO) design. The green marked sequences exhibited optimal thermodynamic properties.

Number	Location (nt)	Sequence ASO (5'-3')
1	145-159	CCAUGAAAUUUUAAU
2	515_534	AUGAGAACAGACGGAA
3	2140-2156	AAAAAGAAAGAAAGAA
4	2323-2339	UCUUUCCAAGGUUCCUU
5	4588-4606	UGCUGCGGGGUUAGAAG
6	6925-6940	AGAAGACUUGAAGGUA
7	7358-7377	AUUGUUGGUGAAAUGUG
8	7353-7368	GGUGAAAUGUGGAAG

In the next step we analysed the thermodynamic properties of our sequences to fulfil to the following properties of a good gapmer: the free energy should be higher than -4kcal/mol for the ASO itself and higher than -16kcal/mol for ASO/ASO homodimers. In addition, the total binding energy, calculated by subtracting the free energy of the target sequence by that of the target/ASO duplex, should ideally range between 21-28 kcal/mol. The GC-content is optimal between 40-60%, preferably less than 50%, and melting temperature should be above 48°C. These different properties were evaluated using the online OligoAnalyzer™ Tool from Integrated DNA technologies (IDT) (Owczarzy et al., 2008).

First, the ASO numbers 1 and 3 did not have an optimal GC content, and ASO numbers 6 and 8 have their melting temperature too low. However, ASO numbers 2, 4, 5 and 7 did all have good thermodynamic properties including good free energy of itself and as homodimer. For all these ASOs we observed a slightly larger binding energy of around 31 to 33 kcal/mol, however the online analyzer tool only takes into account the folding of the specific complementary target sequence, neglecting the folding and energy of the complete transcripts. We went further to analyse these ASOs for off-target effects performing a cBlast search (Altschul et al., 1990)showing that ASO numbers 2 and 4 showed off-targets. ASO sequences 5 and 7, however, did not show any off-target effects and were chosen for further analysis. The ASO sequences 5 and 7 were modified with LNAs on the first and last 3 nucleotides of the gapmer. In addition we modified the backbone with phosphorothioate modications every 2 nucleotides to not affect the melting temperature, but still provide protection from breakdown by RNases.

Our experiment involved treating bone marrow-derived macrophages (BMDMs) obtained from A20 knockout (A20 KO) mice and wild-type (WT) littermate control mice with antisense oligonucleotides (ASOs) for a duration of four hours. Following this, the BMDMs were either stimulated with lipopolysaccharide (LPS) for an additional four hours or left unstimulated. RNA was isolated from the BMDMs, and we analyzed the expression levels of *Miat* (Figure 31). Based on our findings, we observed no significant decrease in *Miat* expression after the addition of the two ASOs compared to the control group. Similarly, there was no notable difference in expression levels when the scrambled ASO was added (Figure 31a). Furthermore, during the LPS-stimulated condition, we did not observe any significant difference in *Miat* expression (Figure 31b). Consequently, we concluded that the ASOs did not effectively modulate the expression of *Miat* as expected.

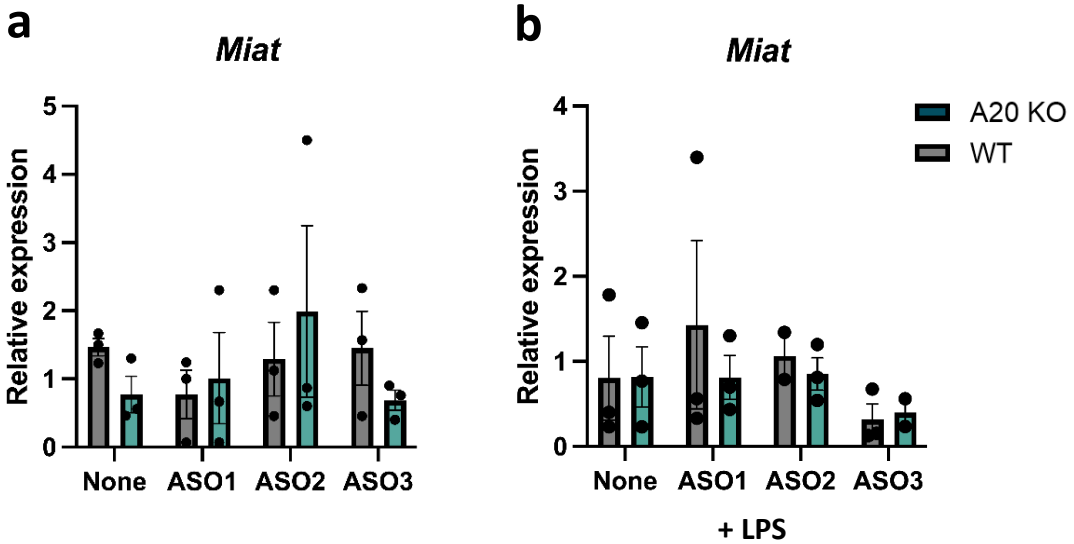

Figure 31. Relative expression of *Miat* in bone marrow derived macrophages (BMDMs) stimulated with antisense oligonucleotides (ASO) and LPS. BMDMs were isolated from WT (n = 3) and A20 KO (n = 3) mice, cultured at 1 x 10^6 cells and stimulated with ASO1 and ASO2 which target *Miat* , as well as a scrambled ASO3 which serves as a negative control. RT-qPCR was performed on RNA isolated from these in either condition of no stimulation **(a)** or lipopolysaccharide (LPS) stimulation (**b**). The y-axis presents the relative expression levels of *Miat*. Values were normalised to the expression of the housekeeping genes *Gapdh* and *Hprt*. Statistical significance was determined using two-way ANOVA with Sidak's multiple comparisons test.

Part 4: Discussion

Over the past decade, the significance of long non-coding RNAs (lncRNAs) has greatly increased due to emerging evidence showcasing their regulatory role in various cellular responses through diverse mechanisms on DNA, RNA and protein level (Statello et al., 2021). While their presumed central and complex role in neuroinflammatory diseases is widely recognized, our understanding of their precise functions remains limited (Tripathi et al., 2021b). Therefore, our study aimed to shed further light on the involvement of lncRNAs in neuroinflammation, with a specific focus on their contribution to neuroinflammatory processes in the experimental autoimmune encephalomyelitis (EAE) mouse model of Multiple Sclerosis (MS).

4.1 Identification of LncRNAs Involved in Neuroinflammation and EAE Pathology

Our *in silico* analyses have revealed the involvement of inflammation-related lncRNAs in both LPS-induced neuroinflammation and EAE neuroinflammation. This discovery highlights the previously overlooked and potentially significant roles of specific lncRNAs within these contexts. By elucidating their potential contributions to the molecular regulation of neuroinflammation, our findings enhance the understanding of these intricate processes and offer valuable insights for further research avenues in neuroinflammatory pathologies.

To gain insights into the general role of lncRNAs in neuroinflammation, we initiated our investigation by analysing the expression patterns of identified lncRNAs in LPS-induced neuroinflammation. Microglia-specific A20 knockout mice have hyperactivated microglia, exacerbating LPS-induced neuroinflammation, as previously demonstrated by the host laboratory (Voet et al., 2018) and further confirmed in our own investigation. In our study using an existing bulk RNAseq dataset of isolated microglia, we have unveiled distinct expression patterns of 10 lncRNAs strongly correlated with elevated levels of LPS-induced neuroinflammation. Notably, the lncRNAs *Malat1, Neat1, Miat, Snhg4, Snhg5, Cdkn2b-as1, Gm28309, Mirt2,* and *Oser-as1* exhibit downregulated expression, which correlates with increased inflammation markers. While a few of these lncRNAs have been studied in the context of microglia and LPS stimulation (Cui et al., 2019; Y. Jiang & Zhang, 2021; Z.-S. Jiang & Zhang, 2018; J. Li et al., 2022a; S.-X. Li et al., 2021; Y. Lyu et al., 2015; J. Wu et al., 2020), their specific expression profiles in microglia in the context of exacerbated neuroinflammation have not been previously established. Furthermore, only a limited number of lncRNAs have been associated with the regulation of A20 (Qi et al., 2020; H.-J. Zhou et al., 2022), thus presenting interesting research opportunities.

Indeed, our findings suggest that the identified lncRNAs play a significant role in the regulation of inflammation by microglia. Considering that A20 serves as an upstream regulator of inflammatory signalling, we propose that these lncRNAs function downstream of A20, as supported by their distinct downregulated expression in microglia obtained from unchallenged and LPS-stimulated $A20^{Cx3cr1\text{-}KO}$ mice compared to control mice. However, the precise mechanism by which these lncRNAs are influenced remains unclear, as determining the exact downstream mediators based on our results is challenging.

Previous studies have characterized the expression of these lncRNAs in response to various modulators associated with inflammation, such as NF-κB, STATs, MAPKs, inflammasome complexes and transcriptional repressors, processes that have previously been shown to be negatively regulated by A20 (Gupta et al., 2020; Tripathi et al., 2021b; Walther & Schulte, 2021). Building upon observations made by the host laboratory (Voet et al., 2018), we support our statement and hypothesize that any or all of these factors may contribute to the downregulation of the lncRNAs. Furthermore, based on their downregulation, we speculate that these identified lncRNAs may exert a negative regulatory role on the inflammatory response, as observed during neuroinflammation in conditions such as in Alzheimer's disease (AD) (Y. Liu et al., 2022b; X. Zhou & Xu, 2015). To gain further insight into the effect of A20 deficiency on the expression of lncRNAs, we would perform chromatin immunoprecipitation (ChIP)-sequencing of the aforementioned inflammation modulators and associated transcription repressors in our experimental settings. This approach will facilitate the identification of interactions between these factors and the promoters of the lncRNAs.

However, we must exercise caution when interpreting our results due to the limitations of our manual method for retrieving expression counts, as it may not align with the standard and accurate methodologies employed in the field. Our approach of mapping sequence data to the mouse genome and manually inspecting genome loci to retrieve expression counts of the lncRNAs introduces potential issues. These include the possibility of retrieving counts from untargeted genes, incorrect numerical count extraction for each gene, and potential normalization biases. Furthermore, while our study successfully revealed the downregulation of specific lncRNAs in microglia from LPS-stimulated $A20^{Cx3cr1\text{-}KO}$ mice, which correlated with increased expression of inflammation markers, it is important to note that further statistical validation should have been conducted to draw accurate conclusions. Regrettably, our manual method had certain limitations that prevented us from including an adequate number of genes for a comprehensive analysis. The constraints and potential biases inherent in our current manual approach for retrieving expression counts necessitate conducting a comprehensive total RNA sequencing analysis. We highly recommend performing a screening analysis using total RNA sequencing to overcome these limitations and obtain more accurate and comprehensive results.

Our analysis of lncRNA expression in LPS-induced neuroinflammation has provided valuable insights into their expression patterns and potential roles within this inflammatory context. These findings serve as a reference point for comparing results obtained from neuroinflammatory conditions such as MS, enhancing our understanding of the broader regulation of inflammation. Consequently, we can identify potential therapeutic targets that may have relevance in various inflammatory diseases.

Recognizing the crucial role of neuroinflammation in MS, our objective was to expand our understanding of lncRNA involvement in this specific context. To achieve this, we investigated inflammation-related lncRNAs in the EAE model. Previous studies have explored the regulatory role of specific lncRNAs such as *Gas5, Malat1*, and *linc-cox2* in EAE but without a comprehensive understanding of the broader significance of lncRNAs in regulating neuroinflammation in the EAE model (Masoumi et al., 2019; Sun et al., 2017; Xue et al., 2019). Additionally, a microarray study examined lncRNAs in EAE mice and activated astrocytes but primarily focused on the brain rather than the spinal cord (X. Liu et al., 2018). To bridge this

research gap, we aimed to identify specific lncRNAs associated with inflammation and exhibiting significant expression in the spinal cord tissue of EAE mice.

In our study, we conducted unbiased total RNA sequencing analysis on spinal cord tissue samples obtained from mice with EAE at two time points: day 9 and day 20 post-immunization. At day 9 of EAE, we observed minimal differential expression, primarily involving genes associated with the initiation of immune responses. Among the differentially expressed genes, we identified only two significant expressed lncRNAs, namely *B230208H11Rik* and *1110038B12Rik*. Furthermore, we noted that the level of neuroinflammation was also limited at this particular time point, which poses a challenge in establishing a direct connection between these lncRNAs and inflammation. Notably, these two annotated lncRNAs have not been previously associated with inflammation or immune responses in the literature. However, by uncovering these understudied lncRNAs, our findings shed light on their potential novelty in contributing to neuroinflammation during the early stages of EAE. Further exploration of their interactions with established inflammatory pathways and immune cells could provide valuable insights into their regulatory mechanisms and their potential as therapeutic targets or biomarkers in the future.

In contrast to the minimal differential expression observed at day 9, we observed a notable increase in neuroinflammation and significant expression of 557 lncRNAs at day 20 post-immunization. As a result, our primary focus was directed towards this specific time point in order to identify lncRNAs that are already known to regulate inflammation. Through this approach, we successfully identified 51 lncRNAs that have been documented in the literature as regulators of inflammation. Moreover, we validated a few of these lncRNAs in a coding non-coding coexpression analysis as well as unknown lncRNAs. It is important to note that while coexpression analysis offers insights into potential regulatory relationships, it should be interpreted cautiously, and additional functional analysis is necessary to fully elucidate their roles. Yet, our contribution is significant as it expands our knowledge of lncRNAs associated with EAE that have not yet been characterized in this specific context.

Interestingly, several lncRNAs identified in our study, such as *Malat1, Neat1, Snhg1, Sox2ot, H19, Norad, and Meg3*, have already been implicated in human patients with MS in previous studies (Akbari et al., 2022; Ghafouri-Fard et al., 2023; Nociti & Santoro, 2021; Torkamandi et al., 2021). It is worth noting that while some of these lncRNAs exhibit expression profiles that align with our observations, others show discrepancies. These differences can be attributed to their identification in specific cell populations or tissues investigated in these previous studies, whereas our focus is solely on the complete spinal cord tissue. To validate our findings in the EAE model against MS patients, we recommend performing single-cell total RNA sequencing on the brain, spinal cord tissue, and eventually blood samples. This approach will enable the analysis of the expression of the identified lncRNAs in specific cell types, providing a more comprehensive characterization of their role in the context of inflammation. By comparing our results with data from MS patients, we will gain further insights into the relevance and potential translational implications of these lncRNAs in human disease.

Finally, it is important to acknowledge the limitations and differences between the EAE mouse model and human MS in terms of disease progression and pathogenesis. The monophasic chronic disease course observed in MOG_{35-55} immunized EAE mice contrasts with the relapsing-remitting disease course typically seen in the majority of MS patients (Kipp et al., 2017). This disparity suggests that the identified lncRNAs in both EAE samples and MS patients

may have distinct roles and mechanisms due to the differential symptoms observed in these two contexts. Moreover, while some lncRNAs may exhibit similarities between mice and humans, not all lncRNAs are well conserved, and they may have different functions in mice compared to humans (Pheasant & Mattick, 2007). Therefore, caution should be exercised when extrapolating findings from mouse models to human disease. Additionally, it is worth noting that certain lncRNAs mentioned earlier have already been associated with inflammation in MS patients, while others may not have been extensively studied in this context. The observed expression patterns of these latter lncRNAs could potentially be influenced by other biological pathways, as evidenced by the significant findings in our gene ontology enrichment analysis. Therefore, it is crucial to consider the broader biological context and the potential involvement of additional pathways when interpreting the expression of these lncRNAs in relation to inflammation.

4.2 Characterization of selected lncRNAs *in vivo*

To enhance our comprehension of the role of lncRNAs in inflammation during EAE, we performed additional *in vivo* and *in vitro* characterization experiments. The primary objective of these experiments was to investigate the functional roles of the identified lncRNAs. As a result, we obtained valuable insights into the specific roles and regulatory mechanisms of these lncRNAs in the context of inflammation, not only in EAE but also potentially in human MS.

4.2.1 Selection of LncRNAs for Further Investigation

Due to limitation in time and high-throughput technology, it is impractical to characterize all 51 lncRNAs. As a result, we adopted a strategic approach and selected four lncRNAs for in-depth analysis. These lncRNAs were chosen based on their expression patterns observed in our preliminary experiments and their relevance to neuroinflammation and EAE as indicated by existing literature. This targeted selection aimed to uncover valuable insights into the potential functions and roles of these lncRNAs in the context of EAE.

Our study has identified a correlation between the downregulation of *Malat1* and general neuroinflammation. However, in the RNA-sequencing analysis of EAE mice at day 20, the expression of *Malat1* did not reach statistical significance. Nevertheless, it is important to note that our analysis revealed a downward trend in the expression of *Malat1,* although the statistical significance was not achieved. Furthermore, one study already demonstrated decreased expression of *Malat1* in the spinal cord of EAE mice, as well as in stimulated splenocytes and primary macrophages. Considering the substantial evidence from previous studies, we found it necessary to include *Malat1* in our investigation to explore its behaviour in our specific EAE models and further elucidate its contribution to neuroinflammation.

We also included the other well characterized lncRNA *Neat1*. This lncRNAs exhibits a correlated downregulation during general neuroinflammation. However, in the context of EAE pathology at day 20, we have observed an upregulation of *Neat1*. Interestingly, existing literature supports the upregulation of *Neat1* in MS patients (Nociti & Santoro, 2021). It is worth noting that the behaviour of *Neat1* can vary depending on the specific cellular context and the nature of the immune response. For instance, *in vitro* experiments using MG63 cells stimulated with LPS have demonstrated a decrease in *Neat1* expression (Dai et al., 2021). These findings suggest that the in vivo autoimmune response in EAE may have a different effect on *Neat1* compared to LPS stimulation. This highlights the complex and context-

dependent regulation of *Neat1* in the context of neuroinflammation and indicates the need for further investigation to fully understand the role of *Neat1* in EAE pathology and its potential implications in MS.

Furthermore, we observed a role for *Zfas1* and *Miat* in both LPS-induced neuroinflammation as well as in the spinal cord of EAE mice. The lncRNA *Zfas1* has primarily been studied in the context of neuronal injury, stroke and Parkinson's disease mouse models models (H. Yang & Chen, 2022; Y. Zhang & Zhang, 2020; Zhu et al., 2022) . Interestingly, while *Miat* has not been specifically investigated in the context of MS and EAE, studies have explored its role in microglial inflammation (J. Li et al., 2022b).). Considering the limited knowledge regarding the involvement of *Zfas1* and *Miat* in neuroinflammation and immune responses, we found it important to include these relatively understudied lncRNAs in our further analysis.

4.2.2 Malat1, Neat1, Miat and Zfas1 Regulate Neuroinflammation in EAE Mice

In our study, we utilized Pggt1b$^{CD4\text{-}KO}$ mice, which lack the β subunit of protein geranylgeranyl transferase-I (GGTase-I), and we observed complete protection from EAE and inflammation, as previously shown by the host lab (unpublished data van Loo group). GGTase-I is responsible for the lipidation of RHO family proteins, which play crucial roles in intracellular signalling pathways, including those involved in inflammation (Akula et al., 2016, 2019). Although this thesis did not aim to explain the mechanisms behind the observed protection from EAE in Pggt1b$^{CD4\text{-}KO}$ mice, we speculate that the differential regulation of RHO proteins in the T-cells leads to increased apoptosis and inhibition of cell migration. As a result, the ability of T-cells to be activated and infiltrate the CNS is impaired. In our study, we confirmed the absence of neuroinflammation in the spinal cord of immunized Pggt1b$^{CD4\text{-}KO}$ mice. This finding has significant implications as it allowed us to investigate the correlation between neuroinflammation and the expression of the selected lncRNAs, while excluding any potential confounding effects of the immunization process. Importantly, we found that the expression patterns of the selected lncRNAs in the knockout mice closely resemble those observed in unchallenged control mice in the sequencing analysis. Specifically, *Malat,* and *Miat* show an upward trend in expression in Pggt1b$^{CD4\text{-}KO}$ EAE mice compared to control EAE mice, while *Zfas1* exhibited the expected downregulation. The lncRNA *Neat1* does not show the expected downregulation as expected from our previous findings. We suggest the possible off-targeting of the *Neat1* primers or a different role in these specific EAE transgenic mice.

We further characterized the role of the lncRNAs in EAE 'hypersensitive' mice models in order to understand their contribution to neuroinflammation in these, possibly revealing how these lncRNAs contribute to their sensitivity.

Our initial focus was on examining the expression profiles of the identified lncRNAs in A20$^{Cx3cr1\text{-}KO}$ (A20 KO) mice. These mice have been previously demonstrated to develop early onset and more severe EAE disease compared to the control mice (Voet et al., 2018), which we could confirm. We observed the presence of neuroinflammation in both groups of EAE mice, with no significant difference observed between the control and A20 KO mice. This finding contrasts with previous results from the host lab, which showed a significant increase in *Il1β* expression in the A20 KO EAE mice compared to the EAE control group (Voet et al., 2018). We suggest that the observed variation in our study could potentially be attributed to the timing of spinal cord isolation for analysis of *Il1β* expression, which was performed at a later time

point compared to the initial study. However, we could confirm high *Il1β* expression in non-immunized A20 KO mice, as previously shown (Voet et al., 2018).

In EAE mice, we observed downregulation of the lncRNAs *Malat1, Neat1, Miat*, with no significant difference between the knockout and control groups. Interestingly, similar downregulation was also observed in unchallenged A20$^{Cx3cr1\text{-}KO}$ mice, which aligns with *our in silico* analysis of these mice. We attribute this observation to the presence of *Il1β* expression in the knockout mice, which is a consequence of Nlrp3 hyperactivation within the CNS of A20 KO mice (Voet et al., 2018). Notably, our identified lncRNAs have previously been associated with Nlrp3 activation in other studies (Dai et al., 2021; Wang et al., 2021; Y. Zhang & Zhang, 2020). However, these results indicate context-specific regulation, likely involving interactions with various miRNAs and proteins. Consequently, we propose a potential context-specific role for these lncRNAs during Nlrp3 activation in the context of EAE. Additionally, our analyses, which include both RNA-seq and qPCR experiments, revealed the downregulation of the lncRNA *Zfas1* in unchallenged A20 knockout mice, followed by its upregulation during EAE. This contrasting expression pattern suggests a different role for *Zfas1* during general neuroinflammation characterized by Nlrp3 activation, such as in the autoimmune reaction during EAE.

In our investigation using OTULIN$^{Cx3cr1\text{-}KO}$ (OTU KO) mice, which exhibit similar characteristics to A20 KO mice and display 'hypersensitivity' to EAE (unpublished data van Loo group), we have discovered intriguing findings regarding the selected lncRNAs. Firstly, we observed comparable regulatory trends to our previous EAE analysis, indicating consistent downregulation of the lncRNAs *Malat1, Neat1,* and *Miat* in the context of EAE. However, in unchallenged OTULIN knockout mice, we noted a contrasting trend of upregulation for the lncRNAs *Malat1, Neat1*, and *Miat*, as opposed to the unchallenged control mice and EAE mice. These results diverge from our observations in unchallenged A20$^{Cx3cr1\text{-}KO}$ mice, where downregulation of these lncRNAs was observed. The contrasting expression patterns in unchallenged OTULIN knockout mice suggest that the absence of OTULIN may have distinct effects on the regulation of these lncRNAs compared to A20 deficiency. To fully comprehend the underlying mechanisms and functional roles of these lncRNAs, further investigations are necessary, including detailed characterization of the OTULIN knockout mice and exploring potential interactions with other molecules and signalling pathways.

Based on our findings, we propose a model that provides a plausible explanation for the observed patterns of lncRNA expression and their potential role in neuroinflammation. According to this model, the lncRNAs initially function as a "brakes" to regulate and suppress neuroinflammatory responses. However, their ability to maintain this regulatory effect is compromised when significant neuroinflammation is present. Our proposition is supported by the observation of lncRNA upregulation in non-immunized OTU KO mice, which exhibit hyperactivated microglia, despite the absence of upregulated neuroinflammation markers. In this condition, we postulate that the deletion of OTULIN results in the upregulation of NF-κB, which initiates a negative feedback loop involving the lncRNAs to deactivate NF-κB and serve as a compensatory mechanism to suppress neuroinflammation. However, when neuroinflammation becomes more pronounced, as evidenced by increased expression of *Il1β* and hyperactivated microglia in non-immunized A20 KO mice, we observe the downregulation of the lncRNAs. We propose that this downregulation may be attributed to downstream mediators of IL-1β receptors or an amplified effect of NF-κB partners.

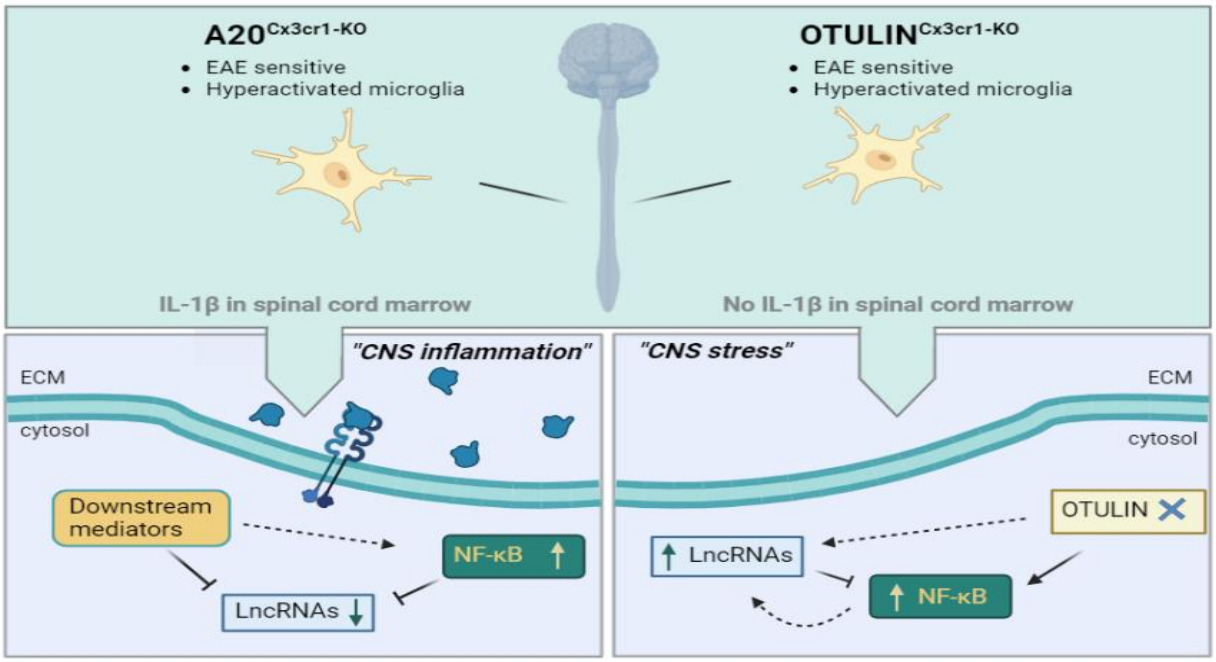

Figure 32. Regulation effect of lncRNAs on inflammation response in the central nervous system (CNS). In this proposed model, we depict the possible regulatory effect of long non-coding (lnc)RNAs on the inflammation response in the CNS. The lncRNAs act as a "safety mechanism" to initially regulate and suppress neuroinflammatory responses. However, their ability to maintain this regulatory effect diminishes in the presence of prominent neuroinflammation. Under "CNS stress" conditions, we postulate that the deletion of OTULIN in microglia (OTULIN$^{Cx3cr1\text{-}KO}$) leads to the upregulation of NF-κB, initiating a negative feedback loop involving the lncRNAs, which inactivate NF-κB and help to suppress neuroinflammation. However, when neuroinflammation becomes more pronounced, the lncRNAs are downregulated. This downregulation may be influenced by downstream mediators of IL-1β receptors or an amplified effect of NF-kB partners, which override the regulatory function of the lncRNAs.

Previous studies have reported the involvement of the lncRNA *Malat1* in feedback loops with NF-κB signaling (Gupta et al., 2020), suggesting a direct connection. However, for the lncRNAs *Neat1* and *Miat*, while they have not been specifically associated with direct NF-κB signalling loops, they have been implicated in indirect interactions with NF-κB signalling pathways (Dai et al., 2021; J. Li et al., 2022a). Regarding the effect of OTULIN KO on NF-κB, it is interesting to note that increased NF-κB activation was not observed in LPS-stimulated primary microglia (unpublished data van Loo group). In our proposed model, we suggest an indirect effect in which the hyperactivation of microglia in OTULIN KO mice leads to an impact on NF-κB signalling in the complete spinal cord. Furthermore, downstream effects of these lncRNAs have been reported in literature, including interactions with signalling pathways involving STATs, MAPKs, and inflammasomes, as mentioned above (Tripathi et al., 2021a). Considering the A20 knockout in microglia, which is known to induce Nlrp3, we propose that Nlrp3 may serve as the main mediator for the observed downregulation of lncRNAs in EAE and in A20$^{Cx3cr1\text{-}KO}$ mice. Nlrp3 activation could potentially influence the expression and function of these lncRNAs, leading to their downregulation in the context of neuroinflammation. To further investigate and validate these hypotheses, we suggest performing single-cell CHIP and total RNA-sequencing experiments in these transgenic mice. These techniques will provide valuable insights into the specific cellular interactions of the lncRNAs with inflammation and help elucidate the intricate mechanisms underlying their regulation in neuroinflammatory processes. Moreover by executing Chromatin Isolation by RNA purification (ChiRP)-

sequencing, we will be able to know which lncRNAs bind to specific DNA sequences with chromatin-remodelers and transcription factors and consequently regulate the expression of inflammation mediators such as NF-κB and many others.

In conclusion, our *in vivo* experiments have shed light on the correlation between neuroinflammation in EAE and the expression profiles of the selected lncRNAs. Through our findings, we have proposed a plausible model for the regulation of these lncRNAs in the context of EAE neuroinflammation, providing insights into their potential mechanisms of action in influencing the inflammatory response and contributing to EAE pathogenesis. Furthermore, our study highlights the utility of the chosen mouse models in understanding the role of lncRNAs in neuroinflammation. These models have allowed us to uncover valuable information about the expression patterns of these lncRNAs in different contexts and their potential implications in neuroinflammation.

4.3 Characterization of Selected LncRNAs *in vitro*

The use of the studied mouse models has provided valuable evidence for the involvement of lncRNAs in neuroinflammation during EAE. Additionally, by investigating the expression of these lncRNAs in stimulated bone marrow-derived macrophages (BMDMs), we have gained direct insights into the influence of specific inflammation signalling pathways on the regulation of these lncRNAs. This approach has allowed us to deepen our understanding of the regulatory roles of lncRNAs in macrophages and their functional impact on the inflammatory response.

Our *in vitro* experiments have provided us with valuable regulatory trends, but we acknowledge the challenges posed by substantial variation among biological replicates, preventing us from drawing statistically significant conclusions. We hypothesize that the observed variability could be attributed to differences in the number of cells used in each replicate. Since certain lncRNAs are expressed at relatively low levels, even minor variations in cell numbers could contribute to noticeable differences between replicates. It is worth noting that such significant variance was not observed for other transcripts, including *Tnf, Il6, Il1β*, and the housekeeping genes. To address this issue in future experiments, it is crucial to take steps to minimize discrepancies in cell numbers during the plating process. Additionally, maintaining a consistent and adequate cell density, and using more than 1×10^6 cells per well, can reduce the impact of cell number variations and improve the statistical significance of the results. In addition, employing targeted RNA-sequencing with a biased approach, such as using pre-designed panels targeting specific lncRNAs of interest, may offer a more sensitive and robust alternative to RT-qPCR. By implementing these measures, we can enhance the reliability and reproducibility of in vitro experiments investigating the regulatory roles of lncRNAs in the context of inflammation and further improve our understanding of their functional impact on the immune response.

Although we were unable to achieve statistically significant results in our *in vitro* experiments due to substantial variation between biological replicates, the observed trends in lncRNA expression suggest a potential relationship between signalling pathways and the regulation of these lncRNAs. While we cannot draw definitive conclusions based on these trends alone, they provide valuable insights that could help explain the results observed in our *in vivo* investigations. Additionally, they indicate the need for further investigation.

Based on our preliminary experiments, we consistently observed a significant presence of the central inflammatory mediator NF-κB. This suggests that NF-κB may play a crucial role as one of the main mediators influencing the expression levels of the studied lncRNAs. The trend of downregulation of the lncRNAs *Malat1* and *Miat* in BMDMs upon NF-κB activation by LPS aligns with our *in vivo* results and *in silico* analyses. However, it is important to note that a previous study has reported conflicting findings regarding the regulation of *Malat1* upon LPS stimulation in BMDMs(Cui et al., 2019). Regarding *Miat*, a previous study demonstrated its upregulation after LPS stimulation in human macrophages (Wang et al., 2021). As lncRNAs can exhibit varying behaviours in different cell types and may differ between mouse and human systems (Pheasant & Mattick, 2007), the differences observed could be due to cell type-specific responses or species-specific variations.

Our study highlights the significant role of the Nlrp3 inflammasome, in addition to NF-κB. The observed upregulation of the lncRNA *Zfas1* in both control and A20 knockout BMDMs under Nlrp3 and NF-κB activation aligns with the results obtained from in vivo experiments conducted in the EAE model. Interestingly, in unchallenged $A20^{Cx3cr1\text{-}KO}$ mice, both the RT-qPCR experiments and in silico analysis demonstrate downregulation of *Zfas1*. This downregulation indicates the involvement of another mediator that is active specifically in $A20^{Cx3cr1\text{-}KO}$ mice and contributes to the decrease in *Zfas1* expression. To better understand this discrepancy, we propose to use the above stated 'multi-omics' approaches to know the transcription modulators of this lncRNA during neuroinflammation and EAE.

Furthermore, understanding the regulatory mechanisms underlying the resolution of inflammation and the induction of an alternative activated state in myeloid cells, such as microglia, is crucial for developing effective therapies to modulate neuroinflammation in the context of MS pathology (Ponomarev et al., 2007). Our study examined IL-4-stimulated BMDMs to investigate these mechanisms. While the results were inconclusive due to variation between biological replicates, we did observe a slight trend of downregulation of *Malat1* and *Neat1* at certain time points, which aligns with the observed expression patterns during EAE pathology (Figure 29). Also in EAE, the presence of such markers indicative of an alternative activated state could be observed. These findings suggest a potential pleiotropic effect of the lncRNAs, where they may contribute to the regulation of other molecular markers involved in the induction of activated states, both anti-inflammatory and proinflammatory. Further investigations are needed to fully elucidate the specific roles and mechanisms by which these lncRNAs exert their regulatory effects in myeloid cells during different inflammatory states.

Last due to the significant role of *Miat* in our results we tried to further characterize this lncRNA in the context of myeloid inflammation. However, based on the expression of *Miat*, we concluded that the gapmers did not work. The lack of significant changes in the expression of *Miat* could have several explanations. One possibility is that the gapmers were not efficiently entering the BMDMs. While lipofectamine is commonly used to facilitate the introduction of molecules into cells, it is known that phosphorothioate modified ASOs can enter cells without the assistance of lipofectamine at appropriate concentrations (Rego et al., 2011). Moreover, previous experimental setups have shown successful uptake of naked modified ASOs into cells via endocytosis (Geary et al., 2015). However, it is also important to consider other factors that could contributed to the lack of observed effects. The efficacy of knockdown may vary depending on the specific sequence and characteristics of the target RNA. Additionally, the gapmers could be susceptible to degradation or sequestration within

the cells, reducing their effectiveness (Geary et al., 2015). Optimization of gapmer concentration and delivery methods, such as exploring different transfection reagents or delivery systems, could also improve their efficiency in entering the cells and reaching the target RNA.

4.4 Conclusions and Future Perspectives

In our study, we identified 51 lncRNAs that are significantly expressed in the spinal cord during the peak of EAE. While some of these lncRNAs have been previously associated with in MS patients, employing 'multi-omics' approaches like single-cell RNA sequencing and CLIP-sequencing would provide deeper insights into their role in regulating inflammation in EAE and MS. Furthermore, a large part of the 557 significant expressed lncRNAs are not yet characterized. While, we used a coding non-coding coexpression network analysis and revealed the potential of some unknown lncRNAs, functional experimentation is needed to know their exact role. However, we opened a road for further research on investigating these lncRNAs in the context of neuroinflammation and MS. Furthermore, to elucidate the contributions of some specific lncRNAs to EAE, we performed comprehensive characterizations of four lncRNAs: *Malat1, Neat1, Miat,* and *Zfas1.* We ultilized A20$^{Cx3cr1\text{-}KO}$ and OTULIN$^{Cx3cr1\text{-}KO}$ mice, which exhibit heightened sensitivity to EAE and display hyperactivated microglia even in unchallenged conditions. During all EAE conditions, we observed downregulation of *Malat1, Neat1 and Miat,* while *Zfas1* showed upregulation. Notably, in the spinal cord of non-immunised A20$^{Cx3cr1\text{-}KO}$ mice, *Malat1, Neat1 and Miat* were downregulated, whereas non-immunised OTULIN$^{Cx3cr1\text{-}KO}$ mice showed upregulation of these lncRNAs. Furthermore, in Pggt1b$^{CD4\text{-}KO}$ EAE mice we observed the expected findings as in unchallenged wild-type mice. All these findings support the notion that *Malat1, Miat*, and *Neat1* act as "brakes" to balance and counteract the inflammatory response. However, conditions of prominent neuroinflammation, such as in EAE, seems to compromise the ability of lncRNAs to restrain inflammation. To validate this hypothesis, we propose conducting the aforementioned 'multi-omics' approach in these transgenic mice. to enhance our understanding of their role in MS pathogenesis. Next, we aimed to investigate the impact of inflammatory pathway activation on the expression of the identified lncRNAs specifically. To achieve this, we examined their expression in BMDMs, which provided insights into their potential role in regulating inflammation in these cells. However, due to significant variation between biological replicates, we were unable to draw definitive conclusions regarding the effect of NF-kB, Nlrp3 inflammasome and STAT6 activation on the lncRNAs. Nonetheless, certain trends aligned with the expression patterns observed *in vivo,* suggesting pleiotropic roles for these lncRNAs in regulating activation of myeloid cells in both pro-inflammatory and anti-inflammatory states. Future studies should focus on optimizing technical details to investigate lncRNA expression in BMDMs, aiming to gain a better understanding of their integration into myeloid inflammation signalling.

Furthermore, in our efforts to gain insights into the role of *Miat* during inflammation, we employed silencing techniques. Although the specific experiments using antisense oligonucleotides (ASOs) did not yield the desired results, it is important to acknowledge that ASOs have shown promise in treating neurological diseases and targeting lncRNAs in previous studies (Wurster & Ludolph, 2018). For example, a study demonstrated the effective delivery of DNA/RNA heteroduplex oligonucleotides (HDOs) conjugated to cholesterol or α-tocopherol to the CNS following subcutaneous or intravenous administration in mice and rats (Nagata et

al., 2021). These HDOs were efficiently distributed throughout the brain, spinal cord, and peripheral tissues, leading to significant suppression (up to 90%) of four target genes in the CNS. Targeting specific lncRNAs through such mechanisms has also shown promise (Hsiao et al., 2016), although further optimization is required to develop effective therapies. Undoubtedly, lncRNAs have emerged as intriguing potential targets for the treatment of neuroinflammatory conditions. Not only because of their significant contributions to pathologies, but also due to their cell and context-specific roles, consequently reducing possible side effects. Our research has significantly contributed to the identification of potential targets in the context of MS and general neuroinflammation. However, there is still much to be discovered in order to fully unravel the therapeutic potential of lncRNAs in these conditions.

Part 5: Materials and Methods

Animals. Conditional A20 knockout mice harboring two loxP sequences flanking exons 4 and 5 ($A20^{FL/FL}$) were generated as previously described . $A20^{FL/FL}$ mice were crossed with Cx3Cr1Ert2-Cre transgenic mice to generate $A20^{Cx3cr1\text{-}KO}$ or to Lysm-Cre transgenic mice to generate $A20^{Myel\text{-}KO}$mice (Catrysse et al., 2014). Mice with conditional loxP-flanked *Otulin* alleles (Verboom et al., 2020) were crossed with Cx3Cr1Ert2-Cre mice to generate $OTULIN^{Cx3cr1\text{-}KO}$ mice. Mice with conditional loxP-flanked *Pggt1b* alleles were a kind gift of Prof. Martin Bergo, Karolinska Institute, Stockholm, Sweden. $Pggt1b^{FL/FL}$ were crossed in house with CD4-Cre transgenic mice to generate $Pggt1b^{CD4\text{-}KO}$ mice.

All alleles were maintained on a C57BL/6 genetic background. Mice were housed in individually-ventilated cages at the VIB Center for Inflammation Research, in a specific pathogen-free animal facility. All experiments on mice were conducted according to institutional, national, and European animal regulations. Animal protocols were approved by the ethics committee of Ghent University

Induction and assessment of EAE. Eight- to 26-week-old littermate mice were immunized subcutaneously with an emulsion of 200 µg $MOG_{35–55}$ (MEVGWYRSPFSRVVHLYRNGK) peptide in 100 µl sterile PBS and an equal volume of complete Freud's adjuvant (CFA, Sigma-Aldrich) supplemented with 10 mg/ml *Mycobacterium tuberculosis* H37RA (Becton Dickinson Bioscience). In addition, mice also received 50 ng of pertussis toxin (Sigma-Aldrich) in 200 µl sterile PBS at the time of immunization and 48 h later. Before MOG injection, mice were anaesthetized with 10 ng xylazine and 10 ng ketamine in 200 µl PBS, per 25 gram body weight. Clinical signs of disease were scored on a scale of 0–5, with 0.5 points for immediate clinical findings as follows: 0, normal; 1, weakness of tail; 2, complete loss of tail tonicity; 3, partial hind limb paralysis; 4, complete hind limb paralysis; 5, forelimb paralysis or moribund. To eliminate any diagnostic bias, mice were scored blindly. In addition, body weight during disease progression was registered.

RNA extraction. Spinal cord tissue of EAE and non-immunized mice was collected and homogenized using 700 µL of lysis buffer (Qiagen miRNeasy isolation kit), followed by mechanical homogenization with beads. The tissue was lysed in a tissue lyser (two times 5 min with a frequency of 20/s), and RNA was extracted according to the manufacturer's instructions (Qiagen, attachments). In addition, RNA was extracted from BMDMs according to the manufacturer's instructions (Biorad, attachments). RNA concentration and purity were determined spectrophotometrically using the Nanodrop (ND-100, Isogen Life Science) Technology.

Total RNA sequencing. Generation of cDNA and library preparation (SMARTer Stranded Total RNA-seq Kit v3 -Pico input mammalian) were performed according to manufacturer's protocols (attachments). The sequencing libraries were sequenced on an Illumina NextSeq™ 550 sequencer. Basecalling and Fastq file generation was performed using standard Illumina software (RTA, Casava). Fastq files were analyzed for data quality using FastQC v0.11.553 (FastQC: a quality control tool for high-throughput sequence data. Available online at: http://www.bioinformatics.babraham.ac.uk/ projects/fastqc.) Sequences were aligned to the

mouse genome assembly GRCm39 as provided by the GENCODE project54 using the Star aligner v2.5.2b55. Aligned reads were counted using featureCounts v1.5.156.

Bioinformatic analysis for RNA sequencing data. The DESeq2 tool in R was used to normalize and statistically analyse differential expression of the transcripts. The GSEA databank was used to perform gene ontology enrichment analysis. The weightened correlation network analysis (WGNA) package was used to identify network hubs and calculate the Pearson's correlation coefficient. In this analysis all annotated long non-coding (lnc)RNAs were included as well as transcripts of NF-κB signalling mediators. Direct connections with the inflammation transcripts with a Pearson's correlation coefficient r > 0,55 were mapped using the Cytoscape tool.

Primary bone marrow derived cell cultures. Bone marrow cells were isolated from tibia and femurs from $A20^{Myel\text{-}KO}$ and control wild-type littermate mice by flushing the bones with RPMI medium 1640 (Thermo Fisher Scientific) through a syringe and a G26 needle on a 100 µM cell strainer. Next, the cells were spun down for 5 min at 1000 rpm and resuspended in RPMI medium 1640 supplemented with 100 ng/ml macrophage colony stimulating factor (MCSF, made inhouse), 10% fetal bovine serum (Thermo Fisher Scientific), 25 units/mL penicillin, 25 µg/mL streptomycin (Thermo Fisher Scientific) and L-glutamine (Lonza), and plated in 9 cm bacterial plates in quadruplicate. Every 48 hours, the medium was refreshed and on day 6 bone marrow derived macrophages (BMDMs) were seeded for further experiments. To determine the precise cell concentration for each biological sample, the cells were harvested and resuspended in RPMI medium supplemented with MCSF. First, after removal of the supernatant, cells were scraped with 10 µL cold PBS and collected in a 50 mL Falcon tube. The cells were pelleted by centrifugation at 1000 rpm for 5 minutes and then resuspended in RPMI medium with MCSF. The cell concentration was determined using an automated cell counter, Luna II TM, by mixing 10 µL of the cell suspension with 10 µL of trypan blue. The cell suspension was further diluted to a concentration of 1 x 10^6 cells/mL for seeding.

BMDM stimulation. BMDMs, obtained from three $A20^{Myel\text{-}KO}$ mice and three control wild-type littermate mice, were plated at a density of 1 x 10^6 cells per well in 6-well plates. The cells were stimulated (or not) with 20 ng/mL lipopolysaccharide (LPS, LPS Ultrapure, E. coli 0111:B4 from Invivogen) for 2, 4, 6, and 24 hours. To activate the NLRP3 inflammasome, BMDMs were primed with 20 ng/mL LPS for 4 hours, followed by stimulation with 20 mM ATP for 45 minutes. Alternatively, cells were treated with 10 ng/mL IL-4 (prepared in-house) for 4, 8, and 24 hours. After the time of stimulation, cells were washed twice with ice-cold Dulbecco's phosphate buffered saline (D-PBS, Invitrogen) and scraped in 500 µL Trizol (Invitrogen) for RNA isolation. In addition, 200 µL supernatant was isolated for further analysis of cytokine levels.

Antisense Oligonucleotides. Antisense oligonucleotides (ASOs) were designed as described in the result section. The secondary structure of *Miat* was analysed using the bioinformatic tool mFOLD to detect open single stranded RNA sequences of at least 15 nt. Potential ASO sequences were further investigated for their thermodynamic properties. The free energy should be higher than -4kcal/mol for the ASO itself and higher than -16kcal/mol for ASO/ASO homodimers. In addition, the total binding energy, calculated by subtracting the free energy of the target sequence by that of the target/ASO duplex, should ideally range between 21-28 kcal/mol. The GC-content is optimal between 40-60%, preferably less than 50%, and melting

temperature should be above 48°C. These different properties were evaluated using the online OligoAnalyzer™ Tool from Integrated DNA technologies (IDT). The following ASOs were ordered at Eurogentech: {A*T*T*}G*T*TG*GT*GA*AA*TG*TG*G*{A*A*G}, {T*G*C*}T*G*CG*GGG*TT*A*{G*A*A}, {A*G*G*}T*A*GT*AG*GT*TG*AT*AT*A*{G*T*G}. {} = Locked nucleic acids, * = phosphorothiate. ASOs were dissolved in TE buffer (Biorad) to a concentration of 1000 µM. The ASOs were administered to the BMDMs for 4 or 24 hours (10 µM) after which they were stimulated with LPS for 4h. RNA was isolated and qPCR was performed, as mentioned above.

Cell death assay. To allow for cell attachment and recovery, 40,000 cells per well were seeded in RPMI medium supplemented with 100 ng/mL macrophage colony-stimulating factor (MCSF, prepared in-house), 10% fetal bovine serum (Thermo Fisher Scientific), 25 units/mL penicillin, 25 µg/mL streptomycin (Thermo Fisher Scientific), and L-glutamine (Lonza). The cells were incubated at 37°C, 5% CO2 overnight. After the incubation, the cells were stimulated with 20 ng/mL LPS, and Sytox green (Invitrogen) and Draq5 (Thermo Fisher Scientific) were added to the medium. After 4 hours, the cells were further stimulated with 20 mM ATP in Sytox green (Invitrogen) and Draq5 (Thermo Fisher Scientific), and cell death was monitored every 10 minutes for 1 hour in the Sartorius Incucyte Live-cell analysis system. The percentage of cell death was calculated as the number of Sytox green-stained cells divided by the total number of cells stained with Draq5 using the Incucyte Base analysis software.

Quantitive real time PCR on BMDMs and spinal cord tissue. After RNA isolation and quantification, cDNA was synthesised from 1000 ng RNA by using the SensiFAST cDNA Synthesis Kit according to the manufacturer's instructions (supplementary). A total of 10 ng cDNA was used for real time quantitative PCR in a total volume of 10 µl with 5 µl LightCycler 480 SYBR Green I Master Mix (Roche) and 1µL of (5 µM) specific primers (Table 1), on a LightCycler 480 (Roche). Real-time PCR reactions were performed in triplicates.

Table 2. Sequences of forward and reverse primers for real-time quantitative PCR analysis on the LightCycler 480.

Gene	Forward primer (5'-3')	Reverse primer (5'-3')
Malat1	GCAGTGTGCCAATGTTTCGT	AGTCTGCTGTTTCCTGCTCC
Neat1	GGCACAAGTTTCACAGGCCTACATGGG	GCCAGAGCTGTCCGCCCAGCGAAG
Miat	GGGAGGTGTATAAAGTGAGAAGCT	GTATCCCAAGGAATGAAGTCTGTCT
Zfas1	TCCCGATATGTCTCGTCCCT	TCACGCTCCATTCAAAGCCC
Tnf	TGTCTTTGAGATCCATGCCGT	TCAAAATTCGAGTGACAAGCCTG
Il6	CCGGAGAGGAGACTTCACAG	TTCTGCAAGTGCATCATCGT
Il1β	AGCTCATATGGGTCCGACAG	GACCTTCCAGGATGAGGACA

Gapdh	TGAAGCAGGCATCTGAGGG	CGAAGGTGGAAGAGTGGGAG
Rpl13	CCTGCTGCTCTCAAGGTT	TGGTTGTCACTGCCTGGTACTT
Hprt	AGTGTTGGATACAGGCCAGAC	CGTGATTCAAATCCCTGAAGT
Arg1	AAAGCTGGTCTGTGGAAAA	ACAGACCGTGGGTTCTTCAC
Il10	GCCTTATCGGAAATGATCCA	TTTTCACAGGGGAGAAATCG
Igf	CTGGTGGATGCTCTTCAGTTC	TGCAGCTTCGTTTTCTTGTTT
Tgfβ	TATCACCTGTGTGCTGATCCA	CAAGCAGTCCTTCCCTTCAG

Bioplex. TNF, IL-6, IL-1β, and IL-10 protein levels in culture supernatant were determined by magnetic bead-based multiplex assay using Luminex technology (Bio-Rad Bio-Plex 200), according to the manufacturers' instructions (supplementary).

Statistics. Results were displayed as mean ± SEM (standard error of the mean). EAE clinical score are analysed using an F-test on repeated measurements. RT-qPCR results of the *in vivo* experiments were analysed using a one-way ANOVA with Tukey correction for multiple comparison in case of the 4 treatments group. For the Pggt1b$^{CD4\text{-}KO}$ mice an unpaired T-test with Welsh-correction was performed. The *in vitro* BMDM experiments were analysed using a two-way ANOVA with Sirlak's correction. Levels of cytokines and expression in BMDM timelapse experiments were analysed using Wilcoxon-sum rank test between the genotypes at every time-point.

References

Ajami, B., Bennett, J. L., Krieger, C., McNagny, K. M., & Rossi, F. M. V. (2011). Infiltrating monocytes trigger EAE progression, but do not contribute to the resident microglia pool. *Nature Neuroscience*, *14*(9), 1142–1149. https://doi.org/10.1038/nn.2887

Ajami, B., Samusik, N., Wieghofer, P., Ho, P. P., Crotti, A., Bjornson, Z., Prinz, M., Fantl, W. J., Nolan, G. P., & Steinman, L. (2018). Single-cell mass cytometry reveals distinct populations of brain myeloid cells in mouse neuroinflammation and neurodegeneration models. *Nature Neuroscience*, *21*(4), 541–551. https://doi.org/10.1038/s41593-018-0100-x

Akbari, M., Eshghyar, F., Gholipour, M., Eslami, S., Hussen, B. M., Taheri, M., Omrani, M. D., & Ghafouri-Fard, S. (2022). Expression analysis of mTOR-associated lncRNAs in multiple sclerosis. *Metabolic Brain Disease*, *37*(6), 2061–2066. https://doi.org/10.1007/s11011-022-01010-8

Akula, M. K., Ibrahim, M. X., Ivarsson, E. G., Khan, O. M., Kumar, I. T., Erlandsson, M., Karlsson, C., Xu, X., Brisslert, M., Brakebusch, C., Wang, D., Bokarewa, M., Sayin, V. I., & Bergo, M. O. (2019). Protein prenylation restrains innate immunity by inhibiting Rac1 effector interactions. *Nature Communications*, *10*(1), 3975. https://doi.org/10.1038/s41467-019-11606-x

Akula, M. K., Shi, M., Jiang, Z., Foster, C. E., Miao, D., Li, A. S., Zhang, X., Gavin, R. M., Forde, S. D., Germain, G., Carpenter, S., Rosadini, C. V, Gritsman, K., Chae, J. J., Hampton, R., Silverman, N., Gravallese, E. M., Kagan, J. C., Fitzgerald, K. A., … Wang, D. (2016). Control of the innate immune response by the mevalonate pathway. *Nature Immunology*, *17*(8), 922–929. https://doi.org/10.1038/ni.3487

Altschul, S. F., Gish, W., Miller, W., Myers, E. W., & Lipman, D. J. (1990). Basic local alignment search tool. *Journal of Molecular Biology*, *215*(3), 403–410. https://doi.org/10.1016/S0022-2836(05)80360-2

Baek, M., Chai, J. C., Choi, H. I., Yoo, E., Binas, B., Lee, Y. S., Jung, K. H., & Chai, Y. G. (2022). Analysis of differentially expressed long non-coding RNAs in LPS-induced human HMC3 microglial cells. *BMC Genomics*, *23*(1), 853. https://doi.org/10.1186/s12864-022-09083-6

Baranzini, S. E., & Oksenberg, J. R. (2017). The Genetics of Multiple Sclerosis: From 0 to 200 in 50 Years. *Trends in Genetics : TIG*, *33*(12), 960–970. https://doi.org/10.1016/j.tig.2017.09.004

Bennett, C. F., & Swayze, E. E. (2010). RNA targeting therapeutics: molecular mechanisms of antisense oligonucleotides as a therapeutic platform. *Annual Review of Pharmacology and Toxicology*, *50*, 259–293. https://doi.org/10.1146/annurev.pharmtox.010909.105654

Bennett, M. L., Bennett, F. C., Liddelow, S. A., Ajami, B., Zamanian, J. L., Fernhoff, N. B., Mulinyawe, S. B., Bohlen, C. J., Adil, A., Tucker, A., Weissman, I. L., Chang, E. F., Li, G., Grant, G. A., Hayden Gephart, M. G., & Barres, B. A. (2016). New tools for studying microglia in the mouse and human CNS. *Proceedings of the National Academy of Sciences of the United States of America*, *113*(12), E1738-46. https://doi.org/10.1073/pnas.1525528113

Berer, K., Gerdes, L. A., Cekanaviciute, E., Jia, X., Xiao, L., Xia, Z., Liu, C., Klotz, L., Stauffer, U., Baranzini, S. E., Kümpfel, T., Hohlfeld, R., Krishnamoorthy, G., & Wekerle, H. (2017). Gut microbiota from multiple sclerosis patients enables spontaneous autoimmune encephalomyelitis in mice. *Proceedings of the National Academy of Sciences of the United States of America*, *114*(40), 10719–10724. https://doi.org/10.1073/pnas.1711233114

Berse, B., Brown, L. F., Van de Water, L., Dvorak, H. F., & Senger, D. R. (1992). Vascular permeability factor (vascular endothelial growth factor) gene is expressed differentially in normal tissues, macrophages, and tumors. *Molecular Biology of the Cell*, *3*(2), 211–220. https://doi.org/10.1091/mbc.3.2.211

Bjornevik, K., Cortese, M., Healy, B. C., Kuhle, J., Mina, M. J., Leng, Y., Elledge, S. J., Niebuhr, D. W., Scher, A. I., Munger, K. L., & Ascherio, A. (2022). Longitudinal analysis reveals high prevalence of Epstein-Barr virus associated with multiple sclerosis. *Science (New York, N.Y.)*, *375*(6578), 296–301. https://doi.org/10.1126/science.abj8222

Bodini, B., Tonietto, M., Airas, L., & Stankoff, B. (2021). Positron emission tomography in multiple sclerosis - straight to the target. *Nature Reviews. Neurology*, *17*(11), 663–675. https://doi.org/10.1038/s41582-021-00537-1

Bogie, J. F. J., Stinissen, P., & Hendriks, J. J. A. (2014). Macrophage subsets and microglia in multiple sclerosis. *Acta Neuropathologica*, *128*(2), 191–213. https://doi.org/10.1007/s00401-014-1310-2

Brkic, M., Balusu, S., Van Wonterghem, E., Gorlé, N., Benilova, I., Kremer, A., Van Hove, I., Moons, L., De Strooper, B., Kanazir, S., Libert, C., & Vandenbroucke, R. E. (2015). Amyloid β Oligomers Disrupt Blood-CSF Barrier Integrity by Activating Matrix Metalloproteinases. *The Journal of Neuroscience : The Official Journal of the Society for Neuroscience*, *35*(37), 12766–12778. https://doi.org/10.1523/JNEUROSCI.0006-15.2015

Butovsky, O., Jedrychowski, M. P., Moore, C. S., Cialic, R., Lanser, A. J., Gabriely, G., Koeglsperger, T., Dake, B., Wu, P. M., Doykan, C. E., Fanek, Z., Liu, L., Chen, Z., Rothstein, J. D., Ransohoff, R. M., Gygi, S. P., Antel, J. P., & Weiner, H. L. (2014). Identification of a unique TGF-β-dependent molecular and functional signature in microglia. *Nature Neuroscience*, *17*(1), 131–143. https://doi.org/10.1038/nn.3599

Butovsky, O., & Weiner, H. L. (2018). Microglial signatures and their role in health and disease. In *Nature Reviews Neuroscience* (Vol. 19, Issue 10, pp. 622–635). Nature Publishing Group. https://doi.org/10.1038/s41583-018-0057-5

Cabili, M. N., Dunagin, M. C., McClanahan, P. D., Biaesch, A., Padovan-Merhar, O., Regev, A., Rinn, J. L., & Raj, A. (2015). Localization and abundance analysis of human lncRNAs at single-cell and single-molecule resolution. *Genome Biology*, *16*(1), 20. https://doi.org/10.1186/s13059-015-0586-4

Cai, L.-J., Tu, L., Huang, X.-M., Huang, J., Qiu, N., Xie, G.-H., Liao, J.-X., Du, W., Zhang, Y.-Y., & Tian, J.-Y. (2020). LncRNA MALAT1 facilitates inflammasome activation via epigenetic suppression of Nrf2 in Parkinson's disease. *Molecular Brain*, *13*(1), 130. https://doi.org/10.1186/s13041-020-00656-8

Caminero, A., Comabella, M., & Montalban, X. (2011). Tumor necrosis factor alpha (TNF-α), anti-TNF-α and demyelination revisited: an ongoing story. *Journal of Neuroimmunology*, *234*(1–2), 1–6. https://doi.org/10.1016/j.jneuroim.2011.03.004

Cao, H., Xu, D., Cai, Y., Han, X., Tang, L., Gao, F., Qi, Y., Cai, D., Wang, H., Ri, M., Antonets, D., Vyatkin, Y., Chen, Y., You, X., Wang, F., Nicolas, E., & Kapranov, P. (2021). Very long intergenic non-coding (vlinc) RNAs directly regulate multiple genes in cis and trans. *BMC Biology*, *19*(1), 108. https://doi.org/10.1186/s12915-021-01044-x

Carninci, P., Kasukawa, T., Katayama, S., Gough, J., Frith, M. C., Maeda, N., Oyama, R., Ravasi, T., Lenhard, B., Wells, C., Kodzius, R., Shimokawa, K., Bajic, V. B., Brenner, S. E., Batalov, S., Forrest, A. R. R., Zavolan, M., Davis, M. J., Wilming, L. G., … RIKEN Genome Exploration Research Group and Genome Science Group (Genome Network Project Core Group). (2005). The transcriptional landscape of the mammalian genome. *Science (New York, N.Y.)*, *309*(5740), 1559–1563. https://doi.org/10.1126/science.1112014

Catrysse, L., Vereecke, L., Beyaert, R., & van Loo, G. (2014). A20 in inflammation and autoimmunity. *Trends in Immunology*, *35*(1), 22–31. https://doi.org/10.1016/j.it.2013.10.005

Cekanaviciute, E., Yoo, B. B., Runia, T. F., Debelius, J. W., Singh, S., Nelson, C. A., Kanner, R., Bencosme, Y., Lee, Y. K., Hauser, S. L., Crabtree-Hartman, E., Sand, I. K., Gacias, M., Zhu, Y., Casaccia, P., Cree, B. A. C., Knight, R., Mazmanian, S. K., & Baranzini, S. E. (2017). Gut bacteria from multiple sclerosis patients modulate human T cells and exacerbate symptoms in mouse models. *Proceedings of the National Academy of Sciences of the United States of America*, *114*(40), 10713–10718. https://doi.org/10.1073/pnas.1711235114

Cheetham, S. W., Faulkner, G. J., & Dinger, M. E. (2020). Overcoming challenges and dogmas to understand the functions of pseudogenes. *Nature Reviews. Genetics*, *21*(3), 191–201. https://doi.org/10.1038/s41576-019-0196-1

Cheng, J., Kapranov, P., Drenkow, J., Dike, S., Brubaker, S., Patel, S., Long, J., Stern, D., Tammana, H., Helt, G., Sementchenko, V., Piccolboni, A., Bekiranov, S., Bailey, D. K., Ganesh, M., Ghosh, S., Bell, I., Gerhard, D. S., & Gingeras, T. R. (2005). Transcriptional maps of 10 human chromosomes at 5-nucleotide resolution. *Science (New York, N.Y.)*, *308*(5725), 1149–1154. https://doi.org/10.1126/science.1108625

Clemson, C. M., Hutchinson, J. N., Sara, S. A., Ensminger, A. W., Fox, A. H., Chess, A., & Lawrence, J. B. (2009). An architectural role for a nuclear noncoding RNA: NEAT1 RNA is essential for the structure of paraspeckles. *Molecular Cell*, *33*(6), 717–726. https://doi.org/10.1016/j.molcel.2009.01.026

Comi, G. (2009). Shifting the paradigm toward earlier treatment of multiple sclerosis with interferon beta. *Clinical Therapeutics*, *31*(6), 1142–1157. https://doi.org/10.1016/j.clinthera.2009.06.007

Constantinescu, C. S., Farooqi, N., O'Brien, K., & Gran, B. (2011). Experimental autoimmune encephalomyelitis (EAE) as a model for multiple sclerosis (MS). *British Journal of Pharmacology*, *164*(4), 1079–1106. https://doi.org/10.1111/j.1476-5381.2011.01302.x

Cui, H., Banerjee, S., Guo, S., Xie, N., Ge, J., Jiang, D., Zörnig, M., Thannickal, V. J., & Liu, G. (2019). Long noncoding RNA Malat1 regulates differential activation of macrophages and response to lung injury. *JCI Insight*, *4*(4). https://doi.org/10.1172/jci.insight.124522

Cullis, P. R., & Hope, M. J. (2017). Lipid Nanoparticle Systems for Enabling Gene Therapies. *Molecular Therapy : The Journal of the American Society of Gene Therapy*, *25*(7), 1467–1475. https://doi.org/10.1016/j.ymthe.2017.03.013

Dai, W., Wang, M., Wang, P., Wen, J., Wang, J., Cha, S., Xiao, X., He, Y., Shu, R., & Bai, D. (2021). lncRNA NEAT1 ameliorates LPS-induced inflammation in MG63 cells by activating autophagy and suppressing the NLRP3 inflammasome. *International Journal of Molecular Medicine*, *47*(2), 607–620. https://doi.org/10.3892/ijmm.2020.4827

Damisah, E. C., Hill, R. A., Rai, A., Chen, F., Rothlin, C. V, Ghosh, S., & Grutzendler, J. (2020). Astrocytes and microglia play orchestrated roles and respect phagocytic territories during neuronal corpse removal in vivo. *Science Advances*, *6*(26), eaba3239. https://doi.org/10.1126/sciadv.aba3239

Dangond, F., Donnelly, A., Hohlfeld, R., Lubetzki, C., Kohlhaas, S., Leocani, L., Ciccarelli, O., Stankoff, B., Sormani, M. P., Chataway, J., Bozzoli, F., Cucca, F., Melton, L., Coetzee, T., & Salvetti, M. (2021). Facing the urgency of therapies for progressive MS - a Progressive MS Alliance proposal. *Nature Reviews. Neurology*, *17*(3), 185–192. https://doi.org/10.1038/s41582-020-00446-9

Das, R., & Chinnathambi, S. (2019). Microglial priming of antigen presentation and adaptive stimulation in Alzheimer's disease. *Cellular and Molecular Life Sciences : CMLS*, *76*(19), 3681–3694. https://doi.org/10.1007/s00018-019-03132-2

Davidovich, C., & Cech, T. R. (2015). The recruitment of chromatin modifiers by long noncoding RNAs: lessons from PRC2. *RNA (New York, N.Y.)*, *21*(12), 2007–2022. https://doi.org/10.1261/rna.053918.115

De Strooper, B., & Karran, E. (2016). The Cellular Phase of Alzheimer's Disease. *Cell*, *164*(4), 603–615. https://doi.org/10.1016/j.cell.2015.12.056

Deng, W., Zhu, X., Skogerbø, G., Zhao, Y., Fu, Z., Wang, Y., He, H., Cai, L., Sun, H., Liu, C., Li, B., Bai, B., Wang, J., Jia, D., Sun, S., He, H., Cui, Y., Wang, Y., Bu, D., & Chen, R. (2006). Organization of the Caenorhabditis elegans small non-coding transcriptome: genomic features, biogenesis, and expression. *Genome Research*, *16*(1), 20–29. https://doi.org/10.1101/gr.4139206

Di Ianni, T., Bose, R. J. C., Sukumar, U. K., Bachawal, S., Wang, H., Telichko, A., Herickhoff, C., Robinson, E., Baker, S., Vilches-Moure, J. G., Felt, S. A., Gambhir, S. S., Paulmurugan, R., & Dahl, J. D. (2019). Ultrasound/microbubble-mediated targeted delivery of anticancer microRNA-loaded nanoparticles to deep tissues in pigs. *Journal of Controlled Release : Official Journal of the Controlled Release Society*, *309*, 1–10. https://doi.org/10.1016/j.jconrel.2019.07.024

Dresselhaus, E. C., & Meffert, M. K. (2019). Cellular Specificity of NF-κB Function in the Nervous System. *Frontiers in Immunology*, *10*, 1043. https://doi.org/10.3389/fimmu.2019.01043

Eftekharian, M. M., Noroozi, R., Komaki, A., Mazdeh, M., Ghafouri-Fard, S., & Taheri, M. (2019). MALAT1 Genomic Variants and Risk of Multiple Sclerosis. *Immunological Investigations*, *48*(5), 549–554. https://doi.org/10.1080/08820139.2019.1576728

Epelman, S., Lavine, K. J., Beaudin, A. E., Sojka, D. K., Carrero, J. A., Calderon, B., Brija, T., Gautier, E. L., Ivanov, S., Satpathy, A. T., Schilling, J. D., Schwendener, R., Sergin, I., Razani, B., Forsberg, E. C., Yokoyama, W. M., Unanue, E. R., Colonna, M., Randolph, G. J., & Mann, D. L. (2014). Embryonic and adult-derived resident cardiac macrophages are maintained through distinct mechanisms at steady state and during inflammation. *Immunity*, *40*(1), 91–104. https://doi.org/10.1016/j.immuni.2013.11.019

Eriksson, M., Andersen, O., & Runmarker, B. (2003). Long-term follow up of patients with clinically isolated syndromes, relapsing-remitting and secondary progressive multiple sclerosis. *Multiple Sclerosis (Houndmills, Basingstoke, England)*, *9*(3), 260–274. https://doi.org/10.1191/1352458503ms914oa

Eshaghi, A., Young, A. L., Wijeratne, P. A., Prados, F., Arnold, D. L., Narayanan, S., Guttmann, C. R. G., Barkhof, F., Alexander, D. C., Thompson, A. J., Chard, D., & Ciccarelli, O. (2021). Identifying multiple sclerosis subtypes using unsupervised machine learning and MRI data. *Nature Communications*, *12*(1), 2078. https://doi.org/10.1038/s41467-021-22265-2

Florou, D., Katsara, M., Feehan, J., Dardiotis, E., & Apostolopoulos, V. (2020). Anti-CD20 Agents for Multiple Sclerosis: Spotlight on Ocrelizumab and Ofatumumab. *Brain Sciences*, *10*(10). https://doi.org/10.3390/brainsci10100758

Flynn, R. A., & Chang, H. Y. (2014). Long noncoding RNAs in cell-fate programming and reprogramming. *Cell Stem Cell*, *14*(6), 752–761. https://doi.org/10.1016/j.stem.2014.05.014

Frischer, J. M., Weigand, S. D., Guo, Y., Kale, N., Parisi, J. E., Pirko, I., Mandrekar, J., Bramow, S., Metz, I., Brück, W., Lassmann, H., & Lucchinetti, C. F. (2015). Clinical and pathological insights into the dynamic nature of the white matter multiple sclerosis plaque. *Annals of Neurology*, *78*(5), 710–721. https://doi.org/10.1002/ana.24497

Gao, H., Danzi, M. C., Choi, C. S., Taherian, M., Dalby-Hansen, C., Ellman, D. G., Madsen, P. M., Bixby, J. L., Lemmon, V. P., Lambertsen, K. L., & Brambilla, R. (2017). Opposing Functions of Microglial and Macrophagic TNFR2 in the Pathogenesis of Experimental Autoimmune Encephalomyelitis. *Cell Reports*, *18*(1), 198–212. https://doi.org/10.1016/j.celrep.2016.11.083

Geary, R. S., Norris, D., Yu, R., & Bennett, C. F. (2015). Pharmacokinetics, biodistribution and cell uptake of antisense oligonucleotides. *Advanced Drug Delivery Reviews*, *87*, 46–51. https://doi.org/10.1016/j.addr.2015.01.008

Gertig, U., & Hanisch, U.-K. (2014). Microglial diversity by responses and responders. *Frontiers in Cellular Neuroscience*, *8*, 101. https://doi.org/10.3389/fncel.2014.00101

Ghafouri-Fard, S., Gholipour, M., Eslami, S., Hussen, B. M., Taheri, M., Samadian, M., & Omrani, M. D. (2023). Abnormal expression of MAPK14-related lncRNAs in the peripheral blood of patients with multiple sclerosis. *Non-Coding RNA Research*, *8*(3), 335–339. https://doi.org/10.1016/j.ncrna.2023.03.006

Gloss, B. S., & Dinger, M. E. (2016). The specificity of long noncoding RNA expression. *Biochimica et Biophysica Acta*, *1859*(1), 16–22. https://doi.org/10.1016/j.bbagrm.2015.08.005

Gong, C., & Maquat, L. E. (2011). lncRNAs transactivate STAU1-mediated mRNA decay by duplexing with 3' UTRs via Alu elements. *Nature*, *470*(7333), 284–288. https://doi.org/10.1038/nature09701

Gordon, S. (2003). Alternative activation of macrophages. *Nature Reviews. Immunology*, *3*(1), 23–35. https://doi.org/10.1038/nri978

Gottschalk, R. A., Martins, A. J., Angermann, B. R., Dutta, B., Ng, C. E., Uderhardt, S., Tsang, J. S., Fraser, I. D. C., Meier-Schellersheim, M., & Germain, R. N. (2016). Distinct NF-κB and MAPK Activation Thresholds Uncouple Steady-State Microbe Sensing from Anti-pathogen Inflammatory Responses. *Cell Systems*, *2*(6), 378–390. https://doi.org/10.1016/j.cels.2016.04.016

Grabert, K., Michoel, T., Karavolos, M. H., Clohisey, S., Baillie, J. K., Stevens, M. P., Freeman, T. C., Summers, K. M., & McColl, B. W. (2016). Microglial brain region-dependent diversity and selective regional sensitivities to aging. *Nature Neuroscience*, *19*(3), 504–516. https://doi.org/10.1038/nn.4222

Gupta, S. C., Awasthee, N., Rai, V., Chava, S., Gunda, V., & Challagundla, K. B. (2020). Long non-coding RNAs and nuclear factor-κB crosstalk in cancer and other human diseases. *Biochimica et Biophysica Acta. Reviews on Cancer*, *1873*(1), 188316. https://doi.org/10.1016/j.bbcan.2019.188316

Györffy, B. A., Kun, J., Török, G., Bulyáki, É., Borhegyi, Z., Gulyássy, P., Kis, V., Szocsics, P., Micsonai, A., Matkó, J., Drahos, L., Juhász, G., Kékesi, K. A., & Kardos, J. (2018). Local apoptotic-like mechanisms underlie complement-mediated synaptic pruning. *Proceedings of the National Academy of Sciences of the United States of America*, *115*(24), 6303–6308. https://doi.org/10.1073/pnas.1722613115

Hacisuleyman, E., Shukla, C. J., Weiner, C. L., & Rinn, J. L. (2016). Function and evolution of local repeats in the Firre locus. *Nature Communications*, *7*(1), 11021. https://doi.org/10.1038/ncomms11021

Harley, J. B., & James, J. A. (2006). Epstein-Barr virus infection induces lupus autoimmunity. *Bulletin of the NYU Hospital for Joint Diseases*, *64*(1–2), 45–50.

Hauser, S. L., Bar-Or, A., Comi, G., Giovannoni, G., Hartung, H.-P., Hemmer, B., Lublin, F., Montalban, X., Rammohan, K. W., Selmaj, K., Traboulsee, A., Wolinsky, J. S., Arnold, D. L., Klingelschmitt, G., Masterman, D., Fontoura, P., Belachew, S., Chin, P., Mairon, N., … OPERA I and OPERA II Clinical Investigators. (2017). Ocrelizumab versus Interferon Beta-1a in Relapsing Multiple Sclerosis. *The New England Journal of Medicine*, *376*(3), 221–234. https://doi.org/10.1056/NEJMoa1601277

Hayden, M. S., & Ghosh, S. (2008). Shared principles in NF-kappaB signaling. *Cell*, *132*(3), 344–362. https://doi.org/10.1016/j.cell.2008.01.020

Heneka, M. T., McManus, R. M., & Latz, E. (2018). Inflammasome signalling in brain function and neurodegenerative disease. *Nature Reviews. Neuroscience*, *19*(10), 610–621. https://doi.org/10.1038/s41583-018-0055-7

Herz, J., Filiano, A. J., Wiltbank, A. T., Yogev, N., & Kipnis, J. (2017). Myeloid Cells in the Central Nervous System. *Immunity*, *46*(6), 943–956. https://doi.org/10.1016/j.immuni.2017.06.007

Hickman, S. E., Kingery, N. D., Ohsumi, T. K., Borowsky, M. L., Wang, L., Means, T. K., & El Khoury, J. (2013). The microglial sensome revealed by direct RNA sequencing. *Nature Neuroscience*, *16*(12), 1896–1905. https://doi.org/10.1038/nn.3554

Hilliard, B., Samoilova, E. B., Liu, T. S., Rostami, A., & Chen, Y. (1999). Experimental autoimmune encephalomyelitis in NF-kappa B-deficient mice:roles of NF-kappa B in the activation and differentiation of autoreactive T cells. *Journal of Immunology (Baltimore, Md. : 1950)*, *163*(5), 2937–2943.

Hsiao, J., Yuan, T. Y., Tsai, M. S., Lu, C. Y., Lin, Y. C., Lee, M. L., Lin, S. W., Chang, F. C., Liu Pimentel, H., Olive, C., Coito, C., Shen, G., Young, M., Thorne, T., Lawrence, M., Magistri, M., Faghihi, M. A., Khorkova, O., & Wahlestedt, C. (2016). Upregulation of Haploinsufficient Gene Expression in the Brain by Targeting a Long Non-coding RNA Improves Seizure Phenotype in a Model of Dravet Syndrome. *EBioMedicine*, *9*, 257–277. https://doi.org/10.1016/j.ebiom.2016.05.011

Huang, Z., Zhao, J., Wang, W., Zhou, J., & Zhang, J. (2020). Depletion of LncRNA NEAT1 Rescues Mitochondrial Dysfunction Through NEDD4L-Dependent PINK1 Degradation in Animal Models of Alzheimer's Disease. *Frontiers in Cellular Neuroscience*, *14*, 28. https://doi.org/10.3389/fncel.2020.00028

Huarte, M. (2015). The emerging role of lncRNAs in cancer. *Nature Medicine*, *21*(11), 1253–1261. https://doi.org/10.1038/nm.3981

Inoue, M., & Shinohara, M. L. (2013). NLRP3 Inflammasome and MS/EAE. *Autoimmune Diseases*, *2013*, 859145. https://doi.org/10.1155/2013/859145

International Multiple Sclerosis Genetics Consortium. (2019). Multiple sclerosis genomic map implicates peripheral immune cells and microglia in susceptibility. *Science (New York, N.Y.)*, *365*(6460). https://doi.org/10.1126/science.aav7188

Jacob, R., Zander, S., & Gutschner, T. (2017). The Dark Side of the Epitranscriptome: Chemical Modifications in Long Non-Coding RNAs. *International Journal of Molecular Sciences*, *18*(11). https://doi.org/10.3390/ijms18112387

Jiang, Y., & Zhang, W. (2021). LncRNA ZFAS1 plays a role in regulating the inflammatory responses in sepsis-induced acute lung injury via mediating miR-193a-3p. *Infection, Genetics and Evolution : Journal of Molecular Epidemiology and Evolutionary Genetics in Infectious Diseases*, *92*, 104860. https://doi.org/10.1016/j.meegid.2021.104860

Jiang, Z., Jiang, J. X., & Zhang, G.-X. (2014). Macrophages: a double-edged sword in experimental autoimmune encephalomyelitis. *Immunology Letters*, *160*(1), 17–22. https://doi.org/10.1016/j.imlet.2014.03.006

Jiang, Z.-S., & Zhang, J.-R. (2018). LncRNA SNHG5 enhances astrocytes and microglia viability via upregulating KLF4 in spinal cord injury. *International Journal of Biological Macromolecules*, *120*(Pt A), 66–72. https://doi.org/10.1016/j.ijbiomac.2018.08.002

Jinno, S., Fleischer, F., Eckel, S., Schmidt, V., & Kosaka, T. (2007). Spatial arrangement of microglia in the mouse hippocampus: a stereological study in comparison with astrocytes. *Glia*, *55*(13), 1334–1347. https://doi.org/10.1002/glia.20552

Jordão, M. J. C., Sankowski, R., Brendecke, S. M., Sagar, Locatelli, G., Tai, Y.-H., Tay, T. L., Schramm, E., Armbruster, S., Hagemeyer, N., Groß, O., Mai, D., Çiçek, Ö., Falk, T., Kerschensteiner, M., Grün, D., & Prinz, M. (2019).

Single-cell profiling identifies myeloid cell subsets with distinct fates during neuroinflammation. *Science (New York, N.Y.)*, *363*(6425). https://doi.org/10.1126/science.aat7554

Kaltschmidt, B., & Kaltschmidt, C. (2009). NF-kappaB in the nervous system. *Cold Spring Harbor Perspectives in Biology*, *1*(3), a001271. https://doi.org/10.1101/cshperspect.a001271

Kassed, C. A., Willing, A. E., Garbuzova-Davis, S., Sanberg, P. R., & Pennypacker, K. R. (2002). Lack of NF-kappaB p50 exacerbates degeneration of hippocampal neurons after chemical exposure and impairs learning. *Experimental Neurology*, *176*(2), 277–288. https://doi.org/10.1006/exnr.2002.7967

Keren-Shaul, H., Spinrad, A., Weiner, A., Matcovitch-Natan, O., Dvir-Szternfeld, R., Ulland, T. K., David, E., Baruch, K., Lara-Astaiso, D., Toth, B., Itzkovitz, S., Colonna, M., Schwartz, M., & Amit, I. (2017). A Unique Microglia Type Associated with Restricting Development of Alzheimer's Disease. *Cell*, *169*(7), 1276-1290.e17. https://doi.org/10.1016/j.cell.2017.05.018

Kierdorf, K., Erny, D., Goldmann, T., Sander, V., Schulz, C., Perdiguero, E. G., Wieghofer, P., Heinrich, A., Riemke, P., Hölscher, C., Müller, D. N., Luckow, B., Brocker, T., Debowski, K., Fritz, G., Opdenakker, G., Diefenbach, A., Biber, K., Heikenwalder, M., … Prinz, M. (2013). Microglia emerge from erythromyeloid precursors via Pu.1- and Irf8-dependent pathways. *Nature Neuroscience*, *16*(3), 273–280. https://doi.org/10.1038/nn.3318

Kimura, T., Ferran, B., Tsukahara, Y., Shang, Q., Desai, S., Fedoce, A., Pimentel, D. R., Luptak, I., Adachi, T., Ido, Y., Matsui, R., & Bachschmid, M. M. (2019). Production of adeno-associated virus vectors for in vitro and in vivo applications. *Scientific Reports*, *9*(1), 13601. https://doi.org/10.1038/s41598-019-49624-w

Kipp, M., Nyamoya, S., Hochstrasser, T., & Amor, S. (2017). Multiple sclerosis animal models: a clinical and histopathological perspective. *Brain Pathology (Zurich, Switzerland)*, *27*(2), 123–137. https://doi.org/10.1111/bpa.12454

Kolb, H., Absinta, M., Beck, E. S., Ha, S.-K., Song, Y., Norato, G., Cortese, I., Sati, P., Nair, G., & Reich, D. S. (2021). 7T MRI Differentiates Remyelinated from Demyelinated Multiple Sclerosis Lesions. *Annals of Neurology*, *90*(4), 612–626. https://doi.org/10.1002/ana.26194

Kopp, F., & Mendell, J. T. (2018). Functional Classification and Experimental Dissection of Long Noncoding RNAs. *Cell*, *172*(3), 393–407. https://doi.org/10.1016/j.cell.2018.01.011

Krasemann, S., Madore, C., Cialic, R., Baufeld, C., Calcagno, N., El Fatimy, R., Beckers, L., O'Loughlin, E., Xu, Y., Fanek, Z., Greco, D. J., Smith, S. T., Tweet, G., Humulock, Z., Zrzavy, T., Conde-Sanroman, P., Gacias, M., Weng, Z., Chen, H., … Butovsky, O. (2017). The TREM2-APOE Pathway Drives the Transcriptional Phenotype of Dysfunctional Microglia in Neurodegenerative Diseases. *Immunity*, *47*(3), 566-581.e9. https://doi.org/10.1016/j.immuni.2017.08.008

Kurreck, J., Wyszko, E., Gillen, C., & Erdmann, V. A. (2002). Design of antisense oligonucleotides stabilized by locked nucleic acids. *Nucleic Acids Research*, *30*(9), 1911–1918. https://doi.org/10.1093/nar/30.9.1911

Lamkanfi, M., & Dixit, V. M. (2012). Inflammasomes and their roles in health and disease. *Annual Review of Cell and Developmental Biology*, *28*, 137–161. https://doi.org/10.1146/annurev-cellbio-101011-155745

Laprell, F., Finkl, K., & Müller, J. (2017). Propagation of Polycomb-repressed chromatin requires sequence-specific recruitment to DNA. *Science (New York, N.Y.)*, *356*(6333), 85–88. https://doi.org/10.1126/science.aai8266

Lassmann, H., van Horssen, J., & Mahad, D. (2012). Progressive multiple sclerosis: pathology and pathogenesis. *Nature Reviews. Neurology*, *8*(11), 647–656. https://doi.org/10.1038/nrneurol.2012.168

Lavin, Y., Winter, D., Blecher-Gonen, R., David, E., Keren-Shaul, H., Merad, M., Jung, S., & Amit, I. (2014). Tissue-resident macrophage enhancer landscapes are shaped by the local microenvironment. *Cell*, *159*(6), 1312–1326. https://doi.org/10.1016/j.cell.2014.11.018

Lemke, D., Klement, R. J., Schweiger, F., Schweiger, B., & Spitz, J. (2021). Vitamin D Resistance as a Possible Cause of Autoimmune Diseases: A Hypothesis Confirmed by a Therapeutic High-Dose Vitamin D Protocol. *Frontiers in Immunology*, *12*, 655739. https://doi.org/10.3389/fimmu.2021.655739

Lewis, N. D., Hill, J. D., Juchem, K. W., Stefanopoulos, D. E., & Modis, L. K. (2014). RNA sequencing of microglia and monocyte-derived macrophages from mice with experimental autoimmune encephalomyelitis illustrates a changing phenotype with disease course. *Journal of Neuroimmunology*, *277*(1–2), 26–38. https://doi.org/10.1016/j.jneuroim.2014.09.014

Li, J., Zou, C.-L., Zhang, Z.-M., & Xue, F. (2022a). Knockdown of lncRNA MIAT attenuated lipopolysaccharide-induced microglial cells injury by sponging miR-613. *Mammalian Genome : Official Journal of the International Mammalian Genome Society*, *33*(3), 471–479. https://doi.org/10.1007/s00335-022-09946-z

Li, J., Zou, C.-L., Zhang, Z.-M., & Xue, F. (2022b). Knockdown of lncRNA MIAT attenuated lipopolysaccharide-induced microglial cells injury by sponging miR-613. *Mammalian Genome : Official Journal of the International Mammalian Genome Society*, *33*(3), 471–479. https://doi.org/10.1007/s00335-022-09946-z

Li, R., Patterson, K. R., & Bar-Or, A. (2018). Reassessing B cell contributions in multiple sclerosis. *Nature Immunology*, *19*(7), 696–707. https://doi.org/10.1038/s41590-018-0135-x

Li, S.-X., Yan, W., Liu, J.-P., Zhao, Y.-J., & Chen, L. (2021). Long noncoding RNA SNHG4 remits lipopolysaccharide-engendered inflammatory lung damage by inhibiting METTL3 - Mediated m6A level of STAT2 mRNA. *Molecular Immunology*, *139*, 10–22. https://doi.org/10.1016/j.molimm.2021.08.008

Li, W., Notani, D., & Rosenfeld, M. G. (2016). Enhancers as non-coding RNA transcription units: recent insights and future perspectives. *Nature Reviews. Genetics*, *17*(4), 207–223. https://doi.org/10.1038/nrg.2016.4

Lisak, R. P., Nedelkoska, L., Benjamins, J. A., Schalk, D., Bealmear, B., Touil, H., Li, R., Muirhead, G., & Bar-Or, A. (2017). B cells from patients with multiple sclerosis induce cell death via apoptosis in neurons in vitro. *Journal of Neuroimmunology*, *309*, 88–99. https://doi.org/10.1016/j.jneuroim.2017.05.004

Liston, A., Dooley, J., & Yshii, L. (2022). Brain-resident regulatory T cells and their role in health and disease. *Immunology Letters*, *248*, 26–30. https://doi.org/10.1016/j.imlet.2022.06.005

Liu, C., Zhang, L., Liu, H., & Cheng, K. (2017). Delivery strategies of the CRISPR-Cas9 gene-editing system for therapeutic applications. *Journal of Controlled Release : Official Journal of the Controlled Release Society*, *266*, 17–26. https://doi.org/10.1016/j.jconrel.2017.09.012

Liu, Y., Cheng, X., Li, H., Hui, S., Zhang, Z., Xiao, Y., & Peng, W. (2022a). Non-Coding RNAs as Novel Regulators of Neuroinflammation in Alzheimer's Disease. *Frontiers in Immunology*, *13*, 908076. https://doi.org/10.3389/fimmu.2022.908076

Liu, Y., Cheng, X., Li, H., Hui, S., Zhang, Z., Xiao, Y., & Peng, W. (2022b). Non-Coding RNAs as Novel Regulators of Neuroinflammation in Alzheimer's Disease. *Frontiers in Immunology*, *13*, 908076. https://doi.org/10.3389/fimmu.2022.908076

Lublin, F. D. (2014). New multiple sclerosis phenotypic classification. *European Neurology*, *72 Suppl 1*, 1–5. https://doi.org/10.1159/000367614

Lucchinetti, C. F., Popescu, B. F. G., Bunyan, R. F., Moll, N. M., Roemer, S. F., Lassmann, H., Brück, W., Parisi, J. E., Scheithauer, B. W., Giannini, C., Weigand, S. D., Mandrekar, J., & Ransohoff, R. M. (2011). Inflammatory cortical demyelination in early multiple sclerosis. *The New England Journal of Medicine*, *365*(23), 2188–2197. https://doi.org/10.1056/NEJMoa1100648

Lund, H., Pieber, M., Parsa, R., Han, J., Grommisch, D., Ewing, E., Kular, L., Needhamsen, M., Espinosa, A., Nilsson, E., Överby, A. K., Butovsky, O., Jagodic, M., Zhang, X.-M., & Harris, R. A. (2018). Competitive repopulation of an empty microglial niche yields functionally distinct subsets of microglia-like cells. *Nature Communications*, *9*(1), 4845. https://doi.org/10.1038/s41467-018-07295-7

Lyman, M., Lloyd, D. G., Ji, X., Vizcaychipi, M. P., & Ma, D. (2014). Neuroinflammation: the role and consequences. *Neuroscience Research*, *79*, 1–12. https://doi.org/10.1016/j.neures.2013.10.004

Lyu, J., Xie, D., Bhatia, T. N., Leak, R. K., Hu, X., & Jiang, X. (2021). Microglial/Macrophage polarization and function in brain injury and repair after stroke. *CNS Neuroscience & Therapeutics*, *27*(5), 515–527. https://doi.org/10.1111/cns.13620

Lyu, Y., Qian, Y., & Fu, L. (2015). [Prediction of regulating network of innate immune signaling molecule hsa-miR-181a in stroke development based on bioinformatics analysis]. *Xi Bao Yu Fen Zi Mian Yi Xue Za Zhi = Chinese Journal of Cellular and Molecular Immunology*, *31*(8), 1042–1047.

Ma, P., Li, Y., Zhang, W., Fang, F., Sun, J., Liu, M., Li, K., & Dong, L. (2019). Long Non-coding RNA MALAT1 Inhibits Neuron Apoptosis and Neuroinflammation While Stimulates Neurite Outgrowth and Its Correlation With MiR-125b Mediates PTGS2, CDK5 and FOXQ1 in Alzheimer's Disease. *Current Alzheimer Research*, *16*(7), 596–612. https://doi.org/10.2174/1567205016666190725130134

Malpass, K. (2012). Multiple sclerosis: “Outside-in” demyelination in MS. *Nature Reviews. Neurology*, *8*(2), 61. https://doi.org/10.1038/nrneurol.2011.217

Martin, R., Bielekova, B., Gran, B., & McFarland, H. F. (2000). Lessons from studies of antigen-specific T cell responses in Multiple Sclerosis. *Journal of Neural Transmission. Supplementum*, *60*, 361–373. https://doi.org/10.1007/978-3-7091-6301-6_26

Masoumi, F., Ghorbani, S., Talebi, F., Branton, W. G., Rajaei, S., Power, C., & Noorbakhsh, F. (2019). Malat1 long noncoding RNA regulates inflammation and leukocyte differentiation in experimental autoimmune encephalomyelitis. *Journal of Neuroimmunology*, *328*, 50–59. https://doi.org/10.1016/j.jneuroim.2018.11.013

Mathys, H., Adaikkan, C., Gao, F., Young, J. Z., Manet, E., Hemberg, M., De Jager, P. L., Ransohoff, R. M., Regev, A., & Tsai, L.-H. (2017). Temporal Tracking of Microglia Activation in Neurodegeneration at Single-Cell Resolution. *Cell Reports*, *21*(2), 366–380. https://doi.org/10.1016/j.celrep.2017.09.039

Mattick, J. S., Amaral, P. P., Carninci, P., Carpenter, S., Chang, H. Y., Chen, L.-L., Chen, R., Dean, C., Dinger, M. E., Fitzgerald, K. A., Gingeras, T. R., Guttman, M., Hirose, T., Huarte, M., Johnson, R., Kanduri, C., Kapranov, P., Lawrence, J. B., Lee, J. T., … Wu, M. (2023). Long non-coding RNAs: definitions, functions, challenges and recommendations. *Nature Reviews. Molecular Cell Biology*. https://doi.org/10.1038/s41580-022-00566-8

Matveeva, O., Bogie, J. F. J., Hendriks, J. J. A., Linker, R. A., Haghikia, A., & Kleinewietfeld, M. (2018). Western lifestyle and immunopathology of multiple sclerosis. *Annals of the New York Academy of Sciences*, *1417*(1), 71–86. https://doi.org/10.1111/nyas.13583

Mayo, L., Cunha, A. P. Da, Madi, A., Beynon, V., Yang, Z., Alvarez, J. I., Prat, A., Sobel, R. A., Kobzik, L., Lassmann, H., Quintana, F. J., & Weiner, H. L. (2016). IL-10-dependent Tr1 cells attenuate astrocyte activation and ameliorate chronic central nervous system inflammation. *Brain : A Journal of Neurology*, *139*(Pt 7), 1939–1957. https://doi.org/10.1093/brain/aww113

Mercer, T. R., Dinger, M. E., & Mattick, J. S. (2009). Long non-coding RNAs: insights into functions. *Nature Reviews. Genetics*, *10*(3), 155–159. https://doi.org/10.1038/nrg2521

Merson, T. D., Binder, M. D., & Kilpatrick, T. J. (2010a). Role of cytokines as mediators and regulators of microglial activity in inflammatory demyelination of the CNS. *Neuromolecular Medicine*, *12*(2), 99–132. https://doi.org/10.1007/s12017-010-8112-z

Merson, T. D., Binder, M. D., & Kilpatrick, T. J. (2010b). Role of cytokines as mediators and regulators of microglial activity in inflammatory demyelination of the CNS. *Neuromolecular Medicine*, *12*(2), 99–132. https://doi.org/10.1007/s12017-010-8112-z

Metodiewa, D., & Kośka, C. (2000). Reactive oxygen species and reactive nitrogen species: relevance to cyto(neuro)toxic events and neurologic disorders. An overview. *Neurotoxicity Research*, *1*(3), 197–233. https://doi.org/10.1007/BF03033290

Mildner, A., Schmidt, H., Nitsche, M., Merkler, D., Hanisch, U.-K., Mack, M., Heikenwalder, M., Brück, W., Priller, J., & Prinz, M. (2007). Microglia in the adult brain arise from Ly-6ChiCCR2+ monocytes only under defined host conditions. *Nature Neuroscience*, *10*(12), 1544–1553. https://doi.org/10.1038/nn2015

Min, H. S., Kim, H. J., Naito, M., Ogura, S., Toh, K., Hayashi, K., Kim, B. S., Fukushima, S., Anraku, Y., Miyata, K., & Kataoka, K. (2020). Systemic Brain Delivery of Antisense Oligonucleotides across the Blood-Brain Barrier with a Glucose-Coated Polymeric Nanocarrier. *Angewandte Chemie (International Ed. in English)*, *59*(21), 8173–8180. https://doi.org/10.1002/anie.201914751

Morrissy, A. S., Griffith, M., & Marra, M. A. (2011). Extensive relationship between antisense transcription and alternative splicing in the human genome. *Genome Research*, *21*(8), 1203–1212. https://doi.org/10.1101/gr.113431.110

Moulder, R., Lönnberg, T., Elo, L. L., Filén, J.-J., Rainio, E., Corthals, G., Oresic, M., Nyman, T. A., Aittokallio, T., & Lahesmaa, R. (2010). Quantitative proteomics analysis of the nuclear fraction of human CD4+ cells in the early phases of IL-4-induced Th2 differentiation. *Molecular & Cellular Proteomics : MCP*, *9*(9), 1937–1953. https://doi.org/10.1074/mcp.M900483-MCP200

Mrdjen, D., Pavlovic, A., Hartmann, F. J., Schreiner, B., Utz, S. G., Leung, B. P., Lelios, I., Heppner, F. L., Kipnis, J., Merkler, D., Greter, M., & Becher, B. (2018). High-Dimensional Single-Cell Mapping of Central Nervous

System Immune Cells Reveals Distinct Myeloid Subsets in Health, Aging, and Disease. *Immunity*, *48*(2), 380-395.e6. https://doi.org/10.1016/j.immuni.2018.01.011

Muraro, P. A., & Uccelli, A. (2010). Immuno-therapeutic potential of haematopoietic and mesenchymal stem cell transplantation in MS. *Results and Problems in Cell Differentiation*, *51*, 237–257. https://doi.org/10.1007/400_2008_14

Nagata, T., Dwyer, C. A., Yoshida-Tanaka, K., Ihara, K., Ohyagi, M., Kaburagi, H., Miyata, H., Ebihara, S., Yoshioka, K., Ishii, T., Miyata, K., Miyata, K., Powers, B., Igari, T., Yamamoto, S., Arimura, N., Hirabayashi, H., Uchihara, T., Hara, R. I., … Yokota, T. (2021). Cholesterol-functionalized DNA/RNA heteroduplexes cross the blood-brain barrier and knock down genes in the rodent CNS. *Nature Biotechnology*, *39*(12), 1529–1536. https://doi.org/10.1038/s41587-021-00972-x

Neumann, H., Kotter, M. R., & Franklin, R. J. M. (2009). Debris clearance by microglia: an essential link between degeneration and regeneration. *Brain : A Journal of Neurology*, *132*(Pt 2), 288–295. https://doi.org/10.1093/brain/awn109

Nimmerjahn, A., Kirchhoff, F., & Helmchen, F. (2005). Resting microglial cells are highly dynamic surveillants of brain parenchyma in vivo. *Science (New York, N.Y.)*, *308*(5726), 1314–1318. https://doi.org/10.1126/science.1110647

Nociti, V., & Santoro, M. (2021). What do we know about the role of lncRNAs in multiple sclerosis? *Neural Regeneration Research*, *16*(9), 1715–1722. https://doi.org/10.4103/1673-5374.306061

Olsson, T., Barcellos, L. F., & Alfredsson, L. (2017). Interactions between genetic, lifestyle and environmental risk factors for multiple sclerosis. *Nature Reviews. Neurology*, *13*(1), 25–36. https://doi.org/10.1038/nrneurol.2016.187

Ostkamp, P., & Schwab, N. (2022). Effects of Latitude and Sunlight on Multiple Sclerosis Severity: Two Peas in a Pod? *Neurology*, *98*(24), 997–998. https://doi.org/10.1212/WNL.0000000000200105

Ousman, S. S., & Kubes, P. (2012). Immune surveillance in the central nervous system. *Nature Neuroscience*, *15*(8), 1096–1101. https://doi.org/10.1038/nn.3161

Owczarzy, R., Tataurov, A. V., Wu, Y., Manthey, J. A., McQuisten, K. A., Almabrazi, H. G., Pedersen, K. F., Lin, Y., Garretson, J., McEntaggart, N. O., Sailor, C. A., Dawson, R. B., & Peek, A. S. (2008). IDT SciTools: a suite for analysis and design of nucleic acid oligomers. *Nucleic Acids Research*, *36*(Web Server), W163–W169. https://doi.org/10.1093/nar/gkn198

Pang, K. C., Frith, M. C., & Mattick, J. S. (2006). Rapid evolution of noncoding RNAs: lack of conservation does not mean lack of function. *Trends in Genetics : TIG*, *22*(1), 1–5. https://doi.org/10.1016/j.tig.2005.10.003

Patel, R. S., Lui, A., Hudson, C., Moss, L., Sparks, R. P., Hill, S. E., Shi, Y., Cai, J., Blair, L. J., Bickford, P. C., & Patel, N. A. (2023). Small molecule targeting long noncoding RNA GAS5 administered intranasally improves neuronal insulin signaling and decreases neuroinflammation in an aged mouse model. *Scientific Reports*, *13*(1), 317. https://doi.org/10.1038/s41598-022-27126-6

Pennell, L. M., & Fish, E. N. (2017). Interferon-β regulates dendritic cell activation and migration in experimental autoimmune encephalomyelitis. *Immunology*, *152*(3), 439–450. https://doi.org/10.1111/imm.12781

Pheasant, M., & Mattick, J. S. (2007). Raising the estimate of functional human sequences. *Genome Research*, *17*(9), 1245–1253. https://doi.org/10.1101/gr.6406307

Pisignano, G., & Ladomery, M. (2021). Epigenetic Regulation of Alternative Splicing: How LncRNAs Tailor the Message. *Non-Coding RNA*, *7*(1). https://doi.org/10.3390/ncrna7010021

Polman, C. H., O'Connor, P. W., Havrdova, E., Hutchinson, M., Kappos, L., Miller, D. H., Phillips, J. T., Lublin, F. D., Giovannoni, G., Wajgt, A., Toal, M., Lynn, F., Panzara, M. A., Sandrock, A. W., & AFFIRM Investigators. (2006). A randomized, placebo-controlled trial of natalizumab for relapsing multiple sclerosis. *The New England Journal of Medicine*, *354*(9), 899–910. https://doi.org/10.1056/NEJMoa044397

Ponomarev, E. D., Maresz, K., Tan, Y., & Dittel, B. N. (2007). CNS-derived interleukin-4 is essential for the regulation of autoimmune inflammation and induces a state of alternative activation in microglial cells. *The Journal of Neuroscience : The Official Journal of the Society for Neuroscience*, *27*(40), 10714–10721. https://doi.org/10.1523/JNEUROSCI.1922-07.2007

Prinz, M., Erny, D., & Hagemeyer, N. (2017). Erratum: Ontogeny and homeostasis of CNS myeloid cells. *Nature Immunology*, *18*(8), 951. https://doi.org/10.1038/ni0817-951d

Prinz, M., & Priller, J. (2014). Microglia and brain macrophages in the molecular age: from origin to neuropsychiatric disease. *Nature Reviews. Neuroscience*, *15*(5), 300–312. https://doi.org/10.1038/nrn3722

Qi, F., Jiang, Z., Hou, W., Peng, B., Cheng, S., Zhang, X., Luo, Z., Dai, Z., Wang, Y., Liu, Y., Wang, Y., & Wang, Z. (2020). The Clock-Controlled lncRNA-AK028245 Participates in the Immune Response via Immune Response Factors OTUD7B and A20. *Journal of Biological Rhythms*, *35*(6), 542–554. https://doi.org/10.1177/0748730420944328

Quarta, A., Berneman, Z., & Ponsaerts, P. (2021). Functional consequences of a close encounter between microglia and brain-infiltrating monocytes during CNS pathology and repair. *Journal of Leukocyte Biology*, *110*(1), 89–106. https://doi.org/10.1002/JLB.3RU0820-536R

Ramaglia, V., Hughes, T. R., Donev, R. M., Ruseva, M. M., Wu, X., Huitinga, I., Baas, F., Neal, J. W., & Morgan, B. P. (2012). C3-dependent mechanism of microglial priming relevant to multiple sclerosis. *Proceedings of the National Academy of Sciences of the United States of America*, *109*(3), 965–970. https://doi.org/10.1073/pnas.1111924109

Ramilowski, J. A., Yip, C. W., Agrawal, S., Chang, J.-C., Ciani, Y., Kulakovskiy, I. V., Mendez, M., Ooi, J. L. C., Ouyang, J. F., Parkinson, N., Petri, A., Roos, L., Severin, J., Yasuzawa, K., Abugessaisa, I., Akalin, A., Antonov, I. V., Arner, E., Bonetti, A., … Carninci, P. (2020). Functional annotation of human long noncoding RNAs via molecular phenotyping. *Genome Research*, *30*(7), 1060–1072. https://doi.org/10.1101/gr.254219.119

Ransohoff, R. M. (2016a). A polarizing question: do M1 and M2 microglia exist? *Nature Neuroscience*, *19*(8), 987–991. https://doi.org/10.1038/nn.4338

Ransohoff, R. M. (2016b). How neuroinflammation contributes to neurodegeneration. *Science (New York, N.Y.)*, *353*(6301), 777–783. https://doi.org/10.1126/science.aag2590

Ray-Jones, H., & Spivakov, M. (2021). Transcriptional enhancers and their communication with gene promoters. *Cellular and Molecular Life Sciences : CMLS*, *78*(19–20), 6453–6485. https://doi.org/10.1007/s00018-021-03903-w

Rego, D., Kumar, A., Nilchi, L., Wright, K., Huang, S., & Kozlowski, M. (2011). IL-6 production is positively regulated by two distinct Src homology domain 2-containing tyrosine phosphatase-1 (SHP-1)-dependent CCAAT/enhancer-binding protein β and NF-κB pathways and an SHP-1-independent NF-κB pathway in lipopolysaccharide-stimulated bone marrow-derived macrophages. *Journal of Immunology (Baltimore, Md. : 1950)*, *186*(9), 5443–5456. https://doi.org/10.4049/jimmunol.1003551

Reich, D. S., Lucchinetti, C. F., & Calabresi, P. A. (2018). Multiple Sclerosis. *The New England Journal of Medicine*, *378*(2), 169–180. https://doi.org/10.1056/NEJMra1401483

Riedhammer, C., & Weissert, R. (2015). Antigen Presentation, Autoantigens, and Immune Regulation in Multiple Sclerosis and Other Autoimmune Diseases. *Frontiers in Immunology*, *6*, 322. https://doi.org/10.3389/fimmu.2015.00322

Roche, P. A., & Cresswell, P. (2016). Antigen Processing and Presentation Mechanisms in Myeloid Cells. *Microbiology Spectrum*, *4*(3). https://doi.org/10.1128/microbiolspec.MCHD-0008-2015

Romero-Barrios, N., Legascue, M. F., Benhamed, M., Ariel, F., & Crespi, M. (2018). Splicing regulation by long noncoding RNAs. *Nucleic Acids Research*, *46*(5), 2169–2184. https://doi.org/10.1093/nar/gky095

Ruiz, F., Vigne, S., & Pot, C. (2019). Resolution of inflammation during multiple sclerosis. *Seminars in Immunopathology*, *41*(6), 711–726. https://doi.org/10.1007/s00281-019-00765-0

Sabaie, H., Salkhordeh, Z., Asadi, M. R., Ghafouri-Fard, S., Amirinejad, N., Askarinejad Behzadi, M., Hussen, B. M., Taheri, M., & Rezazadeh, M. (2021). Long Non-Coding RNA- Associated Competing Endogenous RNA Axes in T-Cells in Multiple Sclerosis. *Frontiers in Immunology*, *12*, 770679. https://doi.org/10.3389/fimmu.2021.770679

Sabel, C. E., Pearson, J. F., Mason, D. F., Willoughby, E., Abernethy, D. A., & Taylor, B. V. (2021). The latitude gradient for multiple sclerosis prevalence is established in the early life course. *Brain : A Journal of Neurology*, *144*(7), 2038–2046. https://doi.org/10.1093/brain/awab104

Saldi, T. K., Gonzales, P. K., LaRocca, T. J., & Link, C. D. (2019). Neurodegeneration, Heterochromatin, and Double-Stranded RNA. *Journal of Experimental Neuroscience*, *13*, 1179069519830697. https://doi.org/10.1177/1179069519830697

Savarin, C., Dutta, R., & Bergmann, C. C. (2018). Distinct Gene Profiles of Bone Marrow-Derived Macrophages and Microglia During Neurotropic Coronavirus-Induced Demyelination. *Frontiers in Immunology*, *9*, 1325. https://doi.org/10.3389/fimmu.2018.01325

Scazzone, C., Agnello, L., Bivona, G., Lo Sasso, B., & Ciaccio, M. (2021). Vitamin D and Genetic Susceptibility to Multiple Sclerosis. *Biochemical Genetics*, *59*(1), 1–30. https://doi.org/10.1007/s10528-020-10010-1

Schuettengruber, B., Chourrout, D., Vervoort, M., Leblanc, B., & Cavalli, G. (2007). Genome regulation by polycomb and trithorax proteins. *Cell*, *128*(4), 735–745. https://doi.org/10.1016/j.cell.2007.02.009

Seifuddin, F., Singh, K., Suresh, A., Judy, J. T., Chen, Y.-C., Chaitankar, V., Tunc, I., Ruan, X., Li, P., Chen, Y., Cao, H., Lee, R. S., Goes, F. S., Zandi, P. P., Jafri, M. S., & Pirooznia, M. (2020). lncRNAKB, a knowledgebase of tissue-specific functional annotation and trait association of long noncoding RNA. *Scientific Data*, *7*(1), 326. https://doi.org/10.1038/s41597-020-00659-z

Shabab, T., Khanabdali, R., Moghadamtousi, S. Z., Kadir, H. A., & Mohan, G. (2017a). Neuroinflammation pathways: a general review. *The International Journal of Neuroscience*, *127*(7), 624–633. https://doi.org/10.1080/00207454.2016.1212854

Shabab, T., Khanabdali, R., Moghadamtousi, S. Z., Kadir, H. A., & Mohan, G. (2017b). Neuroinflammation pathways: a general review. *International Journal of Neuroscience*, *127*(7), 624–633. https://doi.org/10.1080/00207454.2016.1212854

Shemer, A., Grozovski, J., Tay, T. L., Tao, J., Volaski, A., Süß, P., Ardura-Fabregat, A., Gross-Vered, M., Kim, J.-S., David, E., Chappell-Maor, L., Thielecke, L., Glass, C. K., Cornils, K., Prinz, M., & Jung, S. (2018). Engrafted parenchymal brain macrophages differ from microglia in transcriptome, chromatin landscape and response to challenge. *Nature Communications*, *9*(1), 5206. https://doi.org/10.1038/s41467-018-07548-5

Shi, Q., Colodner, K. J., Matousek, S. B., Merry, K., Hong, S., Kenison, J. E., Frost, J. L., Le, K. X., Li, S., Dodart, J.-C., Caldarone, B. J., Stevens, B., & Lemere, C. A. (2015). Complement C3-Deficient Mice Fail to Display Age-Related Hippocampal Decline. *The Journal of Neuroscience : The Official Journal of the Society for Neuroscience*, *35*(38), 13029–13042. https://doi.org/10.1523/JNEUROSCI.1698-15.2015

Sierra, A., Abiega, O., Shahraz, A., & Neumann, H. (2013). Janus-faced microglia: beneficial and detrimental consequences of microglial phagocytosis. *Frontiers in Cellular Neuroscience*, *7*, 6. https://doi.org/10.3389/fncel.2013.00006

Singh, S., Metz, I., Amor, S., van der Valk, P., Stadelmann, C., & Brück, W. (2013). Microglial nodules in early multiple sclerosis white matter are associated with degenerating axons. *Acta Neuropathologica*, *125*(4), 595–608. https://doi.org/10.1007/s00401-013-1082-0

Sparber, P., Filatova, A., Khantemirova, M., & Skoblov, M. (2019). The role of long non-coding RNAs in the pathogenesis of hereditary diseases. *BMC Medical Genomics*, *12*(Suppl 2), 42. https://doi.org/10.1186/s12920-019-0487-6

Statello, L., Guo, C.-J., Chen, L.-L., & Huarte, M. (2021). Gene regulation by long non-coding RNAs and its biological functions. *Nature Reviews. Molecular Cell Biology*, *22*(2), 96–118. https://doi.org/10.1038/s41580-020-00315-9

Stys, P. K., Zamponi, G. W., van Minnen, J., & Geurts, J. J. G. (2012). Will the real multiple sclerosis please stand up? *Nature Reviews. Neuroscience*, *13*(7), 507–514. https://doi.org/10.1038/nrn3275

Sun, D., Yu, Z., Fang, X., Liu, M., Pu, Y., Shao, Q., Wang, D., Zhao, X., Huang, A., Xiang, Z., Zhao, C., Franklin, R. J., Cao, L., & He, C. (2017). LncRNA GAS5 inhibits microglial M2 polarization and exacerbates demyelination. *EMBO Reports*, *18*(10), 1801–1816. https://doi.org/10.15252/embr.201643668

Täuber, H., Hüttelmaier, S., & Köhn, M. (2019). POLIII-derived non-coding RNAs acting as scaffolds and decoys. *Journal of Molecular Cell Biology*, *11*(10), 880–885. https://doi.org/10.1093/jmcb/mjz049

Tavares, R. C. A., Pyle, A. M., & Somarowthu, S. (2019). Phylogenetic Analysis with Improved Parameters Reveals Conservation in lncRNA Structures. *Journal of Molecular Biology*, *431*(8), 1592–1603. https://doi.org/10.1016/j.jmb.2019.03.012

Tian, Y., Liu, B., Li, Y., Zhang, Y., Shao, J., Wu, P., Xu, C., Chen, G., & Shi, H. (2022). Activation of RARα Receptor Attenuates Neuroinflammation After SAH via Promoting M1-to-M2 Phenotypic Polarization of Microglia and Regulating Mafb/Msr1/PI3K-Akt/NF-κB Pathway. *Frontiers in Immunology*, *13*, 839796. https://doi.org/10.3389/fimmu.2022.839796

Torkamandi, S., Bahrami, S., Ghorashi, T., Dehani, M., Bayat, H., Hoseini, S. M., Rezaei, S., & Soosanabadi, M. (2021). Dysregulation of long noncoding RNA MEG3 and NLRC5 expressions in patients with relapsing-remitting multiple sclerosis: is there any correlation? *Genes and Immunity*, *22*(7–8), 322–326. https://doi.org/10.1038/s41435-021-00154-4

Tramacere, I., Del Giovane, C., Salanti, G., D'Amico, R., & Filippini, G. (2015). Immunomodulators and immunosuppressants for relapsing-remitting multiple sclerosis: a network meta-analysis. *The Cochrane Database of Systematic Reviews*, *2015*(9), CD011381. https://doi.org/10.1002/14651858.CD011381.pub2

Trapp, B. D., & Nave, K.-A. (2008). Multiple sclerosis: an immune or neurodegenerative disorder? *Annual Review of Neuroscience*, *31*, 247–269. https://doi.org/10.1146/annurev.neuro.30.051606.094313

Traugott, U., Reinherz, E. L., & Raine, C. S. (1983). Multiple sclerosis. Distribution of T cells, T cell subsets and Ia-positive macrophages in lesions of different ages. *Journal of Neuroimmunology*, *4*(3), 201–221. https://doi.org/10.1016/0165-5728(83)90036-x

Tripathi, S., Shree, B., Mohapatra, S., Swati, Basu, A., & Sharma, V. (2021a). The Expanding Regulatory Mechanisms and Cellular Functions of Long Non-coding RNAs (lncRNAs) in Neuroinflammation. *Molecular Neurobiology*, *58*(6), 2916–2939. https://doi.org/10.1007/s12035-020-02268-8

Tripathi, S., Shree, B., Mohapatra, S., Swati, Basu, A., & Sharma, V. (2021b). The Expanding Regulatory Mechanisms and Cellular Functions of Long Non-coding RNAs (lncRNAs) in Neuroinflammation. *Molecular Neurobiology*, *58*(6), 2916–2939. https://doi.org/10.1007/s12035-020-02268-8

Trotman, J. B., Braceros, K. C. A., Cherney, R. E., Murvin, M. M., & Calabrese, J. M. (2021). The control of polycomb repressive complexes by long noncoding RNAs. *Wiley Interdisciplinary Reviews. RNA*, *12*(6), e1657. https://doi.org/10.1002/wrna.1657

Tsai, S.-J. (2017). Effects of interleukin-1beta polymorphisms on brain function and behavior in healthy and psychiatric disease conditions. *Cytokine & Growth Factor Reviews*, *37*, 89–97. https://doi.org/10.1016/j.cytogfr.2017.06.001

Ueno, M., Fujita, Y., Tanaka, T., Nakamura, Y., Kikuta, J., Ishii, M., & Yamashita, T. (2013). Layer V cortical neurons require microglial support for survival during postnatal development. *Nature Neuroscience*, *16*(5), 543–551. https://doi.org/10.1038/nn.3358

Uszczynska-Ratajczak, B., Lagarde, J., Frankish, A., Guigó, R., & Johnson, R. (2018). Towards a complete map of the human long non-coding RNA transcriptome. *Nature Reviews. Genetics*, *19*(9), 535–548. https://doi.org/10.1038/s41576-018-0017-y

Vainchtein, I. D., Vinet, J., Brouwer, N., Brendecke, S., Biagini, G., Biber, K., Boddeke, H. W. G. M., & Eggen, B. J. L. (2014). In acute experimental autoimmune encephalomyelitis, infiltrating macrophages are immune activated, whereas microglia remain immune suppressed. *Glia*, *62*(10), 1724–1735. https://doi.org/10.1002/glia.22711

van Loo, G., De Lorenzi, R., Schmidt, H., Huth, M., Mildner, A., Schmidt-Supprian, M., Lassmann, H., Prinz, M. R., & Pasparakis, M. (2006). Inhibition of transcription factor NF-kappaB in the central nervous system ameliorates autoimmune encephalomyelitis in mice. *Nature Immunology*, *7*(9), 954–961. https://doi.org/10.1038/ni1372

Vande Walle, L., Van Opdenbosch, N., Jacques, P., Fossoul, A., Verheugen, E., Vogel, P., Beyaert, R., Elewaut, D., Kanneganti, T.-D., van Loo, G., & Lamkanfi, M. (2014). Negative regulation of the NLRP3 inflammasome by A20 protects against arthritis. *Nature*, *512*(7512), 69–73. https://doi.org/10.1038/nature13322

Verboom, L., Martens, A., Priem, D., Hoste, E., Sze, M., Vikkula, H., Van Hove, L., Voet, S., Roels, J., Maelfait, J., Bongiovanni, L., de Bruin, A., Scott, C. L., Saeys, Y., Pasparakis, M., Bertrand, M. J. M., & van Loo, G. (2020). OTULIN Prevents Liver Inflammation and Hepatocellular Carcinoma by Inhibiting FADD- and RIPK1 Kinase-Mediated Hepatocyte Apoptosis. *Cell Reports*, *30*(7), 2237-2247.e6. https://doi.org/10.1016/j.celrep.2020.01.028

Vitkova, M., Diouf, I., Malpas, C., Horakova, D., Kubala Havrdova, E., Patti, F., Ozakbas, S., Izquierdo, G., Eichau, S., Shaygannejad, V., Onofrj, M., Lugaresi, A., Alroughani, R., Prat, A., Larochelle, C., Girard, M., Duquette, P., Terzi, M., Boz, C., … MSBase Study Group. (2022). Association of Latitude and Exposure to Ultraviolet B Radiation With Severity of Multiple Sclerosis: An International Registry Study. *Neurology*, *98*(24), e2401–e2412. https://doi.org/10.1212/WNL.0000000000200545

Voet, S., Mc Guire, C., Hagemeyer, N., Martens, A., Schroeder, A., Wieghofer, P., Daems, C., Staszewski, O., Vande Walle, L., Jordao, M. J. C., Sze, M., Vikkula, H.-K., Demeestere, D., Van Imschoot, G., Scott, C. L., Hoste, E., Gonçalves, A., Guilliams, M., Lippens, S., … van Loo, G. (2018). A20 critically controls microglia activation and inhibits inflammasome-dependent neuroinflammation. *Nature Communications*, *9*(1), 2036. https://doi.org/10.1038/s41467-018-04376-5

Walsh, J. G., Muruve, D. A., & Power, C. (2014). Inflammasomes in the CNS. *Nature Reviews. Neuroscience*, *15*(2), 84–97. https://doi.org/10.1038/nrn3638

Walther, K., & Schulte, L. N. (2021). The role of lncRNAs in innate immunity and inflammation. *RNA Biology*, *18*(5), 587–603. https://doi.org/10.1080/15476286.2020.1845505

Walton, C., King, R., Rechtman, L., Kaye, W., Leray, E., Marrie, R. A., Robertson, N., La Rocca, N., Uitdehaag, B., van der Mei, I., Wallin, M., Helme, A., Angood Napier, C., Rijke, N., & Baneke, P. (2020). Rising prevalence of multiple sclerosis worldwide: Insights from the Atlas of MS, third edition. *Multiple Sclerosis (Houndmills, Basingstoke, England)*, *26*(14), 1816–1821. https://doi.org/10.1177/1352458520970841

Wan, P., Su, W., & Zhuo, Y. (2017). The Role of Long Noncoding RNAs in Neurodegenerative Diseases. *Molecular Neurobiology*, *54*(3), 2012–2021. https://doi.org/10.1007/s12035-016-9793-6

Wang, Z., Kun, Y., Lei, Z., Dawei, W., Lin, P., & Jibo, W. (2021). LncRNA MIAT downregulates IL-1β, TNF-α to suppress macrophage inflammation but is suppressed by ATP-induced NLRP3 inflammasome activation. *Cell Cycle (Georgetown, Tex.)*, *20*(2), 194–203. https://doi.org/10.1080/15384101.2020.1867788

Ward, A. J., Norrbom, M., Chun, S., Bennett, C. F., & Rigo, F. (2014). Nonsense-mediated decay as a terminating mechanism for antisense oligonucleotides. *Nucleic Acids Research*, *42*(9), 5871–5879. https://doi.org/10.1093/nar/gku184

Weng, Q., Wang, J., Wang, J., Wang, J., Sattar, F., Zhang, Z., Zheng, J., Xu, Z., Zhao, M., Liu, X., Yang, L., Hao, G., Fang, L., Lu, Q. R., Yang, B., & He, Q. (2018). Lenalidomide regulates CNS autoimmunity by promoting M2 macrophages polarization. *Cell Death & Disease*, *9*(2), 251. https://doi.org/10.1038/s41419-018-0290-x

Wingerchuk, D. M. (2012). Smoking: effects on multiple sclerosis susceptibility and disease progression. *Therapeutic Advances in Neurological Disorders*, *5*(1), 13–22. https://doi.org/10.1177/1756285611425694

Wolf, Y., Shemer, A., Polonsky, M., Gross, M., Mildner, A., Yona, S., David, E., Kim, K.-W., Goldmann, T., Amit, I., Heikenwalder, M., Nedospasov, S., Prinz, M., Friedman, N., & Jung, S. (2017). Autonomous TNF is critical for in vivo monocyte survival in steady state and inflammation. *The Journal of Experimental Medicine*, *214*(4), 905–917. https://doi.org/10.1084/jem.20160499

Wu, H., Yin, Q.-F., Luo, Z., Yao, R.-W., Zheng, C.-C., Zhang, J., Xiang, J.-F., Yang, L., & Chen, L.-L. (2016). Unusual Processing Generates SPA LncRNAs that Sequester Multiple RNA Binding Proteins. *Molecular Cell*, *64*(3), 534–548. https://doi.org/10.1016/j.molcel.2016.10.007

Wu, J., Wang, C., & Ding, H. (2020). LncRNA MALAT1 promotes neuropathic pain progression through the miR-154-5p/AQP9 axis in CCI rat models. *Molecular Medicine Reports*, *21*(1), 291–303. https://doi.org/10.3892/mmr.2019.10829

Wurster, C. D., & Ludolph, A. C. (2018). Antisense oligonucleotides in neurological disorders. *Therapeutic Advances in Neurological Disorders*, *11*, 1756286418776932. https://doi.org/10.1177/1756286418776932

Xu, W., Zhang, L., Geng, Y., Liu, Y., & Zhang, N. (2020). Long noncoding RNA GAS5 promotes microglial inflammatory response in Parkinson's disease by regulating NLRP3 pathway through sponging miR-223-3p. *International Immunopharmacology*, *85*, 106614. https://doi.org/10.1016/j.intimp.2020.106614

Xue, Z., Zhang, Z., Liu, H., Li, W., Guo, X., Zhang, Z., Liu, Y., Jia, L., Li, Y., Ren, Y., Yang, H., Zhang, L., Zhang, Q., Da, Y., Hao, J., Yao, Z., & Zhang, R. (2019). lincRNA-Cox2 regulates NLRP3 inflammasome and autophagy mediated neuroinflammation. *Cell Death and Differentiation*, *26*(1), 130–145. https://doi.org/10.1038/s41418-018-0105-8

Yamasaki, R., Lu, H., Butovsky, O., Ohno, N., Rietsch, A. M., Cialic, R., Wu, P. M., Doykan, C. E., Lin, J., Cotleur, A. C., Kidd, G., Zorlu, M. M., Sun, N., Hu, W., Liu, L., Lee, J.-C., Taylor, S. E., Uehlein, L., Dixon, D., … Ransohoff, R. M. (2014). Differential roles of microglia and monocytes in the inflamed central nervous system. *The Journal of Experimental Medicine*, *211*(8), 1533–1549. https://doi.org/10.1084/jem.20132477

Yan, W., Chen, Z.-Y., Chen, J.-Q., & Chen, H.-M. (2018). LncRNA NEAT1 promotes autophagy in MPTP-induced Parkinson's disease through stabilizing PINK1 protein. *Biochemical and Biophysical Research Communications*, *496*(4), 1019–1024. https://doi.org/10.1016/j.bbrc.2017.12.149

Yan, Z., Gibson, S. A., Buckley, J. A., Qin, H., & Benveniste, E. N. (2018). Role of the JAK/STAT signaling pathway in regulation of innate immunity in neuroinflammatory diseases. *Clinical Immunology (Orlando, Fla.)*, *189*, 4–13. https://doi.org/10.1016/j.clim.2016.09.014

Yang, H., & Chen, J. (2022). Bone marrow mesenchymal stem cell-derived exosomes carrying long noncoding RNA ZFAS1 alleviate oxidative stress and inflammation in ischemic stroke by inhibiting microRNA-15a-5p. *Metabolic Brain Disease*, *37*(7), 2545–2557. https://doi.org/10.1007/s11011-022-00997-4

Yang, X., Zhang, Y., Chen, Y., He, X., Qian, Y., Xu, S., Gao, C., Mo, C., Chen, S., & Xiao, Q. (2021). LncRNA HOXA-AS2 regulates microglial polarization via recruitment of PRC2 and epigenetic modification of PGC-1α expression. *Journal of Neuroinflammation*, *18*(1), 197. https://doi.org/10.1186/s12974-021-02267-z

Yin, Q.-F., Yang, L., Zhang, Y., Xiang, J.-F., Wu, Y.-W., Carmichael, G. G., & Chen, L.-L. (2012). Long noncoding RNAs with snoRNA ends. *Molecular Cell*, *48*(2), 219–230. https://doi.org/10.1016/j.molcel.2012.07.033

Yu, T., Gan, S., Zhu, Q., Dai, D., Li, N., Wang, H., Chen, X., Hou, D., Wang, Y., Pan, Q., Xu, J., Zhang, X., Liu, J., Pei, S., Peng, C., Wu, P., Romano, S., Mao, C., Huang, M., … Xiao, Y. (2019). Modulation of M2 macrophage polarization by the crosstalk between Stat6 and Trim24. *Nature Communications*, *10*(1), 4353. https://doi.org/10.1038/s41467-019-12384-2

Zhan, J., Qin, W., Zhang, Y., Jiang, J., Ma, H., Li, Q., & Luo, Y. (2016). Upregulation of neuronal zinc finger protein A20 expression is required for electroacupuncture to attenuate the cerebral inflammatory injury mediated by the nuclear factor-kB signaling pathway in cerebral ischemia/reperfusion rats. *Journal of Neuroinflammation*, *13*(1), 258. https://doi.org/10.1186/s12974-016-0731-3

Zhang, P., Cao, L., Zhou, R., Yang, X., & Wu, M. (2019). The lncRNA Neat1 promotes activation of inflammasomes in macrophages. *Nature Communications*, *10*(1), 1495. https://doi.org/10.1038/s41467-019-09482-6

Zhang, Q., Lenardo, M. J., & Baltimore, D. (2017). 30 Years of NF-κB: A Blossoming of Relevance to Human Pathobiology. *Cell*, *168*(1–2), 37–57. https://doi.org/10.1016/j.cell.2016.12.012

Zhang, Y., & Zhang, Y. (2020). lncRNA ZFAS1 Improves Neuronal Injury and Inhibits Inflammation, Oxidative Stress, and Apoptosis by Sponging miR-582 and Upregulating NOS3 Expression in Cerebral Ischemia/Reperfusion Injury. *Inflammation*, *43*(4), 1337–1350. https://doi.org/10.1007/s10753-020-01212-1

Zhao, J., Sun, B. K., Erwin, J. A., Song, J.-J., & Lee, J. T. (2008). Polycomb Proteins Targeted by a Short Repeat RNA to the Mouse X Chromosome. *Science*, *322*(5902), 750–756. https://doi.org/10.1126/science.1163045

Zhou, H.-J., Wang, L.-Q., Zhan, R.-Y., Zheng, X.-J., & Zheng, J.-S. (2022). lncRNA MEG3 restrained the M1 polarization of microglia in acute spinal cord injury through the HuR/A20/NF-κB axis. *Brain Pathology (Zurich, Switzerland)*, *32*(5), e13070. https://doi.org/10.1111/bpa.13070

Zhou, T., Kim, Y., & MacLeod, A. R. (2016). Targeting Long Noncoding RNA with Antisense Oligonucleotide Technology as Cancer Therapeutics. *Methods in Molecular Biology (Clifton, N.J.)*, *1402*, 199–213. https://doi.org/10.1007/978-1-4939-3378-5_16

Zhou, X., & Xu, J. (2015). Identification of Alzheimer's disease-associated long noncoding RNAs. *Neurobiology of Aging*, *36*(11), 2925–2931. https://doi.org/10.1016/j.neurobiolaging.2015.07.015

Zhu, Z., Huang, P., Sun, R., Li, X., Li, W., & Gong, W. (2022). A Novel Long-Noncoding RNA LncZFAS1 Prevents MPP+-Induced Neuroinflammation Through MIB1 Activation. *Molecular Neurobiology*, *59*(2), 778–799. https://doi.org/10.1007/s12035-021-02619-z

Zrzavy, T., Hametner, S., Wimmer, I., Butovsky, O., Weiner, H. L., & Lassmann, H. (2017). Loss of "homeostatic" microglia and patterns of their activation in active multiple sclerosis. *Brain : A Journal of Neurology*, *140*(7), 1900–1913. https://doi.org/10.1093/brain/awx113

Zucchelli, S., Cotella, D., Takahashi, H., Carrieri, C., Cimatti, L., Fasolo, F., Jones, M., Sblattero, D., Sanges, R., Santoro, C., Persichetti, F., Carninci, P., & Gustincich, S. (2015). SINEUPs: A new class of natural and synthetic antisense long non-coding RNAs that activate translation. *RNA Biology*, *12*(8), 771–779. https://doi.org/10.1080/15476286.2015.1060395

Zuker, M. (2003). Mfold web server for nucleic acid folding and hybridization prediction. *Nucleic Acids Research*, *31*(13), 3406–3415. https://doi.org/10.1093/nar/gkg595

Attachments

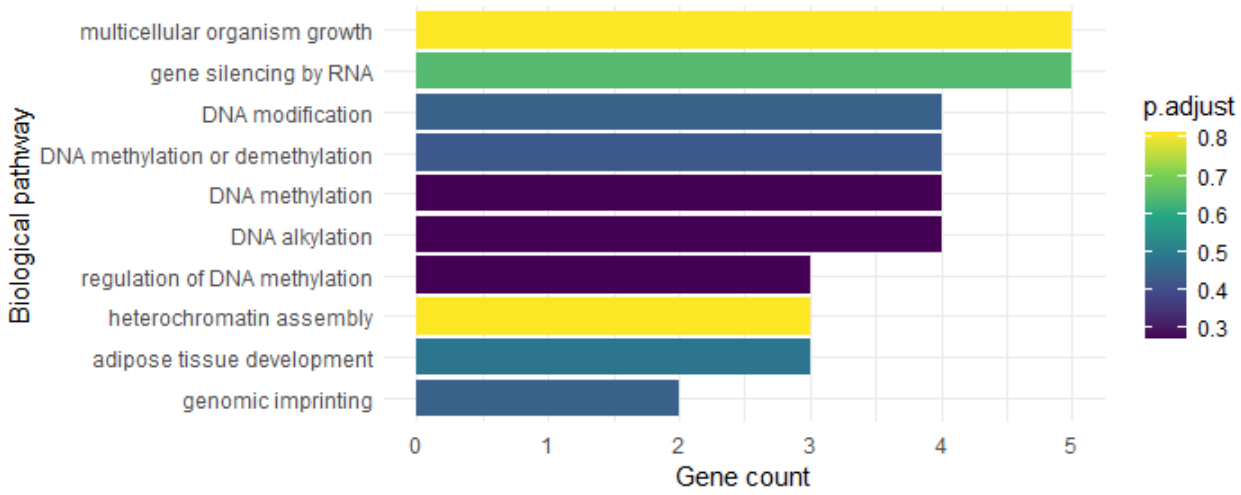

Supplementary figure 1. Top 10 biological pathways based on gene ontology enrichment (GOE) analysis of differentially expressed lncRNAs in spinal cord tissue of experimental autoimmune encephalomyelitis (EAE) mice at 20 post-immunization. RNA isolated from spinal cord tissue of non-immunised control (n = 4) mice and myelin oligodendrocyte glycoprotein (MOG_{35-55}) immunised EAE mice at day 20 (n = 4) post-immunisation, was subjected to total RNA sequencing and downstream processing. Long non-coding (Lnc)RNAs with an adjusted p-value < 0.05 compared to the control, were subjected to GOE. The x-axis displays the number of differentially expressed genes belonging to each biological pathway, while the color gradient indicates the corresponding adjusted p-value (p.adjust). The lower the p-value the more significant the pathway is enriched (more identified differential expressed genes on the total amount of genes belonging to the pathway). The top 10 biological pathways are visualized for both EAE day 9 **(a)** and EAE day 20 **(b).**

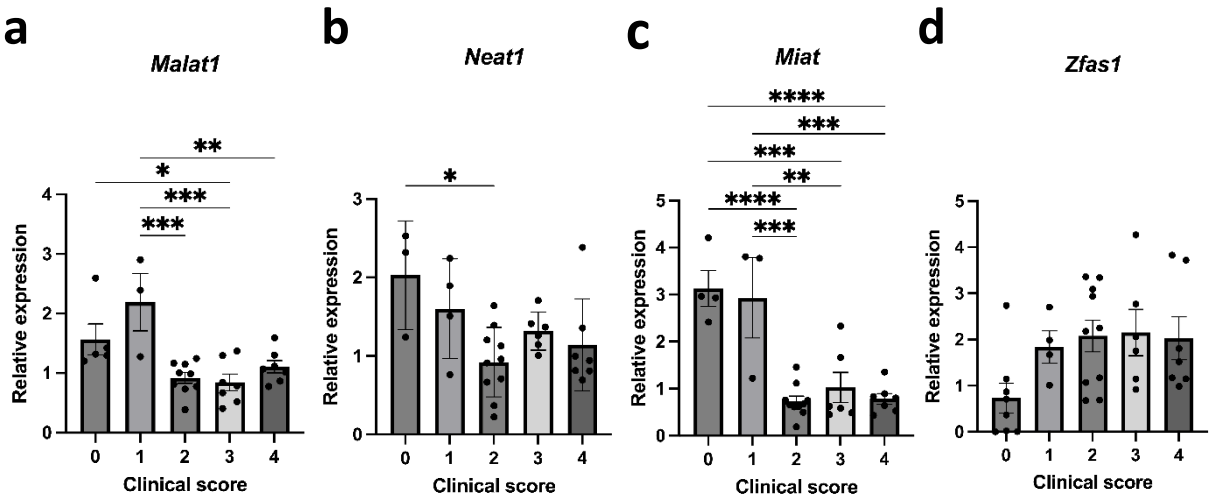

Supplementary Figure 2. Relative gene expression levels of lncRNAs in the spinal cord of experimental autoimmune encephalomyelitis (EAE) pathology at different clinical scores. RT-qPCR was performed on RNA from spinal cord tissue of myelin oligodendrocyte glycoprotein (MOG_{35-55}) peptide immunised WT (WT EAE, n = 8) and A20 KO (A20 KO EAE, n = 8) mice, and non-immunised WT (n = 4) and A20 KO (n = 4) mice 15 days post-immunisation. The y-axis represents the relative gene expression of *Malat1 (**a**), Neat1 (**b**), Miat (**c**)* and *Zfas1 (**d**)*, while the x-axis represents the different clinical scores neglecting the genetic background. All groups were normalised to the expression of the housekeeping genes *Gapdh* and *Hprt*. Statistical significance was determined using one-way ANOVA with Tukey's correction for multiple comparison. *p < 0.05, **p < 0.01, ***p < 0.001, ****p < 0.0001. Results are displayed as mean ± SEM .

cDNA prep. SMARTer Stranded Total RNA-seq Kit v3

SMARTer® Stranded Total RNA-Seq Kit v3 - Pico Input Mammalian User Manual

In order to generate library inserts of an appropriate size for compatibility with Illumina sequencing, RNA molecules obtained from high-quality or partially degraded samples must be fragmented prior to cDNA synthesis. For highly degraded, low-quality starting material, the RNA fragmentation step should be skipped. Please refer to Option 2 for Section V.A for guidance on how to proceed if you are skipping the fragmentation step.

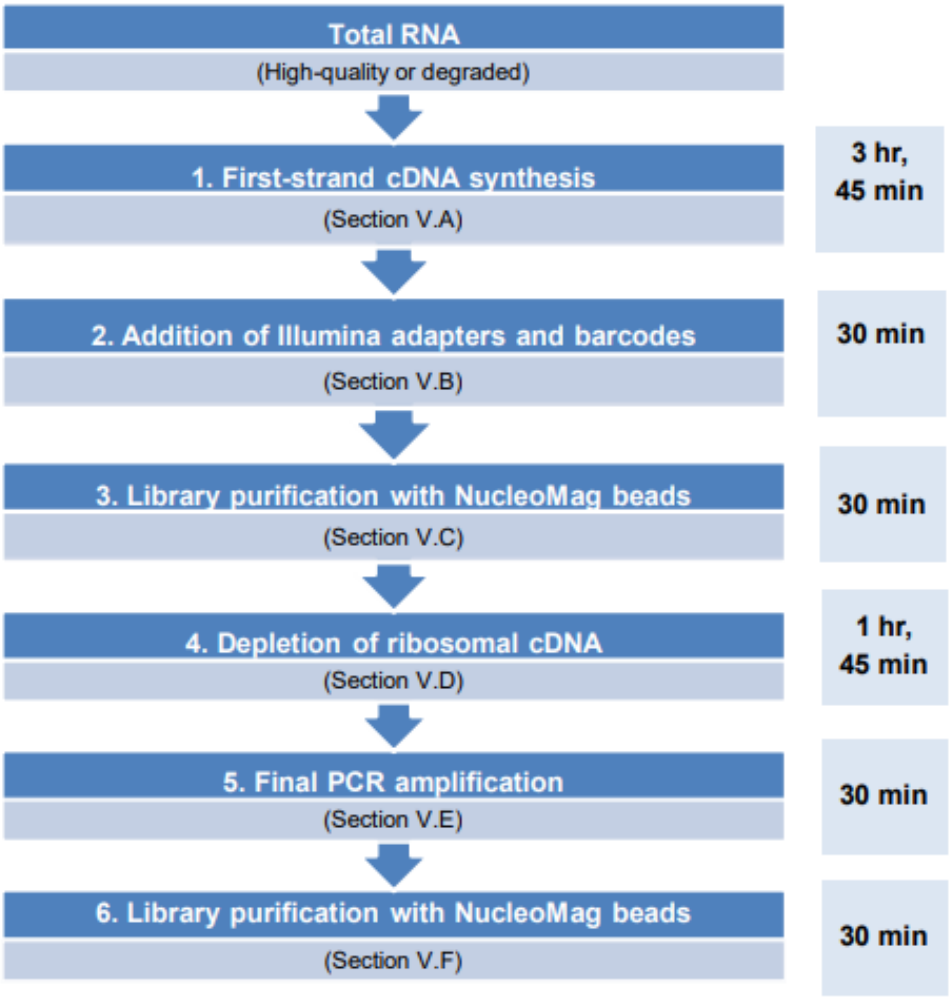

Figure 1. SMARTer Stranded Total RNA-Seq Kit v3 - Pico Input Mammalian protocol overview. This kit features an easy workflow that generates Illumina-compatible RNA-seq libraries in approximately 7 hr 30 min. Actual processing time may vary depending on the number of samples and cycling conditions (e.g., Protocol E takes more than 30 min if using 16 cycles of PCR or if using a thermal cycler with a slow ramping time). First, total RNA is converted to cDNA (Protocol A), and then adapters for Illumina sequencing (with specific barcodes) are added through PCR using a limited number of cycles (Protocol B). The PCR products are purified (Protocol C), and then ribosomal cDNA is depleted (Protocol D). The cDNA fragments from Protocol D are further amplified (Protocol E) with primers universal to all libraries. Lastly, the PCR products are purified once more to yield the final cDNA library (Protocol F). As outlined in Section V, the kit workflow includes three safe stopping points following the completion of Protocols A, B, and E, respectively.

Option 1 (With Fragmentation): Starting from High-Quality or Partially Degraded RNA

1. *To start with RNA samples*, mix the following components on ice:

1–8 µl	RNA
1 µl	SMART Pico Oligos Mix v3
4 µl	5X First-Strand Buffer
0–7 µl	Nuclease-free water
13 µl	Total volume per reaction

Incubate the tubes at 94°C in a preheated, hot-lid thermal cycler for the amount of time recommended in Table 1 or for an experimentally determined, optimal amount of time, then immediately place the samples on an ice-cold PCR chiller rack for 2 min.

NOTE: The samples should be taken out of the thermal cycler immediately after the time indicated to avoid overfragmentation. Make sure to wait by the thermal cycler when the incubation time is over and immediately chill the samples.

NOTE: The next reaction steps (Steps 4–5) are critical for first-strand synthesis and should not be delayed after Step 2. Start Step 3, preparing the First-Strand Master Mix, while your tubes are incubating (Step 2), or have it almost ready before starting Step 2.

2. *To start with cells:*
   a. Prepare RNase Inhibitor Water (RI Water) by combining 199 µl of Nuclease-free water with 1 µl of RNase Inhibitor (scale up as needed). Mix by vortexing and keep on ice until needed.
   b. Prepare a stock solution of 10X Lysis Mix by combining 19 µl of 10X Lysis Buffer and 1 µl of RNase Inhibitor (scale up as needed). Mix by vortexing and keep on ice until needed.
   c. Make sure your cells are in a total volume of 7 µl, in 0.2-ml PCR tubes or strip tubes. If input volume is less than 7 µl, complete with RI Water. Keep sample on ice.

      NOTE: Make sure to include a negative control with 7 µl RI Water, in addition to any other mock or no-cell control.

   d. Prepare enough Shearing Master Mix for all reactions, plus 10%, by combining following:

1 µl	10X Lysis Mix
1 µl	SMART Pico Oligos Mix v3
4 µl	5X First-Strand Buffer
6 µl	Total volume per reaction

   e. Add 6 µl of the Shearing Master Mix to each of your 7 µl cell suspension prepared in Step 2c, and mix by tapping gently, then spin down.
   f. Incubate the tube at 85°C in a preheated, hot-lid thermal cycler for **6 min** then immediately place the samples on an ice-cold PCR chiller rack for 2 min.

3. Prepare enough First-Strand Master Mix for all reactions, plus 10%, by combining the following reagents on ice, in the order shown:

4.5 µl	SMART UMI-TSO Mix v3
0.5 µl	RNase Inhibitor
2 µl	SMARTScribe II Reverse Transcriptase
7 µl	Total volume per reaction

NOTE: The SMART UMI-TSO Mix v3 is very viscous—make sure to homogenize the First-Strand Master Mix very well by pipetting up and down 10 times with a pipette set at a volume larger than the final master mix volume.

4. Add 7 µl of the First-Strand Master Mix to each reaction tube from Step 1 (RNA sample) or Step 2 (cells). Mix the contents of the tubes by vortexing for ~2 sec, then spin the tubes briefly to collect the contents at the bottom.

NOTE: The First-Strand Master Mix is very viscous—make sure to homogenize the content of the tubes very well.

5. Incubate the tubes in a preheated hot-lid thermal cycler with the following program:

42°C	180 min
70°C	10 min
4°C	forever

6. Leave the samples in the thermal cycler at 4°C until the next step.

SAFE STOPPING POINT: Samples can be left overnight in the thermal cycler at 4°C. If not processed the next day, freeze the cDNA at –20°C for up to 2 weeks.

Option 2 (Without Fragmentation): Starting from Highly Degraded RNA

1. Mix the following components on ice:

1–8 µl	RNA
1 µl	SMART Pico Oligos Mix v3
0–7 µl	Nuclease-free water
9 µl	Total volume per reaction

2. Incubate the tubes at **72°C** in a preheated, hot-lid thermal cycler for exactly 3 min, then immediately place the samples on an ice-cold PCR chiller rack for 2 min.
3. Prepare enough First-Strand Master Mix for all reactions, plus 10%, by combining the following reagents on ice, in the order shown.

4 µl	5X First-Strand Buffer
4.5 µl	SMART UMI-TSO Mix v3
0.5 µl	RNase Inhibitor
2 µl	SMARTScribe II Reverse Transcriptase
11 µl	Total volume per reaction

NOTE: The SMART UMI-TSO Mix v3 is very viscous—make sure to homogenize the First-Strand Master Mix very well by pipetting up and down 10 times with a pipette set at a volume larger than the final master mix volume.

4. Add 11 µl of the First-Strand Master Mix to each reaction tube from Step 2. Mix the contents of the tubes by vortexing for ~2 sec, then spin the tubes briefly to collect the contents at the bottom.

   NOTE: The First-Strand Master Mix is very viscous—make sure to homogenize the content of the tubes very well.

5. Incubate the tubes in a preheated hot-lid thermal cycler with the following program:

42°C	180 min
70°C	10 min
4°C	forever

6. Leave the samples in the thermal cycler at 4°C until the next step.

   SAFE STOPPING POINT: Samples can be left overnight in the thermal cycler at 4°C. If not processed the next day, freeze the cDNA at –20°C for up to 2 weeks.

Protocol: Purification of Total RNA, Including Small RNAs, from Animal Tissues

Important points before starting

- If using the miRNeasy Mini Kit for the first time, read "Important Notes" (page 14).
- It is important not to overload the RNeasy Mini spin column, as overloading will significantly reduce RNA yield and quality. Read "Determining the amount of starting material" (page 14).
- If working with RNA for the first time, read Appendix E (page 52).
- For optimal results, stabilize harvested tissues immediately in RNAprotect Tissue Reagent or Allprotect Stabilization Reagent. Tissues can be stored in the reagent for up to 1 day at 37°C, 7 days at 15–25°C, or 4 weeks at 2–8°C, or archived at –30°C to –15°C or –90°C to –65°C.
- Fresh, frozen or RNAprotect-or AllProtect-stabilized tissues can be used. Tissues can be stored for several months at –90°C to –65°C. Do not allow tissues to thaw during weighing or handling prior to disruption in QIAzol Lysis Reagent. Homogenized tissue lysates (in QIAzol Lysis Reagent, step 3) can also be stored at –90°C to –65°C for several months. To process frozen homogenized lysates, incubate at 37°C in a water bath until completely thawed and salts are dissolved. Avoid prolonged incubation, which may compromise RNA integrity. Continue with step 4.
- Generally, DNase digestion is not required since the combination of QIAzol and RNeasy technologies efficiently removes most of the DNA without DNase treatment. In addition, miRCURY LNA miRNA PCR Assay and most other assays for mature miRNA are not affected by the presence of small amounts of genomic DNA. However, further DNA removal may be necessary for certain RNA applications that are sensitive to very small amounts of DNA. In these cases, small residual amounts of DNA can be removed by on-column DNase digestion (see Appendix B, page 44) or by DNase digestion after RNA purification (please contact QIAGEN Technical Service for a protocol).

- Buffer RWT may form a precipitate upon storage. If necessary, redissolve by warming and then place at room temperature (15–25°C).
- QIAzol Lysis Reagent and Buffer RWT contain a guanidine salt and are therefore not compatible with disinfecting reagents containing bleach. See page 5 for safety information.
- Except for phase separation (step 7), all protocol and centrifugation steps should be performed at room temperature. During the procedure, work quickly.

Things to do before starting

- Buffers RWT and RPE are supplied as concentrates. Before using for the first time, add the required amounts of ethanol (96–100%), as indicated on the bottle, to obtain a working solution.
- If performing optional on-column DNase digestion, prepare DNase I stock solution as described in Appendix B (page 44).

Procedure

1. Excise the tissue sample from the animal or remove it from storage. Determine the amount of tissue. Do not use more than 50 mg flash-frozen tissue, 25 mg liver, thymus, spleen or RNAprotect-stabilized tissue, or 100 mg adipose tissue.

   Unless you are working with RNAprotect Tissue- or AllProtect-stabilized tissue, do not allow the tissue to thaw before placing in QIAzol Lysis Reagent.
2. If the entire piece of tissue can be used for RNA purification, place it directly into 700 µl QIAzol Lysis Reagent in a suitably sized vessel for disruption and homogenization.

   If only a portion of the tissue is to be used, determine the weight of the piece to be used and place it into 700 µl QIAzol Lysis Reagent in a suitably sized vessel for disruption and homogenization.

RNA in tissues is not protected after harvesting until the sample is stabilized in RNAprotect Tissue Reagent or AllProtect Reagent, flash-frozen or disrupted and homogenized in step 3. Frozen animal tissue should not be allowed to thaw during handling.

Note: Use a suitably sized vessel with sufficient headspace to accommodate foaming, which may occur during homogenization.

3. Homogenize immediately using the TissueLyser II, TissueLyser LT, TissueRuptor II or another method until the sample is uniformly homogeneous (usually 20–40 s).

   See "Disrupting and homogenizing starting material", page 19, for a more detailed description of disruption and homogenization methods.

   Note: Homogenization with the TissueRuptor II or the TissueLyser II/TissueLyser LT (see Appendix C, page 48, or the appropriate *TissueLyser Handbook*) generally results in higher total RNA yields than with other homogenization methods.

   Foaming may occur during homogenization, especially of brain tissue. If this occurs, let the homogenate stand at room temperature (15–25°C) for 2–3 min until the foam subsides before continuing with the protocol.

   Note: Homogenized tissue lysates can be stored at –90°C to –65°C for several months.

4. Place the tube containing the homogenate on the benchtop at room temperature for 5 min.

   This step promotes dissociation of nucleoprotein complexes.

5. Add 140 µl chloroform to the tube containing the homogenate and cap it securely.

   Shake the tube vigorously for 15 s.

   Thorough mixing is important for subsequent phase separation.

6. Place the tube containing the homogenate on the benchtop at room temperature for 2–3 min.

7. Centrifuge for 15 min at 12,000 x *g* at 4°C. After centrifugation, heat the centrifuge up to room temperature if the same centrifuge will be used for the next centrifugation steps.

   After centrifugation, the sample separates into 3 phases: an upper, colorless, aqueous phase containing RNA; a white interphase; and a lower, red, organic phase. For tissues with an especially high fat content, an additional, clear phase may be visible below the red, organic phase. The volume of the aqueous phase should be approximately 350 µl.

   Note: If you want to purify a separate miRNA-enriched fraction, follow the steps in Appendix A (page 40) after performing this step.

8. Transfer the upper aqueous phase to a new collection tube (supplied). Add 1.5 volumes (usually 525 µl) of 100% ethanol and mix thoroughly by pipetting up and down several times. Do not centrifuge. Continue without delay with step 9.

   A precipitate may form after addition of ethanol, but this will not affect the RNeasy procedure.

9. Pipet up to 700 µl of the sample, including any precipitate that may have formed, into an RNeasy Mini spin column in a 2 ml collection tube (supplied). Close the lid gently and centrifuge at ≥8000 x *g* (≥10,000 rpm) for 15 s at room temperature. Discard the flow-through.*

   Reuse the collection tube in step 10.

10. Repeat step 9 using the remainder of the sample. Discard the flow-through.*

    Reuse the collection tube in step 11.

    Optional: If performing optional on-column DNase digestion (see "Important points before starting"), follow the steps in Appendix B (page 44) after performing this step. 11.

* Flow-through contains QIAzol Lysis Reagent and is therefore not compatible with bleach. See page 5 for safety information.

11. Add 700 µl Buffer RWT to the RNeasy Mini spin column. Close the lid gently and centrifuge for 15 s at ≥8000 x *g* (≥10,000 rpm) to wash the column. Discard the flow-through.*

    Skip this step if performing the optional on-column DNase digestion (page 44).

    Reuse the collection tube in step 12.

12. Pipet 500 µl Buffer RPE into the RNeasy Mini spin column. Close the lid gently and centrifuge for 15 s at ≥8000 x *g* (≥10,000 rpm) to wash the column. Discard the flow-through.

    Reuse the collection tube in step 13.

13. Add another 500 µl Buffer RPE to the RNeasy Mini spin column. Close the lid gently and centrifuge for 2 min at ≥8000 x *g* (≥10,000 rpm) to dry the RNeasy Mini spin column membrane.

    The long centrifugation dries the spin column membrane, ensuring that no ethanol is carried over during RNA elution. Residual ethanol may interfere with downstream reactions.

    Note: Following centrifugation, remove the RNeasy Mini spin column from the collection tube carefully so the column does not contact the flow-through. Otherwise, carryover of ethanol will occur.

14. **Optional**: Place the RNeasy Mini spin column into a new 2 ml collection tube (not supplied), and discard the old collection tube with the flow-through. Centrifuge in a microcentrifuge at full speed for 1 min.

    Perform this step to eliminate any possible carryover of Buffer RPE or if residual.

    flow-through remains on the outside of the RNeasy Mini spin column after step 13.

15. Transfer the RNeasy Mini spin column to a new 1.5 ml collection tube (supplied). Pipet 30–50 µl RNase-free water directly onto the RNeasy Mini spin column membrane. Close the lid gently and centrifuge for 1 min at ≥8000 x *g* (≥10,000 rpm)

    to elute the RNA.

Protocol of RNA isolation using the Biorad Aurorum Total RNA mini kit

Aurum™ Total RNA Mini Kit

Spin Format
Protocol Overview*

Cultured cells

Adherent
Rinse vessel with PBS, aspirate.

Lyse in vessel if # of cells <2 x 10^6.

Nonadherent
Rinse with PBS.

Transfer up to 2 x 10^6 cells, centrifuge 2 min.

Decant supernatant.

Add 350 µl lysis solution. Pipet up and down 12x.

Add 350 µl 70% EtOH. Pipet up and down.

Bacterial cells

Transfer up to 2.4 x 10^9 cells into a capped 2 ml tube. Centrifuge at maximum speed 1 min. Decant supernatant.

Add 100 µl of 500 µg/ml lysozyme. Pipet up and down.

Incubate at room temp. for 5 min.

Add 350 µl lysis solution. Pipet up and down 12x.

Add 250 µl 70% isopropyl alcohol. Pipet up and down.

Yeast cells

Transfer up to 3 x 10^7 cells into a capped 2 ml tube. Centrifuge at maximum speed 1 min. Decant supernatant.

Add 1 ml of 50 U/ml lyticase in lyticase dilution buffer. Pipet up and down.

Incubate at room temp. for 10 min. Centrifuge at 5,000 rpm for 5 min. Discard supernatant.

Add 350 µl lysis solution. Pipet up and down 12x.

Add 350 µl 70% EtOH. Pipet up and down.

Continue with the following steps for all sample types:

Insert RNA binding column into a 2 ml capless tube.

Transfer lysate.
Centrifuge 30 sec. Discard filtrate.

Homogenized lysate

Add 700 µl low stringency wash.
Centrifuge 30 sec. Discard filtrate.

700 µl low stringency wash

Dilute 5 µl reconstituted* DNase I with 75 µl DNase dilution solution.

Add 80 µl diluted DNase I.
Incubate 15 min at room temp. Centrifuge 30 sec. Discard filtrate.

80 µl DNase I in dilution solution

Add 700 µl high stringency wash.
Centrifuge 30 sec. Discard filtrate.

700 µl high stringency wash

Add 700 µl low stringency wash.
Centrifuge 1 min. Discard filtrate. Centrifuge additional 2 min.

700 µl low stringency wash

x 2

Place RNA binding column into a 1.5 ml capped tube.

Add 80 µl 70°C elution solution onto membrane stack.
Incubate 1 min. Centrifuge 2 min to elute.

80 µl elution solution

* Refer to manual for detailed protocol.

Aurum Total RNA Mini Kit: Cat. #732-6820

BIO-RAD

For more information, call Technical Service at 1-800-4BIORAD (1-800-424-6723). Visit us on the Web at **www.bio-rad.com**

8. Run Assay

Considerations

- Bring all assay components and samples to room temperature (RT) before use
- Use calibrated pipets and pipet carefully, avoiding bubbles
- Pay close attention to vortexing, shaking, and incubation instructions; deviating from the protocol may result in assay variability
- Assay incubations are carried out on a shaker at 850 ± 50 rpm at RT. Cover the plate with sealing tape
- After each assay step, select the appropriate Bio-Plex Pro Wash Station program or perform the appropriate manual wash step noted in Table 9

Table 9. Summary of wash options and protocols.

	Bio-Plex Pro Wash Station	Handheld Magnet
Assay Step	**Magnetic Program**	**Manual Wash Steps**
Add beads to plate	MAG x2	2 x 100 µl
Sample incubation	MAG x3	3 x 100 µl
Detection antibody incubation		
SA-PE incubation		

Adding Coupled Beads, Samples, Standards, Blank, and Controls

1. Cover the unused wells of the assay plate with sealing tape.
2. Vortex the diluted (1x) beads for 30 sec at medium speed. Pour into a reagent reservoir and transfer 50 µl to each well of the assay plate.

Tip: A multichannel pipet is highly recommended for ease of use and efficiency.

3. Wash the plate two times with 100 µl Bio-Plex Wash Buffer per well using the wash method of choice.
4. Vortex the diluted samples, standards, blank, and controls at medium speed for 5 sec. Transfer 50 µl of each to the appropriate well of the assay plate, changing the pipet tip after every volume transfer.
5. Cover the plate with a new sheet of sealing tape. Incubate on shaker at 850 ± 50 rpm for 30 min at RT.

Note: Be consistent with this incubation time and shaker setting for optimal assay performance and reproducibility.

Preparing and Adding Detection Antibodies

1. While the samples are incubating, use Tables 10 and 11 to calculate the volume of detection antibodies and detection antibody diluent HB needed to prepare a 1x stock. Detection antibodies should be prepared 10 min before use.
2. Add the required volume of detection antibody diluent HB to a 5 ml polypropylene tube.
3. Vortex the 10x or 20x stock detection antibodies for 5 sec at medium speed, then perform a 30 sec spin to collect the entire volume at the bottom of the tube.
4. Dilute detection antibodies to 1x by pipetting the required volume into the 5 ml tube. Vortex the tube.

Table 10. Premixed panel.

Number of Wells	10x Detection Antibodies, µl	Detection Antibody Diluent HB, µl	Total Volume, µl
96	300	2,700	3,000

Table 11. Mixing singleplex assays.

Number of Wells	Singleplex #1 20x Detection Antibodies, µl	Singleplex #2 20x Detection Antibodies, µl	Detection Antibody Diluent HB, µl	Total Volume, µl
96	150	150	2,700	3,000

5. After incubating the beads, samples, standards, blank, and controls, slowly remove and discard the sealing tape.
6. Wash the plate three times with 100 µl wash buffer per well.
7. Vortex the diluted (1x) detection antibodies at medium speed for 5 sec. Transfer into a reagent reservoir and dispense 25 µl to each well of the assay plate using a multichannel pipet.
8. Cover the plate with a new sheet of sealing tape. Incubate on shaker at 850 ± 50 rpm for 30 min at RT.

Preparing and Adding Streptavidin-PE (SA-PE)

1. While detection antibodies are incubating, use Table 12 to calculate the volume of SA-PE and assay buffer needed to prepare a 1x stock. SA-PE should be prepared 10 min before use.
2. Add the required volume of assay buffer to a 15 ml polypropylene tube.
3. Vortex the 100x stock SA-PE for 5 sec at medium speed. Perform a 30 sec spin to collect the entire volume at the bottom of the tube.
4. Dilute SA-PE to 1x by pipetting the required volume into the 15 ml tube. Vortex and protect from light until ready to use.

Table 12. Preparation of 1x SA-PE from 100x stock.

Number of Wells	100x SA-PE, µl	Assay Buffer, µl	Total Volume, µl
96	60	5,940	6,000

5. After detection antibody incubation, slowly remove and discard the sealing tape.
6. Wash the plate three times with 100 µl of wash buffer per well.
7. Vortex the diluted (1x) SA-PE at medium speed for 5 sec. Pour into a reagent reservoir and transfer 50 µl to each well using a multichannel pipet.
8. Cover the plate with a new sheet of sealing tape. Incubate on shaker at 850 ± 50 rpm for 10 min at RT.
9. After the streptavidin-PE incubation step, slowly remove and discard the sealing tape.
10. Wash the plate three times with 100 µl of wash buffer per well.
11. To resuspend beads for plate reading, add 125 µl assay buffer to each well. Cover the plate with a new sheet of sealing tape. Shake at room temperature at 850 ± 50 rpm for 30 sec. Slowly remove and discard the sealing tape before placing the plate on the reader.
12. Refer to Table 13 for instrument settings.